INFORMATION PROCESSING BY THE FIRST OPTIC GANGLION IN DIPTERANS

Thesis by

David Woods Arnett

In Partial Fulfillment of the Requirements

For the Degree of

Doctor of Philosophy

California Institute of Technology

Pasadena, California

1971

(Submitted November 20, 1970)

ACKNOWLEDGEMENTS

I would like to express my deep gratitude to Dr. Gilbert McCann for the encouragement and steadfast support given me throughout my years at the California Institute of Technology. I am also indebted to Dr. K. I. Naka for his good humor and invaluable discussions.

I also wish to express my appreciation to M. Clay, D. Hodgetts, B. Ellert and D. Aranovich for their technical assistance and to Mrs. E. Fox for typing this manuscript.

This work was done while I held a National Institute of Health Traineeship.

ABSTRACT

Information processing properties of the dipteran first optic ganglion were studied by observing and analyzing the discharge behavior of two units in the intermediate chiasma and the slow potential behavior of two units in the first optic ganglion. Both types of chiasma units (on-off, on-maintained) were centripetal and corresponded to second order units in the first optic ganglion. The on-off unit was characterized by a transient discharge following the onset and cessation of a light pulse presented anywhere in the receptive field which had an elliptical configuration with average major and minor half directional sensitivity angles of 5.5 and 4.3 degrees, respectively. The receptive field of the on-maintained unit was composed of three roughly circular regions arranged adjacently along a line, and stimulation of the center region elicited a sustained on discharge while stimulation of either adjacent region elicited an off discharge. The average half directional sensitivity angle of the center on region was 2.5 degrees which compared well with the acceptance angle of the photoreceptors. The orientation of the major axes of the on-off and on-maintained unit receptive fields was always that of the medio-lateral axis of the compound eye.

The on and off regions of the on-maintained unit receptive field were antagonistic, for stimulation of either off region inhibited or suppressed a discharge resulting from on region stimulation.

Furthermore, the off response was inhibited by on region stimulation if the cessation of on region stimulation preceded, by not more than 200 msec., the cessation of off region stimulation.

The discharge patterns of both units were independent of the stimulus spectral wavelength, and all units studied, of both types, possessed the same spectral sensitivity which was characterized by two peaks of approximately equal maximum sensitivity centered at 350 mμ and 485 mμ. It was concluded that these units belonged to the system served by photoreceptors 1-6 and that a photopigment with two absorption peaks was responsible for the observed spectral sensitivities. Neither unit displayed any sensitivity to the plane of polarized light.

Positive slow potentials were recorded from the first optic ganglion with fine micropipettes, and they were believed to originate from the photoreceptor axons. A hyperpolarizing slow potential, most likely of intracellular origin, was also recorded, but its properties were not studied in detail.

Based on their information processing properties, the on-off and on-maintained units were identified with the two type I monopolar neurons of each cartridge. A model was developed which adequately explained the behavior of both types of units, and its structure was compared with the known anatomical structure of the first optic ganglion.

TABLE OF CONTENTS

CHAPTER	TITLE	PAGE
I	INTRODUCTION	1
II	MATERIALS AND METHODS	11
III	LIGHT EVOKED RESPONSES	37
IV	DIRECTIONAL SENSITIVITY AND RECEPTIVE FIELD ORGANIZATION	65
V	SPECTRAL AND POLARIZATION SENSITIVITY	108
VI	FUNCTIONAL INTERACTIONS	142
VII	DISCUSSION OF RESULTS	157
	LIST OF REFERENCES	186

CHAPTER I

INTRODUCTION

The study of vision is as old as civilization itself and has not been solely the interest of scientists, but artists and philosophers as well. No one needs to be told how important vision is to his existence, for everyone, at one time or another, has experienced a strong dependence on this sense while undergoing a voluntary temporary loss of sight. Nearly every form of life from the single-celled amoeba to man has evolved a form of light sensitivity in conformity with the particular pressures of natural selection. Elementary forms sense only the presence of light which in some cases signals a source of food and in others an approach of danger. The most complex forms of light sensors or eyes belong to vertebrates, such as fishes, birds, and mammals, and to invertebrates such as insects and crustaceans. Through observation of vision dependent behavior of animals of these two phyla, such as the attentive stalking of a cat or the beautiful flight maneuvers of a dragonfly, it is clear that their eyes though differing greatly in design (camera type eyes, compound eyes) are capable of sensing complex spatial-temporal patterns of light. It is not so much a question of how light is detected as it is in the case of elementary light sensors, but instead, of how the visual nervous system abstracts and organizes information contained in highly structured light patterns. Closer observation of behavior

dependent on vision in some of these animals reveals that their eyes are able to detect other characteristics of light as well, such as its spectral composition and polarization.

The compound eye of the fly provides a favorable preparation in which to study how the eye and the visual nervous system are structurally and functionally organized to handle the relevant information contained in spatial, temporal, spectral, and polarized light patterns. Success in this endeavor requires a quantitative approach, and the compound eye of the fly is advantageous in this respect because its structure is highly ordered and therefore readily amenable to an algebraic description. The compound eye is composed of several thousand independent optical elements each being describable in terms of its optical axis orientation and directional sensitivity. Therefore it is possible to describe quantitatively the stimulus presented to the compound eye in terms of a set of equations depending only on the parameters of the optical systems and the applied light distribution. Furthermore, anatomical studies [9, 33, 34, 50, 75, 77, 78, 79, 80] have shown that the optic lobe of the fly is, likewise, highly structured from a relatively small number of components (approximately one million), and there is no evidence of any adaptive behavior in the fly. Consequently, the structural rigidity and specificity make the compound eye of the fly well suited for a quantitative description. In addition, the fly is a readily available material and is easily handled, and

there is an increasing amount of information about the detailed anatomy of the compound eye. However, the fly is not without disadvantages, and its chief one which has been the limiting factor in research of this type in the past is the difficulty in observing the desired signal in the visual system due primarily to its size.

There are three basic approaches in the study of vision in the compound eye, and each extracts a distinct type of information. The behavioral approach utilizes quantitative observations of vision dependent behavior to answer questions pertaining to the existence of sensitivity to particular properties of light, such as color [16, 22, 37, 48], polarization [18, 23, 24, 36, 42], and spatial-temporal organization [20, 51, 52], to the limits of vision [51, 70], and to general mechanisms of vision [69]. This approach lumps the functional and structural details of the compound eye and visual nervous system into a black box having as its input the light stimulus and as its output the observed behavior such as flight torque, landing response, or phototaxis. The behavioral approach does not provide an understanding of the neural mechanisms responsible for the observed behaviors, but it does provide information which is useful in the design of experiments in the other approaches. The structural approach [9, 34, 50, 75, 77, 78, 79, 80] utilizes light and electron microscopy to investigate the elaborate neural structure of the visual nervous system. Such an approach opens the black box and places the study on the cellular and sub-cellular

level. There is little doubt that a complete understanding of the neural mechanisms of compound eye vision is impossible without a comprehensive knowledge of the structure of the system. Another recently developed approach [6, 31, 58, 59] utilizes the method of single unit analysis. The single unit approach provides information about light evoked neural behavior, and when correlated with information from the structural approach makes it possible to combine structure and function at the cellular level to arrive at the neural mechanisms responsible for vision.

Information carried in a light pattern is expressed in terms of its spatial-temporal organization and its spectral and polarization pattern. Due to the demands placed upon them, flying insects developed the ability to detect certain types of information in light patterns. Some of these types of information are also detected by the vertebrate eye; others are specific to the compound eye and, others are species specific. Studies [16, 24, 42, 37] using the behavioral approach have shown that the compound eyes of many insects are sensitive to the plane of light polarization and to radiation whose spectrum is similar to that of humans but shifted by approximately 100 mμ to shorter wavelengths. In fact, color discrimination has also been demonstrated in some insects [16, 49]. Studies of the optomotor reaction in flies have revealed that their compound eyes detect the direction of motion of a moving light stimulus which seems to be an ability also possessed by some

vertebrate eyes. Fast flying insects such as bees, flies, and dragonflies must be capable of abstracting information from a rapidly changing light environment, and studies have found that the compound eyes of these insects have a frequency response an order of magnitude higher than vertebrate eyes.

Recent neural anatomical studies of the fly visual system have revealed a highly ordered structure. As a first approximation, the neural structure of the fly compound eye and optic lobe can be divided into several serially organized subsystems which have a morphological identity.

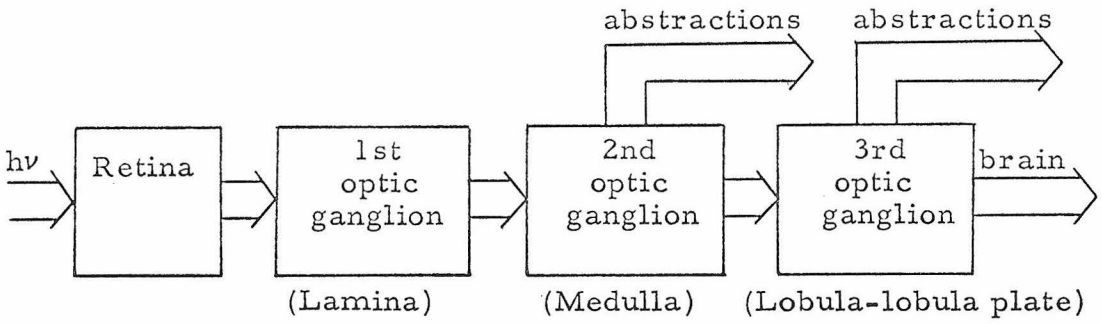

Although existing feedback paths between subsystems are not indicated, the schematic model is quite general and helpful when considering the basic structure and function of the fly visual system. Due to the specially developed optical and photon absorbing properties of the retina, only the functionally relevant information in the light stimulus falling on the retina is actually retained in the multidimensional signal leaving the retina. Each subsystem makes specific transformations on the signals it receives and

creates functionally important abstractions on these signals, such as the abstraction of information concerning the direction and rate of a moving light pattern. The consequences of these transformations and abstractions are manifested in the various light induced behaviors. As the neuroanatomists provide more structural information, refinements can be made in the model. In fact, the model could be structurally refined, as a great amount is already known about the elaborate structure of the retina and first optic ganglion; however, the single unit approach has not provided enough insight into the cellular functions corresponding to these refinements to justify their incorporation into the model.

The above model represents a hierarchy of information transformations. Complete understanding of how information is processed by the fly visual nervous system will only come after studies on the cellular level are made at each stage in the information processing hierarchy. Structural information on the cellular level will come from histological studies, and cellular functional information will come from the analysis of single neuron behavior (slow and spike potentials) at each level of the system. Although the method of single unit analysis is relatively new, it has provided considerable information concerning cellular function. The transducing properties of photoreceptor cells in the retina of several insects [4, 11, 12, 57, 86] have been revealed by inserting micropipettes into them and recording their membrane potential

changes in response to specific types of light stimulation. Slow potential changes [56, 72, 90] have been recorded from the first optic ganglion in an attempt to elucidate the nature of the information transformation taking place at this level. Although spike discharges have not been observed in the retina or first optic ganglion of the fly, they appear to be the mode of information transmission at higher levels of the visual nervous system. Comprehensive studies [7, 8, 19, 53] have been made of a set of single units in the third optic ganglion and the brain which abstract information about the direction of moving light patterns. These studies have revealed that the units responsible for this abstraction are intimately involved in the optomotor response mechanism. However, the exact neural mechanism of directionally selective motion detection is still unknown and can only be determined after precursory units have been studied.

Attempts [6, 7] to observe the behavior of such precursory units in the first and second optic ganglia of the fly have met with only partial success due to the small size and dense packing of these neurons in the neuropile. The behavior of several types of units in the second optic ganglion have been observed and analyzed, but they represent a relatively small subset of the class of units responsible for the information processing at this level. Unsuccessful attempts [6, 31, 56, 72] have been made to record spike discharge activity in the first optic ganglion although slow potentials

have been recorded from single cells in this region. The absence of spike discharge from the first optic ganglion is perplexing because it is difficult to understand how slow potentials could passively transmit information to the relatively distant second optic ganglion.

The reported absence of spike discharge potentials from the first optic ganglion and the need to study the functional behavior of units presynaptic to the directionally selective motion detection units in the third optic ganglion provided the impetus for the study, reported in this thesis, of single units in the first optic ganglion. Furthermore, extensive knowledge was available about the transducing properties of the retina and about the detailed structural organization of the retina and first optic ganglion. Therefore, the study of single second order units in the first optic ganglion would provide information concerning the characteristics of the signal transformation at this level which could be correlated with the existing structural evidence to provide a cellular level model explaining the transformations.

By employing special recording procedures, it was possible to observe single unit discharge behavior in the intermediate chiasma. The observed signals corresponded to output signals of the first optic ganglion. With this ability to observe output signals from the first optic ganglion, several interesting questions concerning the role of the first optic ganglion in information

processing could be posed. For example,

1. How is information concerning the spectrum of the stimulus coded in the discharge patterns of these units, and is there evidence of wavelength discrimination mechanisms?

2. What transformations, if any, are made on the transduced light polarization information by the first optic ganglion?

3. What is the organization of the spatial transformation?

4. What transformations are made on the temporal properties of the light stimulus?

5. How can the information transformations be explained in terms of the synaptic structure of the first optic ganglion?

6. What relevance are these transformations to the abstraction of motion detection?

The study described in this thesis was directed toward providing answers to such questions as these. This thesis is organized into three parts. The first part describes the materials and methods used and is found in Chapter II. The second part, found in

Chapters III, IV, V and VI, presents the results of the experiments. The conclusions are discussed in the third part which appears in Chapter VII.

CHAPTER II

MATERIALS AND METHODS

Introduction

This chapter begins with a description of the specimen preparation used in extracellular and slow potential recording experiments. The following section describes the methods employed for recording extracellular spike potentials and slow potentials, followed by a description of the stimulating equipment used to elicit the recorded responses. The chapter concludes with a detailed account of the methods of data analysis.

Specimen Preparation

All experiments described in this thesis utilized insects of the order Diptera as the biological material under investigation. Most of the data were obtained from Phaenicia sericati and to a lesser extent Calliphora erythrocephala; however, responses similar to those to be described for these two species were also observed in Musca domestica and Sarcophaga. These animals were bred and raised in our laboratory. Specimens selected for an experiment ranged in age from 3-12 days post-emergence, and, generally, females were selected due to the observation that male preparations were less stable. No differences in neural behavior were observed between preparations of opposite sex.

The mechanical stability of preparations used in extracellular potential recording experiments was not critical which allowed the animals to be used intact. For such experiments, the selected specimen was mounted intact on a special ball joint stand by dental wax (Periphery wax) applied with a small heat loop. The specimen was secured in such a way that the thorax and head were completely immobile, but the abdomen was left free to move so that respiration was unrestricted. No anesthesia of any type was used. The optic lobe of the right eye was exposed by tilting the head forward by approximately 30 degrees and removing a triangular flap of exoskeleton from the posterior surface of the head. Various globular tissues were carefully removed from the head capsule without damaging the neural tissue or tracheal system. Afterwards, ringer's solution [71] (9. gm NaCl, .2 gm KCl, .2 gm $CaCl_2$, 4. gm glucose per 1000 mL buffered to pH 7.2 with phosphate buffer) was added, if required, and a platinum indifferent electrode was secured so that it made good electrical contact with the heamolymph circulating through the head capsule. A preparation was judged good if only slight pulsation of the tracheal air sacks and heamolymph could be observed. In such a preparation, the retina and all optic ganglia could be visually identified.

The mechanical stability of preparations for slow potential recording experiments was of great importance. Most movements

were eliminated by removing the head from the thorax. The isolated head was secured to the stand so that the head was rotated by 90 degrees from its position in extracellular experiments as described above (i. e., the right eye was above the left eye, and the mouthparts were to the right). The lamina and the retina were exposed by cleanly slicing away the lateral half of the right eye; thereby, making it possible to drive a vertically oriented micropipette into the desired neural tissue. In good preparations, the entire length of individual ommatidia could be observed along with a clear demarcation of the lamina ganglionaris. The platinum indifferent electrode made contact with a small pool of ringer's solution which wet a part of the head exoskeleton, and the preparation was placed in a high humidity environment (r. h. > 90%) to reduce drying. It was possible to record extracellular discharge activity, typical of that found in intact preparations, from selective motion detection units in the lobulla-lobullar plate region in isolated head preparations.

Recording Methods

The results presented in this thesis were derived from two types of data. Extracellular spike potentials constituted the major type of data while slow potentials were used much less extensively. Because the methods used to obtain both types of data differed, they will be described separately. Several different types of extracellular potential recording microelectrodes were tested

(stainless steel, tungsten, electrolyte filled glass pipettes, suction electrodes, Wood's metal filled glass pipettes); however, etched tungsten electrodes were found to be superior for two reasons. First, the noise level of the microelectrode in the standard recording situation was low enough to easily discriminate a 50 microvolt pulse of .1 msec duration. Second, the recording surface of the microelectrode was relatively large (2 microns) as shown by the scanning electron micrographs of a tungsten microelectrode in figure 2.1 which provided a greater recording life once a single unit had been isolated than did microelectrodes with smaller recording surfaces.

The tungsten microelectrode was etched to the desired shape using the procedure described by Hubel [35]. To reduce the inherent noise associated with a tungsten-electrolyte interface, a platinum black surface was plated on the microelectrode tip in a two step process. A layer of gold was first plated on the tungsten to serve as an adhering base for the platinum surface plated in the second step. The microelectrodes were then coated with three layers of epoxy resin (Hysol AC4396) which served as an excellent and strong insulator (figure 2.1A). Immediately before a microelectrode was to be used, the insulation at the tip was removed by passing a brief pulse of current through the microelectrode while the tip made contact with the platinum plating solution (figure 2.1B). In addition to breaking the insulation, an active layer of platinum

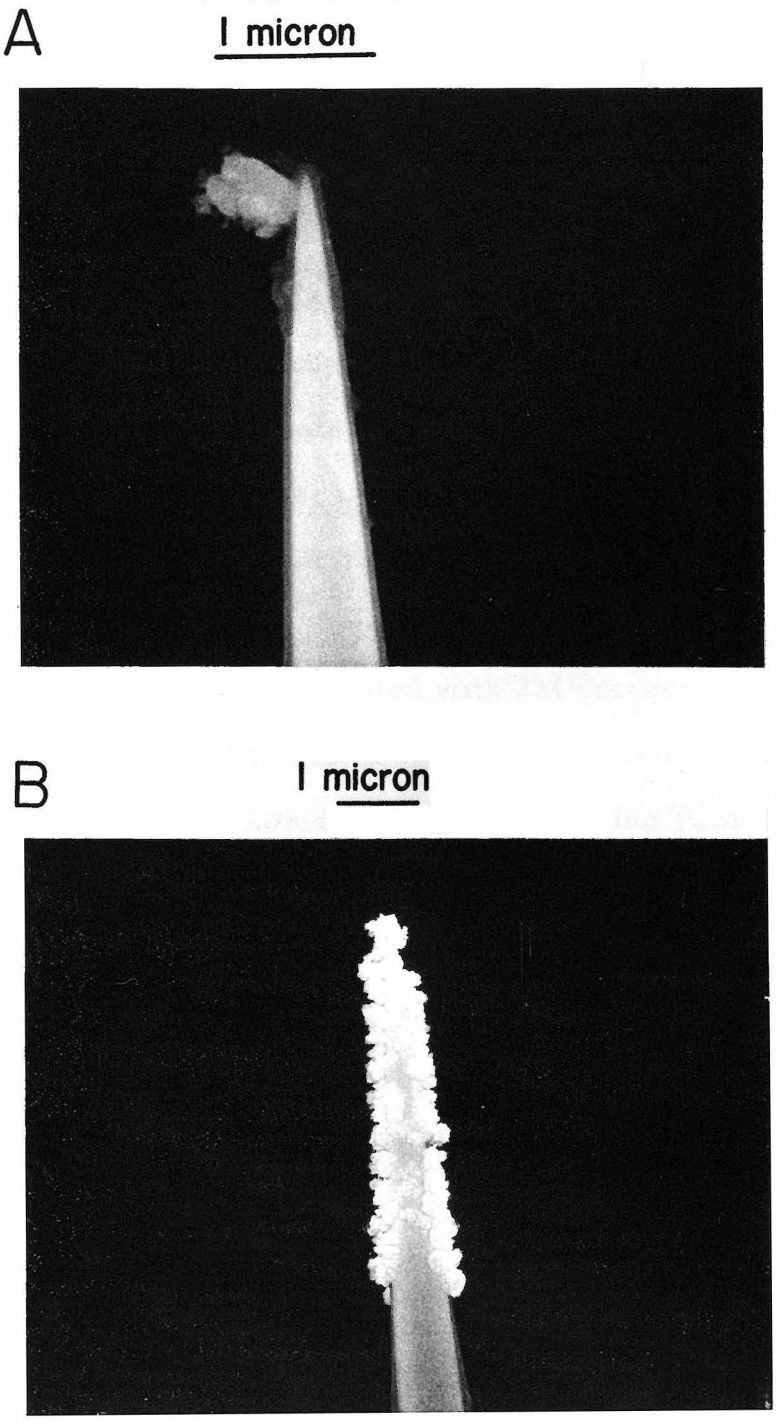

Figure 2.1 Scanning electronmicrographs of tungsten microelectrodes

A. Microelectrode coated with an epoxy resin insulator (and piece of dirt)

B. Microelectrode after plating the tip with platinum black

black was deposited on the tip. During an experiment, the microelectrode was positioned by a standard gear drive micromanipulator. Although it was possible to determine with good accuracy the point of microelectrode insertion into the optic lobe, it was impossible to judge the depth of penetration, for the tissue was sufficiently compliant to allow considerable tissue deformation near the site of the microelectrode penetration. Fortunately, it was not necessary to know the location of the microelectrode tip to any better accuracy than the specific neuropile or chiasma penetrated.

Glass micropipettes filled with 2M potassium citrate were used to record slow potential from the lamina and retina. The micropipettes were drawn from capillary tubing (Corning #7740) with a vertical puller (DKI 700c) and were filled by the standard diffusion technique. An acceptable micropipette had a tip diameter less than .5 microns and a resistance of greater than 100 Megohms. The micropipettes were positioned by a hydraulic micromanipulator which decoupled the micropipette from mechanical perturbations introduced by the experimenter.

The discharge potentials recorded by the extracellular microelectrodes were amplified and stored on magnetic tape as shown in the schematic diagram of figure 2.2. The d.c. offset was not used during extracellular potential recording experiments, for the input to the preamplifier was, in this case, a.c. coupled.

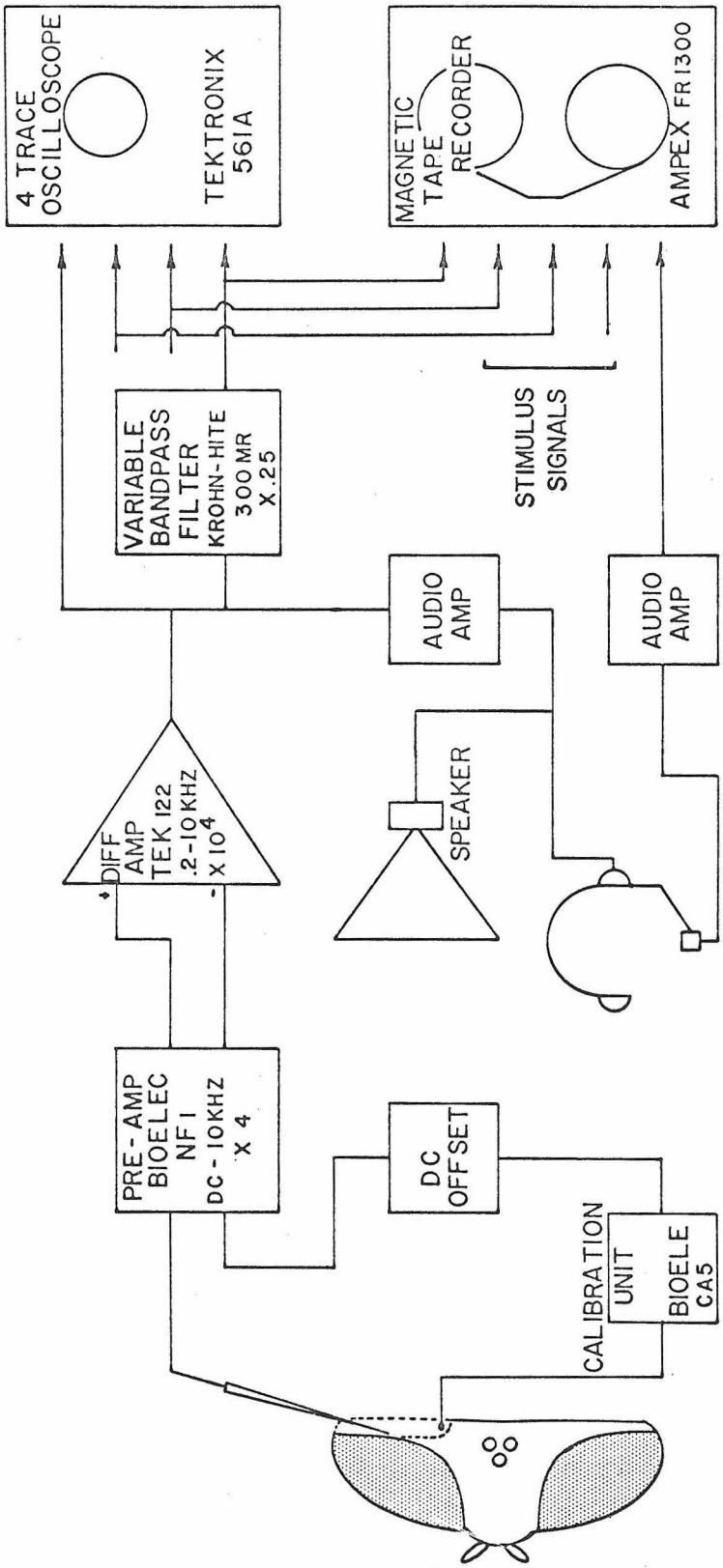

Figure 2.2 Schematic diagram of the electronics used for handling the relevant experimental signals

The variable bandpass filter was found to be a useful tool for enhancing the signal to noise ratio. When two extracellular microelectrodes were used, the potential recorded by the second microelectrode was processed in a similar manner. Slow potentials recorded with micropipettes were processed in the same manner except that the preamplifier was direct coupled and followed by a direct coupled amplifier in parallel with the capacitive coupled differential amplifier and the variable bandpass filter. The capacitive coupled channel allowed higher gain for better observation while the direct coupled channel preserved the potential waveforms and was stored on magnetic tape. The stimulus signals recorded on tape varied depending upon the experiment (wedge position, waveform of stimulus channel 1, of stimulus channel 2) and will be apparent when the experiments are later described. The signals recorded on magnetic tape were later reproduced for analysis by computer methods and for photographic purposes.

Stimulus Equipment

The light stimulus used in the course of these experiments can be characterized with respect to the following classes of attributes:

1. Spectral composition (λ)
2. Angular orientation of the plane of polarization (α)
3. Spatial attributes (multi-dimensional)
4. Temporal attributes (multi-dimensional)

The multi-dimensionality of parameters belonging to classes 3 and 4 precluded their identification, but they will become apparent when specific stimuli are described. Two separate stimulating facilities were utilized to generate stimuli having the above parameters at the control of the experimenter. One facility illustrated in figure 2. 3 utilizing direct stimulation was specially designed to provide the experimenter with control of classes one and two and will be described first. The other facility utilized reflected light which made it possible to manipulate the parameters of classes three and four.

The primary source of light (S_1) for the direct stimulator was a 150 watt xenon arc lamp (Hanovia 901C1) driven by a regulated power supply (Bausch and Lomb). The quartz condensing system (L_1, L_2) focused the light at the plane of the pinhole (Ph); however, a frosted quartz diffuser (D_1) was inserted behind the condensing lenses to make the intensity distribution at the pinhole uniform and to reduce the amount of supplied light. Before reaching the pinhole, the light was filtered by distilled water in a quartz cell (C) which removed most of the infra-red component. The light beam was interrupted by a rotary solenoid actuated shutter (Sh), and the signal of stimulation was derived from a photodiode (Pd) placed behind the shutter. Light passing through the pinhole was accurately attenuated by a 4 log unit neutral density circular wedge (Kodak, Inconel on quartz, W) which was mounted on a precision potentiometer to provide an electrical read-out of the wedge

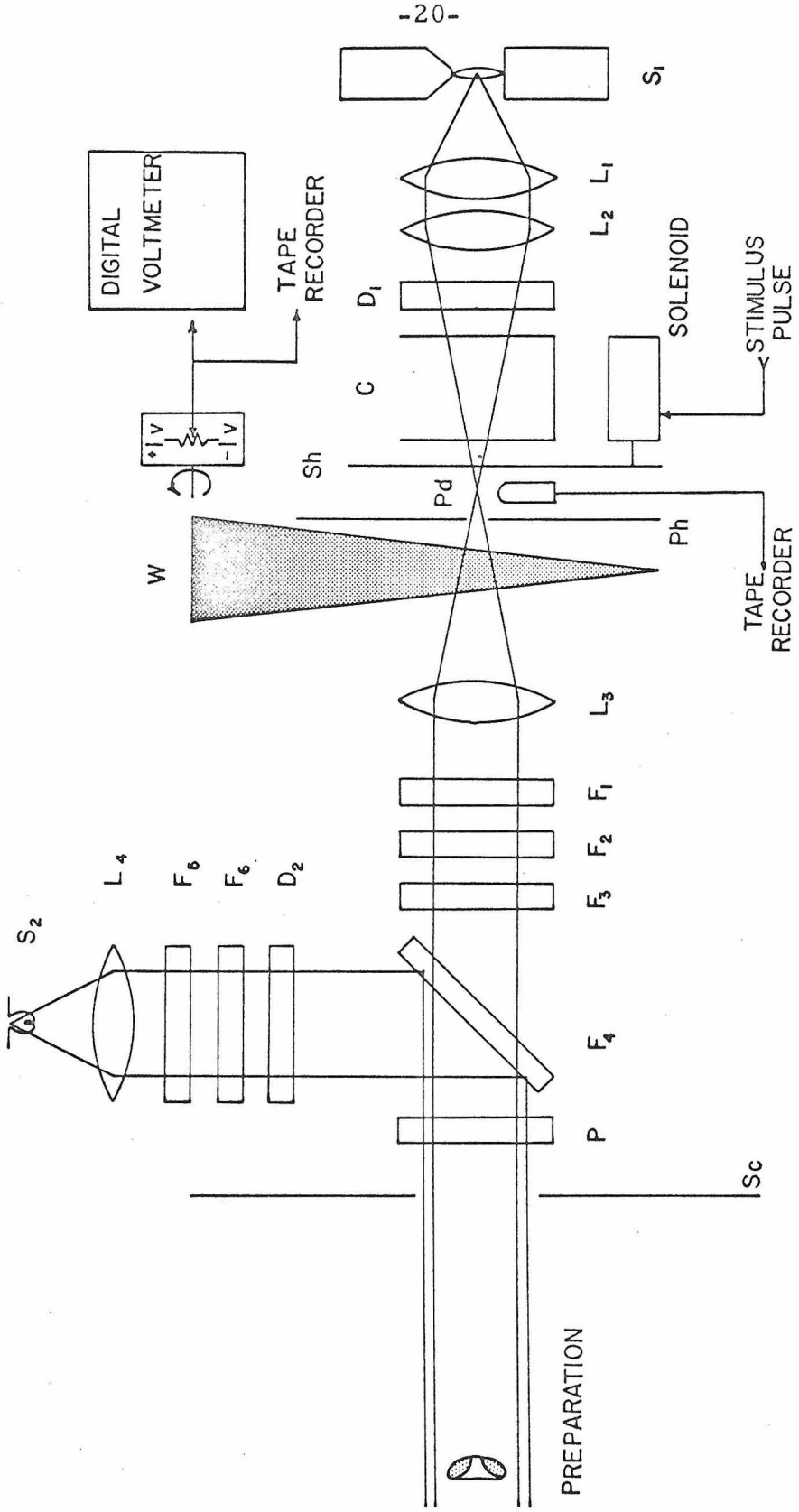

Figure 2.3 Schematic diagram of the direct stimulating apparatus

position. After the light was collimated by the quartz achromat (L_3), it passed through a maximum of three 2" x 2" filters (F1, F2, F3) consisting of narrow and wide band interference filters (Balzer, Filtraflex A-UV, B-HO) and one log unit neutral density filters (Inconel on quartz, Kodak). When the secondary source (S_2) was utilized, a 1 log unit neutral density filter (Inconel on quartz, Kodak, F_4) was introduced at 45 degrees to the primary beam so that the two beams were added. A polarizer (P) could be inserted into the combined beams, and the angle of the plane of polarization could be changed in steps of 30 degrees. After passing through a hole in the screen (Sc, white cardboard 2 ft. square), both concentric beams of uniform intensity were incident directly on the compound eye. The diameter of the smaller primary beam was 6 mm which was large enough to illuminate the entire head of the preparation. A 6 volt tungsten filament bulb (S_2) provided the light for the second beam which was used for supplying a steady adapting stimulus. After being collimated, the beam passed through a narrow band interference filter (F_5), a wratten neutral density filter (F_6) and a diffuser (D_2) before being added to the primary beam.

The spectral composition of the primary beam was controlled by narrow band interference filters (Balzer, Filtraflex R-UV B-40). The bandwidths (50% of maximum transmission) and center wavelengths (wavelength of maximum transmission)

are listed in table 2.1 for all interference filters used during the course of these experiments. The intensity of the stimulus was calibrated with a Reeder thermopile (RBL-500) placed in the position normally occupied by the preparation, and the calibration measurements were taken from a Keithley Microammeter (150B) whose input was the thermopile signal.

The preparation was attached to a specially design movable platform carrying the micromanipulator as diagrammed in figure 2.4. So placed, the compound eye occupied the center of a spherical coordinate system (θ, ϕ) through which the stimulus beams also passed. The platform could be rotated in the orthogonal great circles defining the spherical coordinate system without causing significant translational movement of the compound eye due to imperfect centering of the preparation with respect to the uniform intensity stimulating beam. To assure that the stimulus was effectively a point source, a light sensor was built from two separated pinhole masks followed by a photomultiplier tube such that the optical window was less than .1 degree. The directional radiation of the stimulating beam was measured to be small compared to the optical window of the sensor, and therefore, small enough with respect to the directional sensitivity of photoreceptors to be considered as effectively from a point source. Thus the directionality of the stimulation relative to the compound eye could be changed by moving the compound eye instead of the light source.

Interference Filter Table

Center Wavelength (millimicrons)	Band Width (millimicrons)	Peak Transmission (percent)
326	20	25
349	20	25
358	20	25
377	20	25
385	20	25
403	11	29
416	19	32
430	13	39
454	9	42
463	13	32
471	9	40
480	10	42
491	10	38
500	7	43
513	10	40
523	8	37
535	10	40
552	11	40
575	7	34
600	7	43
624	9	40
660	9	35

Table 2.1 Principal characteristics of the interference filters utilized.

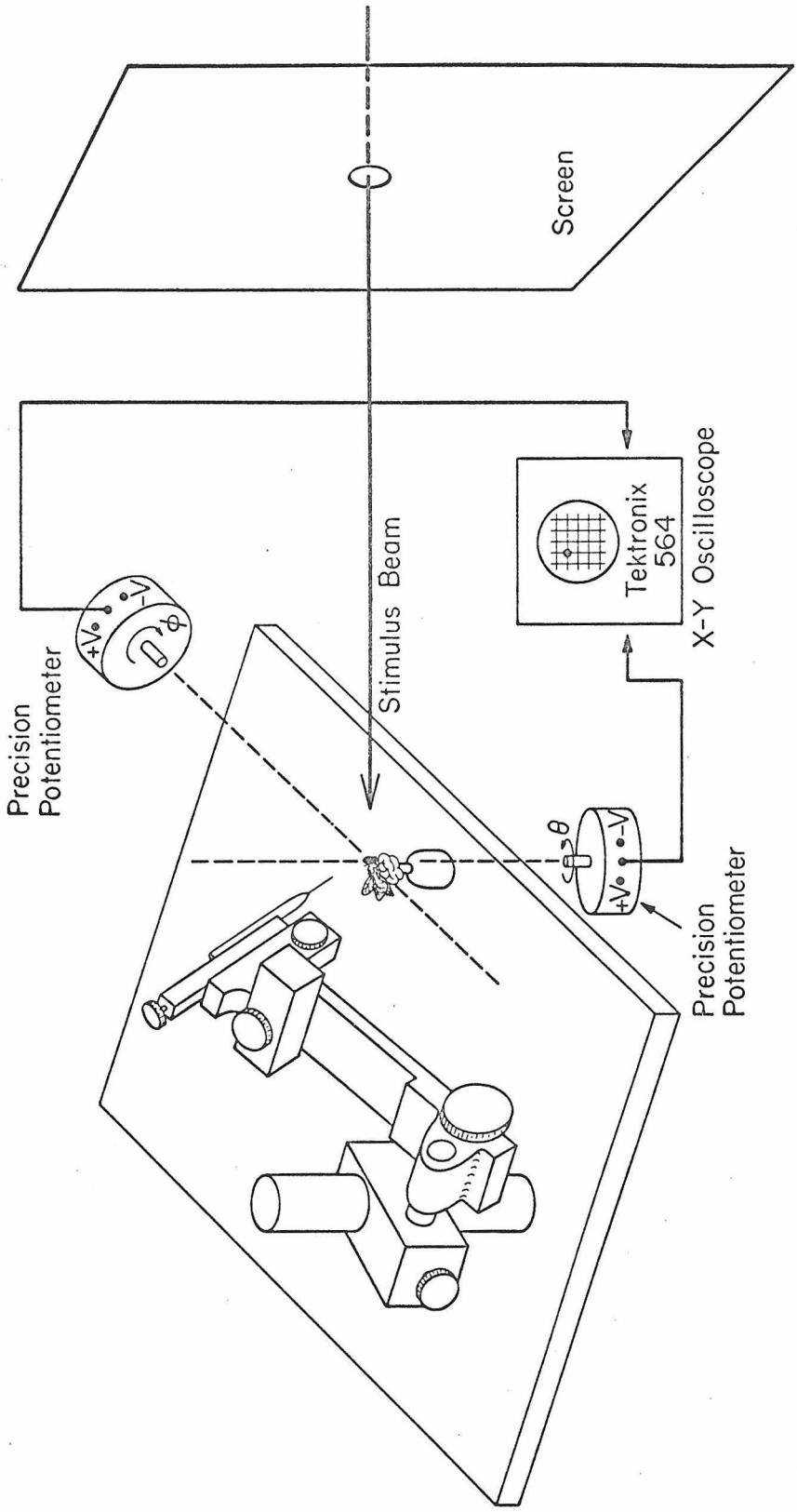

Figure 2.4 Schematic diagram of the movable platform carrying the preparation and microelectrode

Since the micromanipulator carrying the microelectrode was rigidly fixed to the platform supporting the preparation, it was possible to adjust the microelectrode position until a satisfactory unit discharge or slow potential was recorded. Having done this, the location of the receptive field was determined by projecting small spots of light generated from a hand-held source onto the screen (Sc). In general, the receptive field center was not initially coincident with the stimulation light beam passing through the 1/4" diameter hole in the center of the screen (Sc). It was therefore necessary to rotate the platform in the θ and ϕ directions until the receptive field center was coincident with the axis of the stimulating beam. Values for θ and ϕ were obtained from precision potentiometers mechanically coupled to the platform and were displayed as a point on an X-Y operated CRT. The accuracy of orientation was approximately .1 degree. After an experiment was completed, the location of the receptive field relative to the retinal geometry was determined by placing a small aperture microscope along the axis of the stimulating beam and observing the transmission pseudopupils resulting from rear illumination of the compound eye. In summary, this stimulating environment provided the opportunity for accurate control of the intensity of monochromatic (u. v. -visible), polarized or non-polarized light presented to the compound eye from an effective point source oriented arbitrarily with respect to the eye. Experiments pertaining to spectral sensitivity, polarization

sensitivity, and directional sensitivity were carried out using this stimulating apparatus.

The stimulus environment [7] used when studying single unit discharge behavior as a function of various spatial and temporal light intensity programs consisted of a six-foot diameter reflecting sphere upon which light patterns were projected. The preparation and microelectrode carrying micromanipulator were placed at the center of the sphere; therefore, five centimeters on the interior surface of the sphere subtended three degrees at the compound eye. Uniform background illumination was provided by two banks of 6 VDC tungsten filament light bulbs which indirectly illuminated the entire interior surface of the sphere. Specific light stimuli consisting of stationary spots, annuli, and stationary and moving striped patterns of light were generated from two specially designed light pattern projectors. Stimulation with moving striped patterns was provided by a tungsten filament projector through which a constant velocity film loop was moved. The direction and velocity of the loop was controllable, and film loops could be interchanged. A solenoid driven shutter interrupted the projected light, and the timing of the shutter could be adjusted so that immediately after it opened, the edges of a moving striped pattern would always fall in the same location on the sphere. This was necessary when averaging responses in order to preserve the temporal details in the average discharge characteristic to transiently presented

moving striped patterns. Complex spatial and temporal patterns were derived from a three channel tungsten filament projector. Each channel was capable of projecting different stationary light patterns, and since each channel was independently controlled, projection of complex temporal sequences of different spatial patterns was possible. The spectral characteristic of the stimuli derived from these projectors was that of a tungsten filament source.

Data Processing

The success of an investigation of any phenomenon depends upon the formulation of the problem (i. e., asking the right questions and defining pertinent variables) and the observability of the formulated experimental variables. Studies of many neural phenomenon are plagued by the complexity of the phenomenon observed and by limited observations due principally to the size of the structures involved. Consequently, neurophysiologists have confined their attentions to isolated parts of the total system in hopes of synthesizing an understanding of the phenomenon from understandings of its parts. The advantage of this reasoning are that formulations are simplified, but complete observation is less likely. Furthermore, the sum of the parts does not always equal the whole.

Working on the cellular or single unit level requires the observation of the state of a single unit as experimental input variables are strategically manipulated. In the case of single units

in the visual system of the compound eye, the experiment variables are those previously defined, and the state of a single unit is defined to be its membrane potential. Unfortunately, observation of membrane potential change is difficult and is frequently replaced by the more readily observable extracellular discharge potential. However, the use of single unit spike discharge as an experiment variable has one particular shortcoming not shared by the use of the more desired membrane potential. That is, the amount of information contained in a spike discharge response to a particular stimulus is far less than that contained in the slow membrane potential of the same unit to the same stimulus. Slow membrane potentials are encoded into propagating spike potentials by a threshold phenomenon. This process is essentially one of data reduction. However, noise or apparent random fluctuation whether intrinsic in origin or from uncontrolled inputs is present in the slow membrane potential which, in magnitude, is generally small compared to the magnitude of the signal component in the membrane potential. This, of course, depends upon the unit and the stimulus as discussed by Bullock [10]. The threshold encoder accounts for the data reduction between the membrane potential and the discharge and at the same time decreases the apparent signal to noise ratio. It is not known whether the frequently observed random appearance of discharge patterns is truly due to noise or whether it only appears that way due to our interpretation

of the discharge pattern. Nevertheless, a detailed and quantitative understanding of the system requires the signal (as neurophysiologist defines it, not necessarily as the postsynaptic neuron defines it) to noise ratio be enhanced by forming an average from sequential discharge trials to identical stimuli. This is not necessary with membrane potentials. Therefore, what is gained in observability by using discharge behavior as the experimental signal is partially lost by the necessity to reduce statistical fluctuation by sequential averaging. Either the animal doesn't have this problem due to its interpretation of discharge patterns or it does, but solves it by parallel average or by smoothing.

Most experiments described in this thesis utilized spike discharge potentials as the experimental output, and appropriate averages were calculated by a computer implemented data collection and analysis system [19, 48]. Before the data acquisition and analysis system is described, a mathematical formulation of discharge data [25, 54, 55, 66, 67] will be given. It is assumed that all spike potentials from a given neuron are indistinguishable and that they are instantaneous. Under these assumptions, the information conveyed in a spike train is necessarily contained in the time of occurrence of individual spikes or the time of events (TOE's). Therefore, only the TOE's of a spike train need be abstracted which represents an enormous amount of data reduction. A spike train is therefore mathematically represented by a set of TOE's.

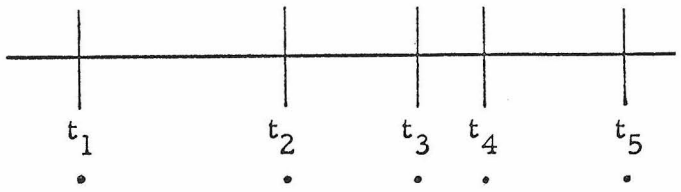

t_j = time of occurrence of j^{th} spike

$r = \{t_1, t_2, \ldots . t_j, \ldots .\}$

The response representation r contains all the information carried by the spike train, but without a similar representation of the stimulus very little of it can be revealed. Given the important parameters of the stimulus (duration, intensity, wavelength), it can likewise be mathematically represented by a sequence of TOE's corresponding to the initiation of each stimulus.

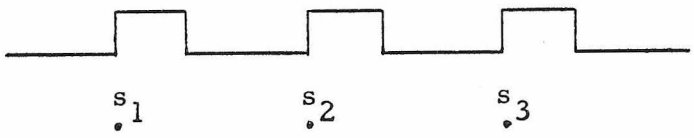

s_i = time of occurrence of i^{th} stimulus

$s = \{s_1, s_2 \ldots . s_i \ldots .\}$

A basic abstraction on the data (r, s) results by forming a histogram of stimulus-response latencies (τ_{ij}) and is called the post stimulus time (PST) histogram. The PST histogram has several equivalent interpretations depending on the basic formulation. If the spike train is formulated as a sample function of a stochastic point process (probabilistic approach), then the PST histogram approximates

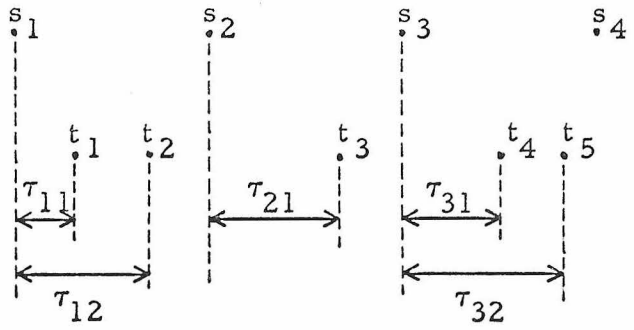

the probability of a spike at time τ given that the stimulus was presented at time 0 (i. e., Prob $[^{\text{spike at } t = \tau}/_{\text{stimulus at } t = 0}]$). Alternatively, if the spike train is formulated to comprise a stimulus evoked signal component and a noise component, then the PST histogram represents the average discharge elicited by the stimulus. As the number of trials accumulates, the PST histogram approaches the stimulus evoked signal component (i. e., the magnitude of the noise component decreases approximately as $1/\sqrt{N}$ where N is the number of trials in the average). Autocorrelation and crosscorrelation are generalizations of the PST average. Instead of compiling a histogram of stimulus-response latencies (τ_{ij}), a histogram is formed from response-response latencies (ℓ_{ij}). For autocorrelation the two sets of response TOE's defining the latencies (l_{ij}) are identical; however, the more useful crosscorrelation uses TOE's representing two separate spike trains. In effect, the crosscorrelogram is a PST histogram of the TOE's representing one spike train with respect to the TOE's representing another spike

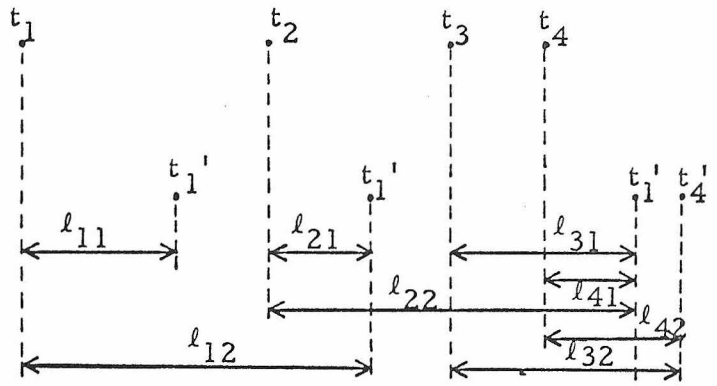

train. The crosscorrelogram approximates the probability of a spike at time τ in unit B given a spike in unit A at a time 0 (i. e., Prob[B spike at $t = \tau$ / A spike at $t = 0$]).

The mathematical formulation of spike trains in terms of sequences of TOE's and the mathematical operations thereupon are particularly well suited for computer implementation. In fact, the necessity of high speed computation is readily appreciated upon considering the task of computing an average which is itself necessary if detailed understanding is desired through studies involving discharge observations. For example, consider the computation involved in forming the crosscorrelation of spike train A with spike train B, each represented by 2000 TOE's. If the average discharge rate is 20 spikes/sec and the interval of interest is one second, then on the average 20 latencies must be calculated and sorted into the proper bins of the histogram for each of the 2000 TOE's of spike train A. The amount of calculation is prohibitive unless high speed computation is possible.

The basic configuration of the data acquisition and analysis system used in processing experimental data is shown in figure 2.5. The LORI was essentially a special-purpose computer and served as an interface between the experimental data and the central computer. It was equipped with a high speed analog to digital converter (500 kHz), a 10-channel multiplexer, and several digital clocks and could accept either of two basic data modes (continuous, TOE) on any of the 10 LORI channels. Continuous mode signals such as slow potentials and wedge position were fed directly into the desired LORI channels, and the LORI processed the signals by sampling them at variable rates up to 500 kHz. The sample values were transmitted to the central processor and stored in bulk memory. A TOE mode signal consisted of a string of negative pulses and was fed to any one of the LORI channels. The occurrence of a negative pulse (an event) triggered the LORI to transmit the contents (time of event) of a 27 bit clock to the central processor where it was stored in bulk memory. The clock rate could be preset to correspond with the desired accuracy; usually a clock rate of 50 kHz was used which corresponded to a TOE accuracy of 20 micro-seconds. The clock values transmitted to the central processor corresponded to the TOE s of the mathematical representation of spike trains if the negative pulses fed to the LORI were themselves triggered by spike potentials. This was accomplished as shown in figure 2.5 by triggering the scope sweep internally from the reproduced spike

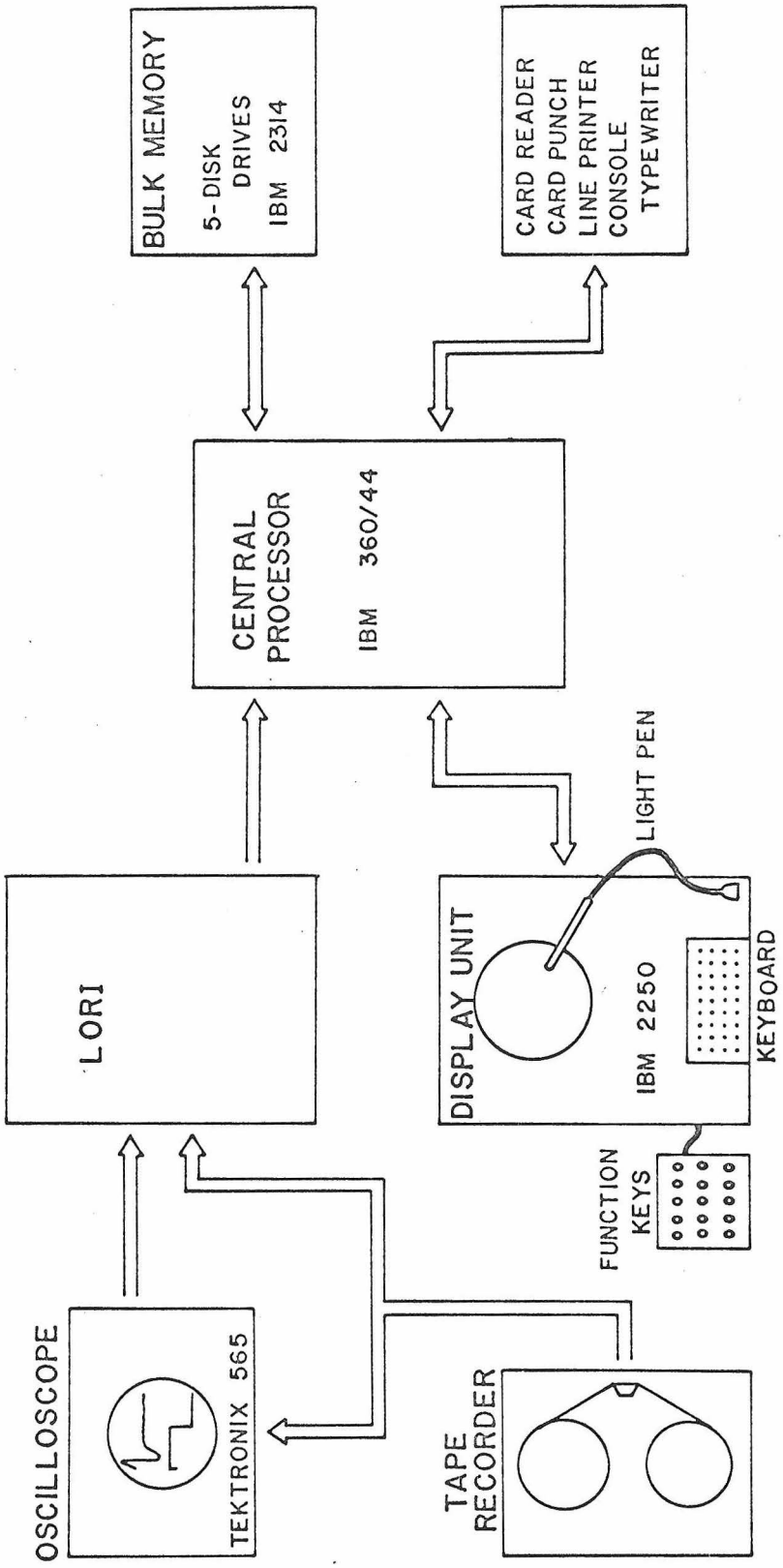

Figure 2.5 Basic configuration of the data acquisition and analysis system

potential (or stimulus signals) while the negative gate signal was fed to one of the LORI channels. For each TOE mode signal transmitted by the LORI, an independent oscilloscope time base was required; however, the maximum number of TOE channels used was only three (two spike trains and one stimulus). Occasionally two separable spike trains were recorded on a single electrode. One string of negative pulses was derived entirely from the larger spikes while the other string was derived from both the larger and smaller spikes. Thus one set of stored TOE's corresponded to the larger spikes only, but the other set of TOE's represented both the larger and smaller spikes. The TOE's corresponding to the smaller spikes were determined by executing one of the data analysis programs which simply formed an exclusive "or" operation on the two TOE data sets. In summary, data acquisition was achieved through the LORI which provided a channel through which continuous and TOE mode signals were transmitted to the central processor.

Having transmitted the data (TOE's, sample values) to the central processor (IBM 360/44) where it was stored in bulk memory (3 IBM 2314 Disk units), the next step was to analyze the data. Interaction with the computer during the analysis phase was made through the IBM 2250 display terminal via the light pen, keyboard, and function keys. It was located close to the LORI and had a 21 inch CRT on which the results of mathematical operations on the data and procedural information were displayed. All data sets

were identified by a name which was specified during the acquisition phase. Analysis of a data set was initiated by selecting an appropriate analysis algorithm from the library of analysis subroutines each of which corresponded to an appropriate function key.

For example, consider forming a PST histogram of the TOE's contained in the data set "SPIKE" which correspond to discharges, relative to the TOE's of the data set "STIM" which correspond to onsets of repeated stimulation. The first step would be to initiate the PST histogram algorithm by pressing the function key designated for this process. Subsequently, the PST process identification page would appear on the display unit CRT requiring the names of the data sets to be used in the algorithm. Display of the parameter identification page would follow after the dataset names SPIKE and STIM were supplied. After values for three parameters (minimum latency, maximum latency, bin width) were typed into the computer, execution of the process would begin. Upon completion, the computed histogram would appear on the CRT, and if any changes in the parameters were desired, they could be made and the computation restarted; or the process could be terminated if the desired information was revealed and a new one initiated. The diversity of the algorithm library and the interactive nature of the system made it a most powerful and flexible tool for revealing detailed information in neurophysiological data.

CHAPTER III

LIGHT EVOKED RESPONSES

Introduction

Considerable attention has been devoted to light evoked behaviors of arthropods [18, 36] and, in particular, insects [16, 24, 26, 49, 69]. These studies have helped to reveal the ability of the compound eye to utilize information in a light signal, but alone they have not elucidated the neural mechanisms responsible for vision. Numerous electrophysiological studies [4, 5, 32, 57, 73, 86] of single photoreceptor cells in the compound eyes of several insects have established their transducing properties, and recently electrophysiological studies [6, 7, 32, 53, 76] of the discharge behavior of a wide range of interneurons in the optic lobe of several insects have revealed some of the information handling properties of the compound eye on the cellular level. The research described in this thesis was a continuation of these efforts to understand the cellular mechanism of information processing in the compound eye of the fly. In particular, the study concentrated on the visual information processing properties of two second order units and their relationship to established neural structure.

The first part of this chapter is devoted to the efforts of others concerning the anatomy and electrophysiology of the first optic ganglion or lamina ganglionaris of flies. Following this is a

description of the discharge properties of two second order units recorded from the intermediate chiasma. The chapter concludes with an account of the results of experiments aimed at locating the origin of these discharges within the hierarchy of the visual nervous system.

Anatomy and Electrophysiology of the First Optic Ganglion

The compound eyes of dipterans consist of a large number of ommatidia (approximately 5500 in Calliphora erythrocephala), each of which contains eight photoreceptor cells [50, 79]. The axon of each photoreceptor cell passes through the basement membrane and enters the first optic ganglion. Two axons from each ommatidium corresponding to the superior and inferior central photoreceptor cells by-pass the first optic ganglion without making synaptic connections and terminate in the medulla or second optic ganglion. The remaining six photoreceptor axons originating from each ommatidium terminate in the first optic ganglion after undergoing a very specific geometrical transformation found only in the compound eyes of dipterans which have unfused rhabdomeres [9, 75, 77]. Corresponding to each ommatidium in the retina, there is a cartridge in the first optic ganglion, and the geometrical transformation is such that each of the six photoreceptor axons from a single ommatidium terminates in a different cartridge [9, 78]. Studies [41, 86] have shown that due to the unfused rhabdomeric structure of each ommatidium, the optical axes of all photoreceptor

cells, excluding the two central cells of each ommatidium, differ by an amount determined by the optics of the dioptric apparatus and the inter-rhabdomere spacing. In fact, the organization of the geometrical transformation and the optics of the compound eye are so specific that the axons of the six photoreceptor cells terminating in each cartridge correspond to photoreceptor cells in different ommatidia but which have coincident optical axes as schematically illustrated in figure 3.1a.

Associated with each cartridge are six primary photoreceptor axons (R_{1-6}), two second order type I monopolar cells (L_1, L_2), two second order type II monopolar cells (L_3, L_4), and two or more "centrifugal" fibers (α, β). The synaptology of the first optic ganglion [75, 77, 80] has not been completely established, but it is apparent that each of the two type I monopolar cells of each cartridge makes synaptic contact with all six of the terminating photoreceptor axons composing the crown of the cartridge. Furthermore, it is likely that synaptic interaction exists between the two type I monopolar cells of each cartridge and possibly between the type I monopolar cells of adjacent cartridges via the synaptic plexus. For each cartridge two sets of "centrifugal" fibers make synaptic contact with each of the six photoreceptor axons and the two giant monopolar cells. Actually, the directionalities of these synaptic contacts have not been adequately established, and the term "centrifugal" fibers has been used because their cell bodies are more centrally located. Furthermore, it is not known whether the

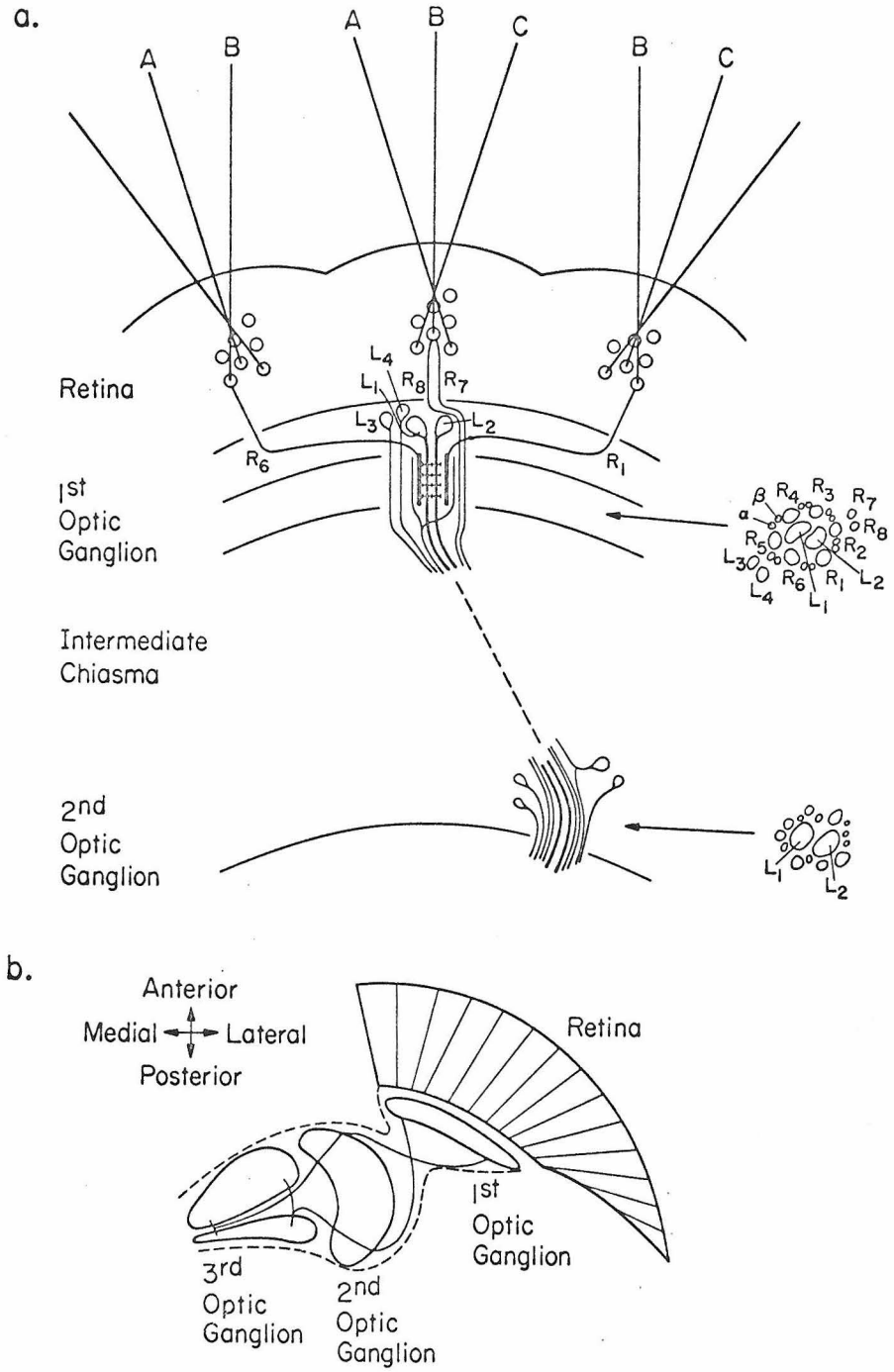

Figure 3.1 Schematic diagram of the relevant anatomical features of the optic lobe (a) Basic neural circuitry of the first optic ganglion R_i = photoreceptor #i, L_1, L_2 = type I monopolar cells, $L_3 L_4$ = type II monopolar cells, α, β = centrifugal fibers. (b) Gross morphology of the optic lobe.

"centrifugal" fiber systems associated with different cartridges are, in fact, independent or where the fibers originate. An additional complicating factor in the structure of the first optic ganglion is the presence of epithelial glial cells which send capitate projection into small invaginations of the photoreceptor axon membranes, thereby suggesting a function other than a merely nutritive or supportive role. Very little is known about type II monopolar cells except that they appear to be second order neurons and to send their axons around the cartridge rather than through it as the type I monopolar cells.

The two axons of the type I monopolar cells of a cartridge join the two by-passing long visual fibers and the two corresponding type II monopolar cell axons and make their way to the second optic ganglion where they terminate. The tract of fibers between the first and second optic ganglia formed from similar sets of fibers associated with each cartridge is called the intermediate chiasma. This tract of fibers undergoes a geometrical transformation illustrated in figure 3.1b which sends fibers belonging to medially located cartridges to posterior regions of the second optic ganglion and fibers belonging to laterally located cartridges to anterior regions of the second optic ganglion. This anatomical transformation represents a complete inversion along the medial-lateral axis of the compound eye; however, there is no alteration of the projection pattern along the dorsal-ventral axis. Within the intermediate chiasma the fibers entwine but generally remain organized into

small bundles corresponding to each cartridge. The highly structured organization of the first optic ganglion in terms of an array of cartridges is preserved in the second optic ganglion in terms of an array of columns. Each column receives its input in the form of a bundle of fibers corresponding to a particular cartridge.

Anatomically, the first optic ganglion is highly organized with enough complexity to conceivably support a considerable amount of integration. However, previous attempts to study its information processing properties through the observation of discharge activity from units in the first optic ganglion failed [6, 31, 56, 72], although, two types of slow potential changes were recorded with micropipettes from the first optic ganglion and were analyzed [56, 72, 74, 90]. In flies, positive slow potentials from the first optic ganglion were reported which had a waveform in response to a light pulse similar to that of the photoreceptor membrane potential change. These positive slow potential changes were believed to be of extracellular origin but closely related to the neural mechanisms of integration in the first optic ganglion. In fact, micro-spot stimulation experiments [72] indicated that a potential change could only be elicited by stimulating one or more of six ommatidia whose geometrical arrangement corresponded to the anatomical transformation such that the axon of a photoreceptor cell in each of the six effective ommatidia terminated in the same cartridge (which presumably generated the observed potential

change). In locusts, hyperpolarizing slow potential changes were recorded [74] which appeared to be of intracellular origin. It was reported that during the course of these slow potential experiments in the fly not one indication of a spike-like potential change was observed. This raises the serious question of how signals are communicated between the first and second optic ganglia (a distance of approximately 200 microns).

Spike Discharges in the Intermediate Chiasma

The answer to the question of communication and to the nature of neural integration occurring in the first optic ganglion was approached by recording extracellular discharge potentials from single fibers in the intermediate chiasma. Two classes of units, based on their discharge behavior to light pulses, were discovered. The average discharge pattern of a typical unit belonging to the first class (designated the on-off class) is shown in figure 3.2. The stimulus was a set of ten .5 second pulses of monochromatic light (λ = 471 mμ) each differing in intensity by 0.4 log units. The stimuli were delivered to the most sensitive part of the receptive field by the direct stimulating apparatus. The PST's were formed from 6 trials like the one shown in figure 3.3. It so happened that two units (one belonging to each class) were recorded simultaneously from the same electrode, however, only the TOE's of the larger on-off unit contributed to the PST histograms of figure 3.2.

The on-off unit was quiescent in the dark and exhibited truly

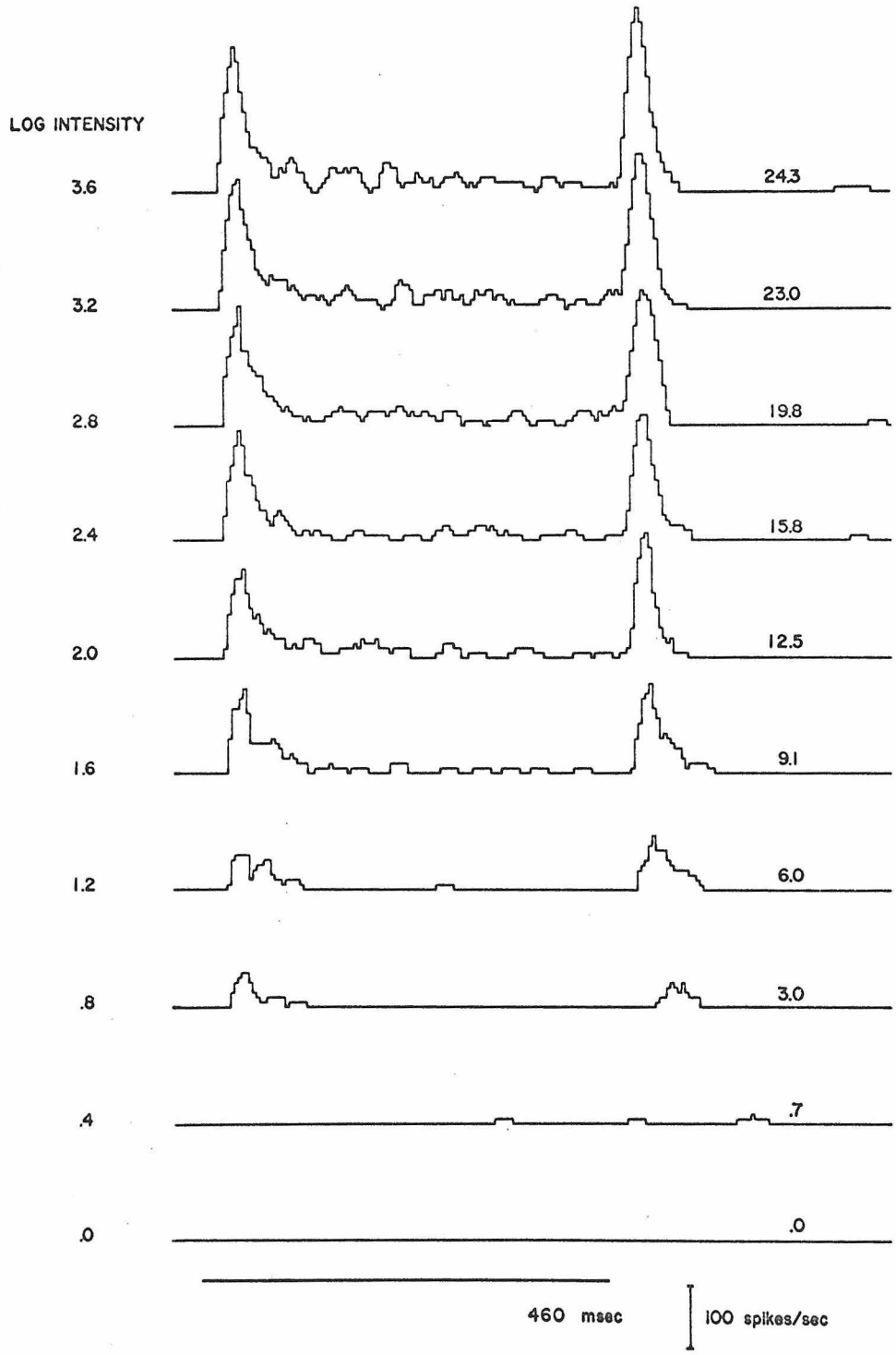

Figure 3.2 Multiple PST histograms of a typical on-off unit corresponding to different intensity stimuli. Right hand column of figures denote the average number of spikes/stimulus based on 6 trials. λ = 471 mμ. B. W. = 4 msec.

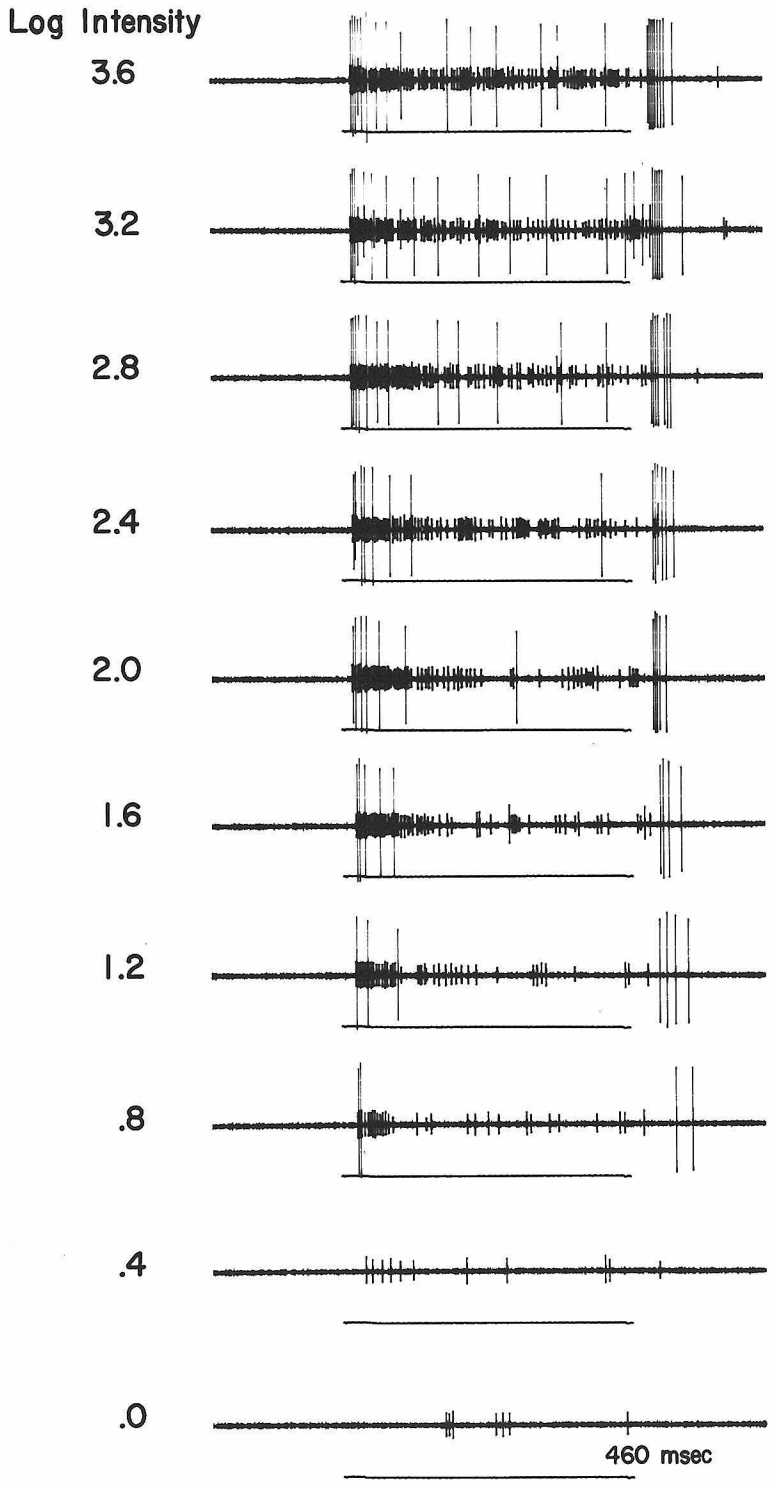

Figure 3.3 Typical discharge of both units to increasing stimulus intensities

on-off discharge behavior for light stimuli having intensities within one log unit of threshold. At higher levels of light intensity the on discharge became more prolonged and lasted the length of the stimulus duration (460 msec). However, the on-off unit did not produce a maintained discharge to sufficiently intense stimulation, for steady light stimulation at intensity levels up to six log units above threshold was ineffective in eliciting a maintained discharge.

Higher levels of light intensity did not affect the on and off discharge in the same fashion. More intense stimulation caused the on discharge to reach higher instantaneous discharge rates and to exhibit activity over longer periods of time, never to reach sustained activity; whereas the off discharge responded to more intense stimulation with greater instantaneous discharge rates but without any appreciable effect on the time course of the off discharge. This is in contradistinction to the nature of the off discharge from on-off units in some vertebrate retinas, where more intense stimulation causes successively longer delays and durations of the off discharge [63, 64, 65].

The dependence of the on-off unit response magnitude, defined as the total number of spikes elicited by a half second pulse of light, on the intensity of the stimulus is shown in figure 3. 4. Curves a and b were fitted to the data by hand and represent the response-log intensity relation for two units. These two units were chosen because their response-log intensity relationships enclosed all others (i. e.,

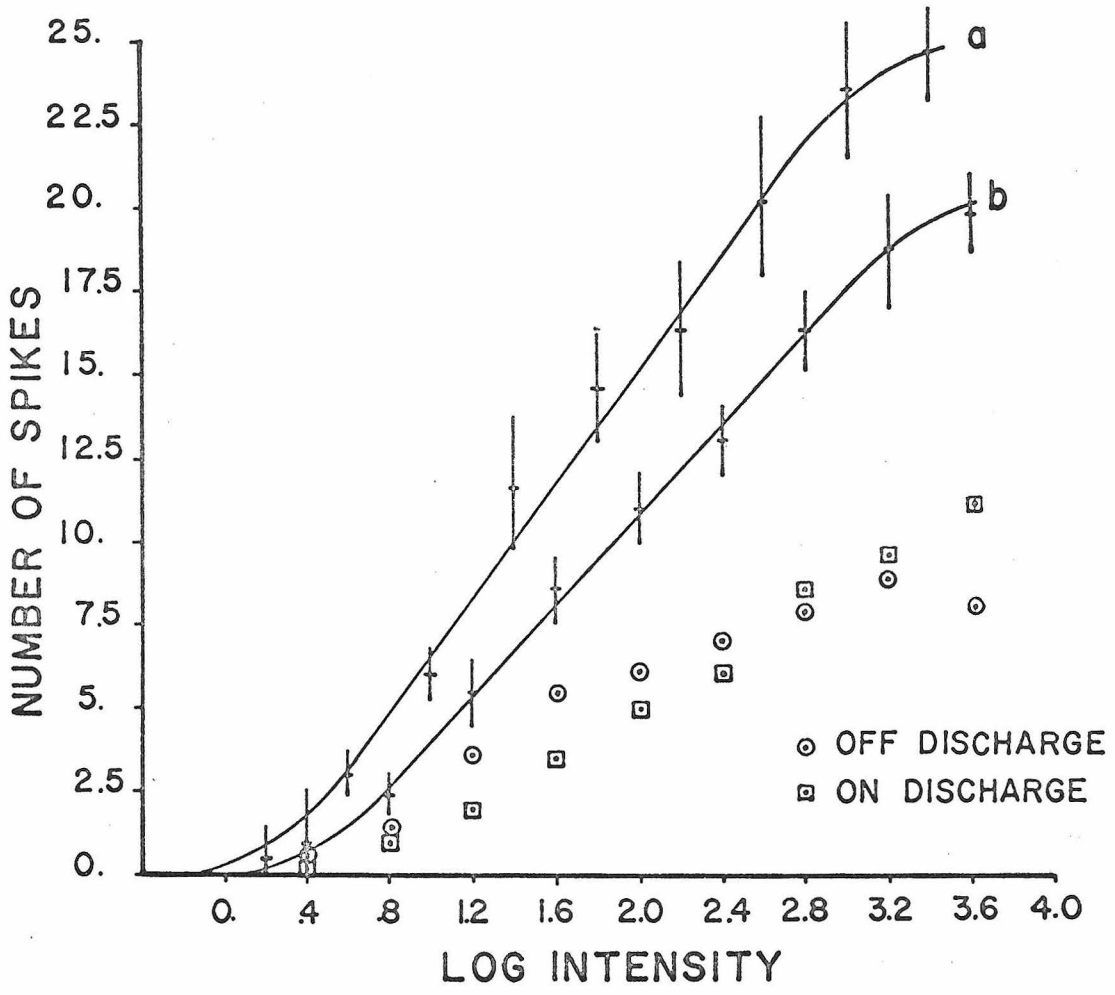

Figure 3.4 Typical response-log intensity characteristics of the on-off unit. The mean (and ± 1 S.D.) numbers of spikes elicited by 460 msec. light pulses are plotted against the relative stimulus intensities. (λ = 471 mμ). The characteristics of the two on-off units (a, b) represent response-log intensity extremes. ⊡ = number of <u>on</u> discharges ⊙ = number of <u>off</u> discharges.

the response-log intensity relationships of all on-off units studied fell within the limits defined by curves a and b). The response magnitude points represent means calculated from seven trials at each stimulus intensity and are plotted with error intervals corresponding to ± one standard deviation. The response-log intensity relationship has a linear region corresponding to small stimulus intensities followed by a log-linear region extended over approximately 2.5 log units of stimulus intensity and ending with a region of saturation approximately 4 log units above threshold. Also shown in figure 3.4 are typical data points corresponding to the magnitude of the on discharge (defined as the number of spikes elicited during the stimulus) and the off discharge (defined as the number of spikes elicited after the cessation of the stimulus) as a function of the stimulus intensity. The threshold response was generally found to be an on discharge, but as the stimulus intensity was increased, the magnitude of the off discharge increased more rapidly. However, the dynamic range of the magnitude of the on discharge was greater due, probably, to the appearance of sustaining type discharge at higher intensity levels.

Units belonging to the second class were called on-maintained units. The average discharge behavior of a typical unit to the same stimulus program as presented to the on-off unit is shown in figure 3.5. In fact, the stimulus used to elicit discharge from the on-off unit of figure 3.2 was exactly the same as that used to elicit discharge from the on-maintained unit of figure 3.5, for both units were

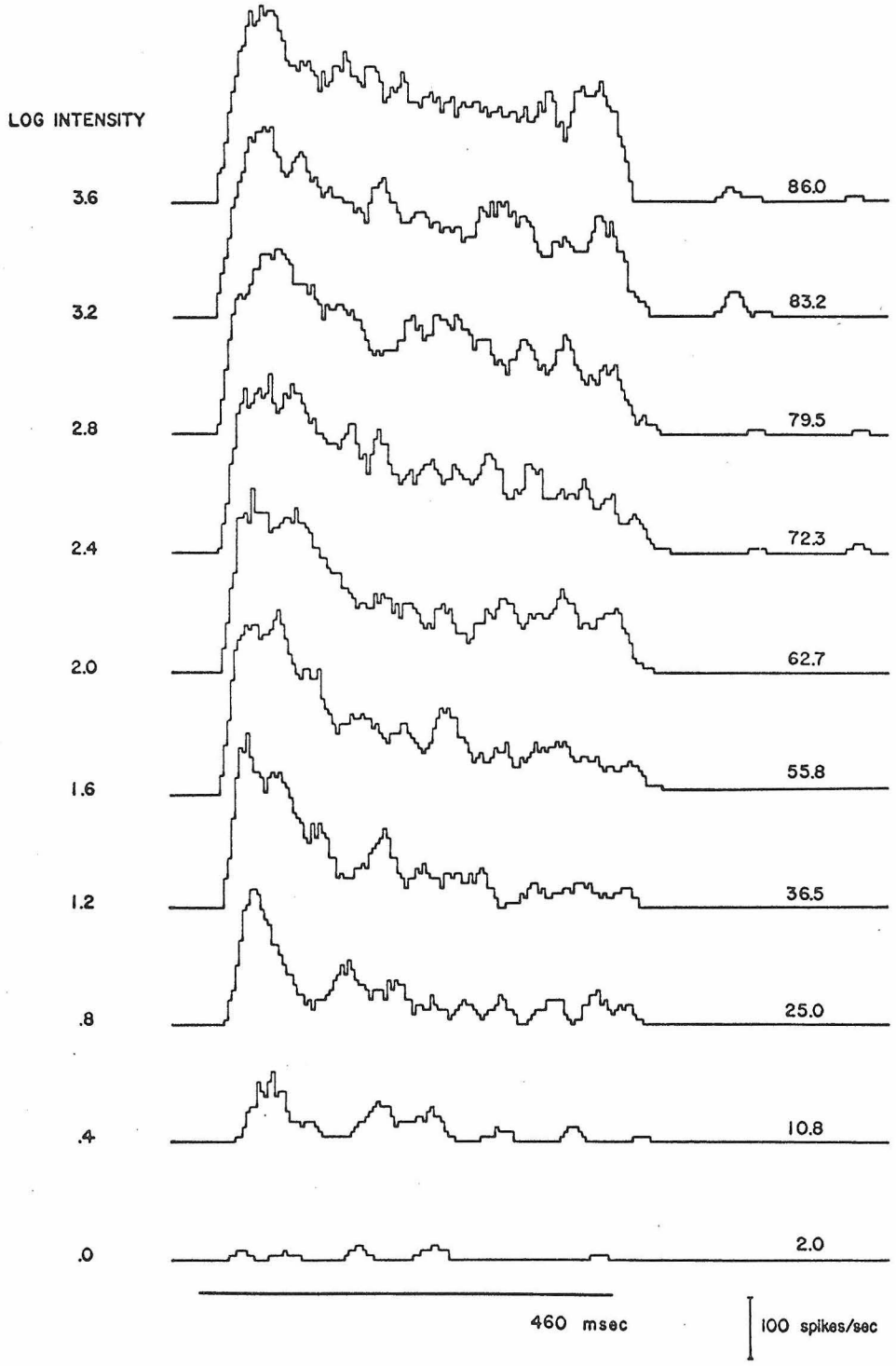

Figure 3.5 Multiple PST histograms of a typical on-maintained unit corresponding to different stimulus intensities. Right hand column of figures denote the average number of spikes/stimulus based on 6 trials. λ = 461 mμ B.W. = 4 msec.

recorded simultaneously. A sample stimulus trial is shown in figure 3. 3. The TOE's representing the smaller on-maintained spike potentials were obtained as described in the data analysis section of Chapter II. The average discharge behavior of the on-maintained unit differed considerably from that of the on-off unit. If the stimulus was centrally located in the receptive field, then it elicited discharges throughout the duration of the stimulus but "not" afterwards. In the dark the unit was also quiescent, and for low stimulus intensities, it had a large transient component and a smaller steady state component. As the stimulus intensity increased, the instantaneous discharge rate of both components increased to saturation, however, the steady state component seemed to be influenced more. In steady illumination the on-maintained unit discharged continuously.

The dependency of the on-maintained unit response magnitude on the intensity of stimulation is shown in figure 3. 6. Here, as before, two units representing extreme cases were plotted. Although the maximum response magnitude (number of spikes elicited) of the on-maintained unit was approximately four times higher than that of the on-off unit, the forms of their response-log intensity relationship were similar.

There were other significant differences between the two classes of units besides the form of their discharge behavior. Frequently examples of both classes of units were recorded simultaneously with one microelectrode as shown in figure 3. 3. In all such cases, the size of the on-off unit spike potential was greater than

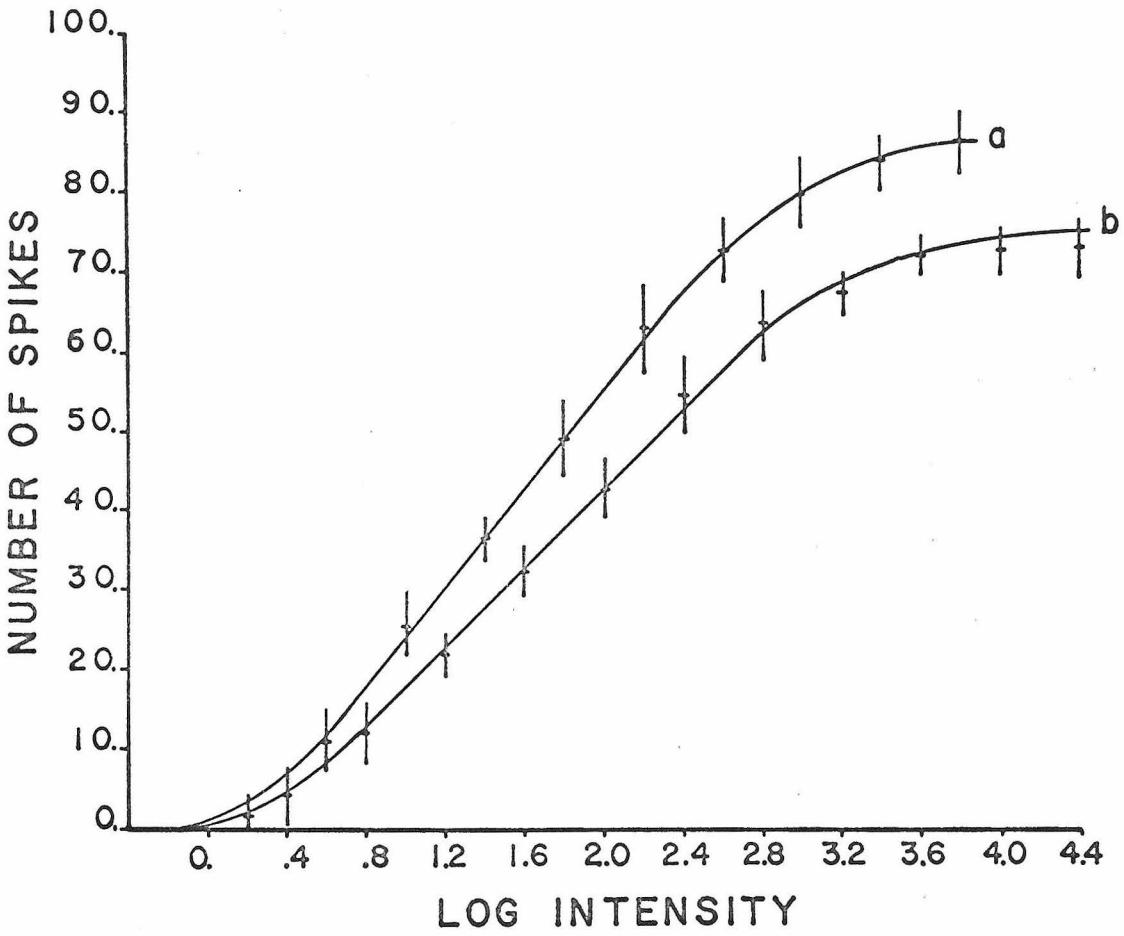

Figure 3.6 Typical response-log intensity characteristics of the on-maintained unit. The mean (and $\pm$ 1 S. D.) numbers of spikes elicited by 460 msec. light pulses are plotted against the relative stimulus intensities (λ = 471 mμ). The characteristics of the two on-maintained units (a, b) represent response-log intensity extremes.

that of the on-maintained unit. In fact, the size of the on-maintained unit spike potential never exceeded 200 μv in any preparation; whereas the on-off unit was seldom observed having spike potentials less than this. The on-off unit was more readily studied, not because there was necessarily a higher percentage of them, but because the relatively larger size of their spike potentials made them easier to detect and isolate. The relative number of units of each class studied (on-off units $\{94\}$, on-maintained units $\{67\}$) did not accurately indicate the true proportion of each class existing in the chiasma, for frequently discharges of on-maintained units could be recognized in the background noise, but they could not be sufficiently isolated to permit study. Simultaneous records from one microelectrode, as in figure 3. 3, were most often obtained when recording an exceptionally large on-off unit spike. In such cases, one or more on-maintained units could be observed having their receptive fields overlapping the receptive field of the on-off unit which implied that they were physically close together. However, there were also occasions when two on-maintained or two on-off units were recorded simultaneously. The two simultaneously recorded units in figure 3. 3 had nearly coincident receptive fields, and the stimulus was supplied approximately midway between the centers of the two receptive fields. The records revealed that the on-maintained unit was approximately 0. 8 log units more sensitive to this stimulation. The difference between the relative thresholds of on-off and on-maintained units was a characteristic distinction, and relative threshold determinations at the

receptive field centers revealed an average difference of 1.2 log units with the on-maintained unit being more sensitive.

Origin of Discharges

To ascertain the origin of the spike potentials recorded from the intermediate chiasma, a series of experiments were performed in which micropipettes were inserted into the first optic ganglion of isolated head preparations. On two occasions spike potentials were recorded extracellularly in response to light stimulation. Although both records were short and of poor quality, they nevertheless indicated, contrary to the observations of others [56, 72], that spike potentials existed in the first optic ganglion, and the discharge patterns elicited by pulses of light were similar to those of the on-maintained unit and clearly different from those of the on-off unit. In fact, there was no on-off type behavior in the slow potentials recorded from the first optic ganglion.

Two distinctly different types of slow potentials were recorded from the first optic ganglion. One type was characterized by hyperpolarizing potentials. A family of hyperpolarizing potential changes elicited by a sequence of one-half second light pulse of successively greater intensity is shown in figure 3.7. The hyperpolarizing potential was normally initiated from a negative resting potential of 20-30 mv. The existence of a resting potential and the ease with which the response was lost suggested that the potential was of intracellular origin which agreed with the conclusion of Shaw [74]. The

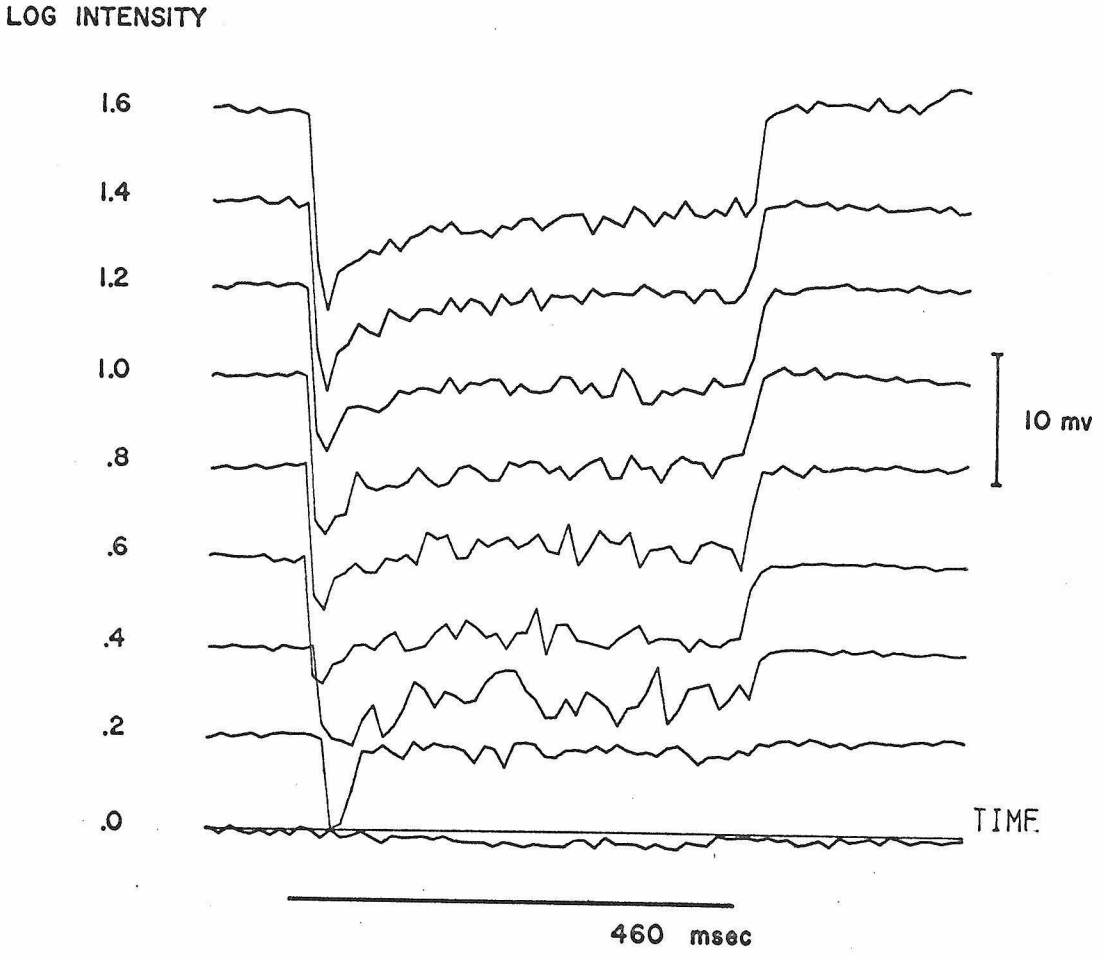

Figure 3.7 A series of typical hyperpolarizing slow potential changes recorded from the first optic ganglion in reponse to different stimulus intensities λ = 471 mμ Sampling rate = 100 samples/sec.

most notable feature of the potential change besides its hyperpolarization was the extremely noisy nature of the response for stimulus intensities near and moderately above threshold. More intense stimulation than shown in the figure caused the potential to saturate, and the waveform became smooth and in some cases less negative.

Much more frequently, positive slow potential changes were recorded by micropipettes in the first optic ganglion. These potentials were extraordinarily stable and did not appear to be associated with a resting potential. Typical responses of this type of slow potential to a sequence of increasing stimulus intensities are shown in figure 3.8. For the range of light intensities used, the magnitude of the polarization never exceeded 40 mv and rarely 30 mv. These factors implied that the potential was of extracellular origin which was the conclusion held by Mote [56] concerning similar potentials recorded from the first optic ganglion of another species of fly. Scholes [72] did not commit himself but held that the potentials represented cartridge integration, for he claimed to show that the potential could only be elicited by stimulating any one of six ommatidia in the characteristic trapezoid configuration. More will be said about the information transmitted by these slow potentials in later chapters, but within the scope of these experiments, it was apparent that slow potentials having <u>on-off</u> characteristics either were difficult to record or were not present in the first optic ganglion. When compared to the waveform characteristics of the two

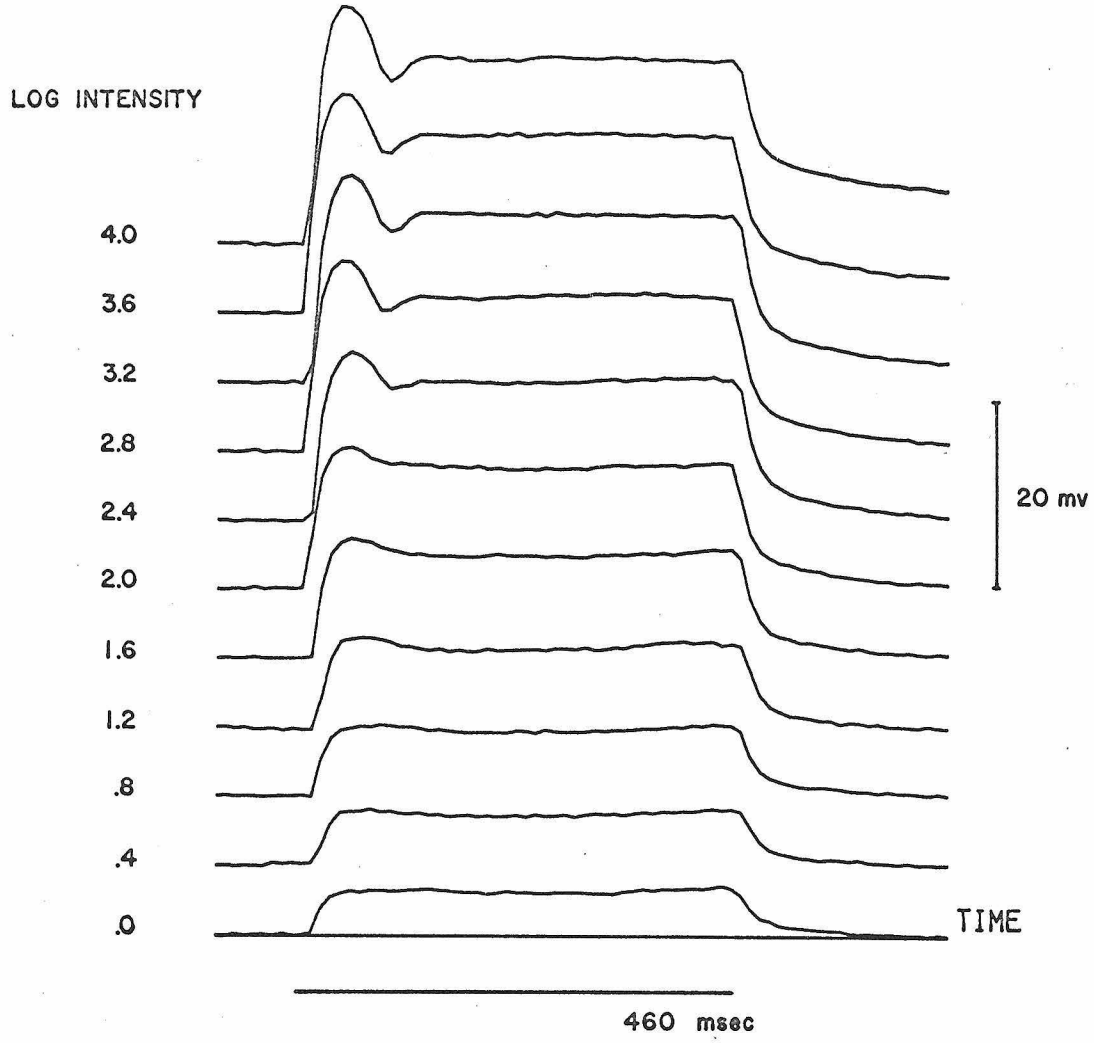

Figure 3.8 A series of typical positive slow potential changes recorded from the first optic ganglion in response to different stimulus intensities. λ = 471 mμ. Sampling rate = 100 sample/sec.

types of slow potentials, the average discharge characteristics of the on-maintained unit of figure 3.5 seemed to more closely resemble that of the positive slow potential, although both had a transient and static on response.

Several investigators [6, 7, 31, 53, 76] have studied the discharge properties of higher order neurons in the second and third optic ganglia of insects and have observed that on-off discharge behavior to transient stimulation was quite prevalent. A series of experiments was performed to determine whether it was possible to record the chiasma on-off unit in the second optic ganglion. Initially, it was thought to be possible, for a unit with similar on and off discharge characteristics was recorded. However, more detailed studies of this unit disclosed that although it responded with an on and off discharge, it was not the on-off unit found in the intermediate chiasma, but rather a higher order unit with a larger receptive field. The average discharge behavior of this unit to a stimulus series of increasing intensity is shown in figure 3.9. Its similarity to the average discharge characteristics of the on-off unit is apparent, but closer examination reveals that its off discharge is more prominent. These results and those to be discussed suggested that on-off discharge was indeed prevalent in the second optic ganglion and that the successfully isolated units were not responsible for the discharge of the on-off unit found in the intermediate chiasma.

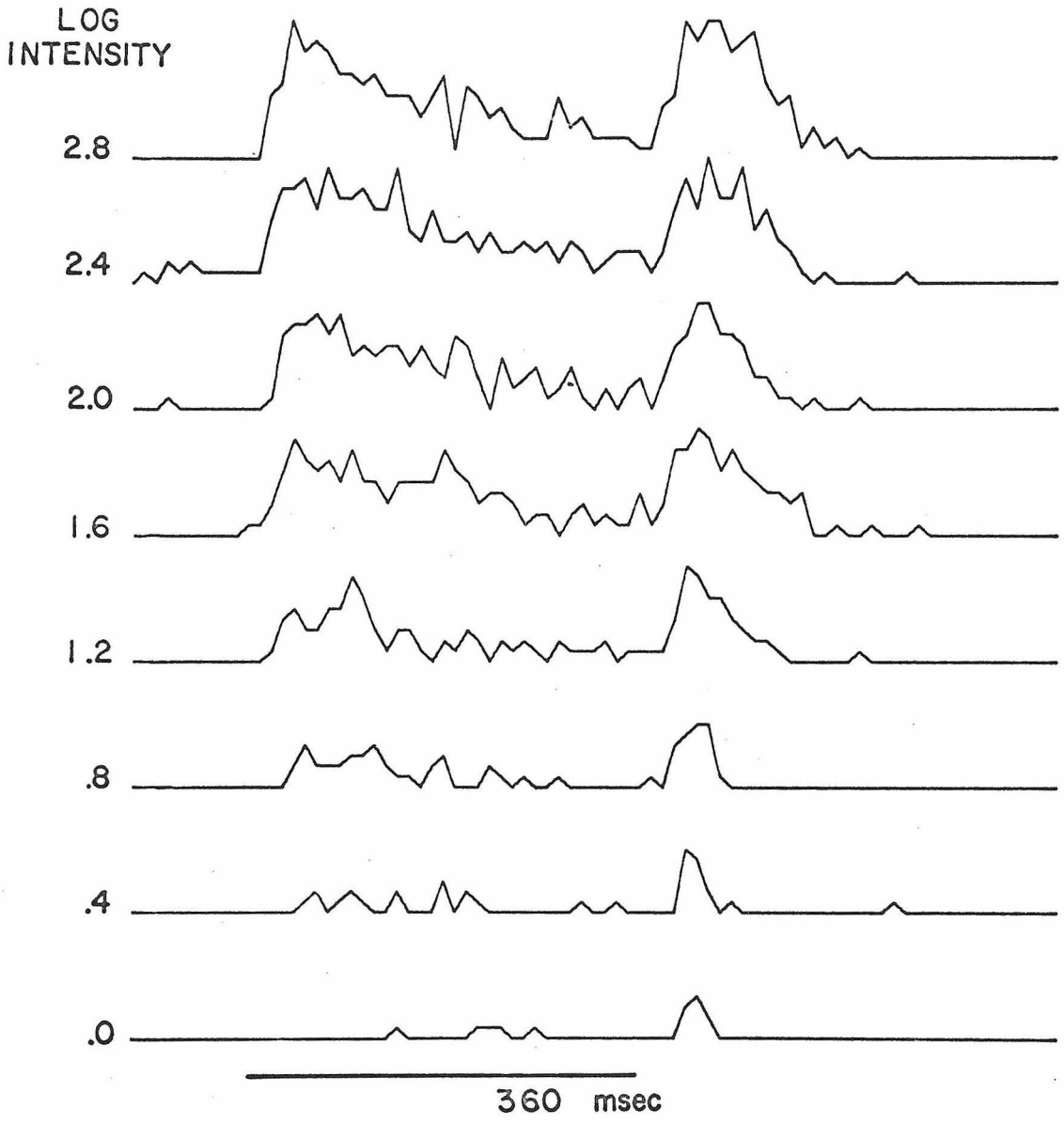

Figure 3.9 Multiple PST histograms of a typical medulla on-off unit corresponding to different stimulus intensities λ = 471 mμ. B.W. = 10 msec.

The spike discharges and slow potentials elicited by stimulus sequences of increasing intensity were also analyzed in terms of their response latency so that a temporal ordering of units could be established. Response latency for spike discharges was defined as the time between the stimulus initiation and the occurrence of the first spike, and for slow potentials, it was defined to be the time between the initiation of stimulation and the moment the slow potential reached one-half of its maximum value. Strictly speaking, the temporal order of two responses could not be determined unless the two responses were recorded simultaneously which was possible for several unit combinations. However, a first approximation to the temporal order was possible by plotting the response latency - log intensity relation for the different units recorded separately. Response latency - log intensity curves are plotted in figure 3.10A for both types of slow potentials, the on-off and on-maintained units. The response latency - log intensity curves for the slow potentials were plotted separately because they were not comparable to the curves derived from spike discharge since more intense stimulation was required and the latency definition differed. Since the hyperpolarizing potential reached saturation more rapidly than did the positive slow potential, only a small number of response latencies were determined; however, the latency points suggested that the positive slow potential was primary with respect to the hyperpolarizing slow potential. These data,

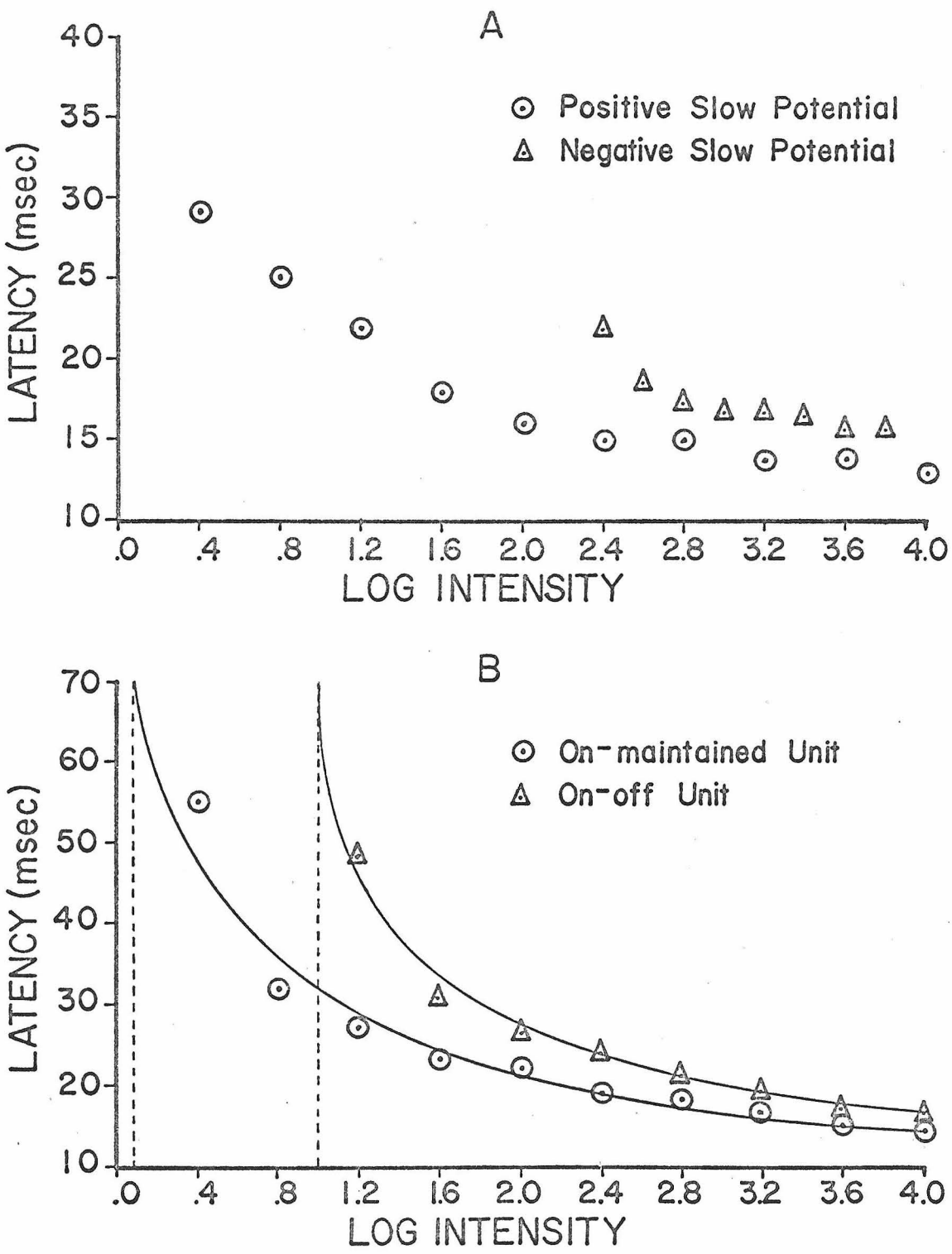

Figure 3.10 Typical response latency-log intensity curves (A) Response latency-log intensity curves for the slow potentials of the first optic ganglion (B) Response latency-log intensity curves for simultaneously recorded on-off and on-maintained units. The dashed lines represent asymptotes set by the response thresholds.

however, were not sufficient to conclude that one potential was primary to the other, but they did establish the time scale of these responses. Scholes [72] made a similar comparison between photoreceptor potential latencies and the latencies of positive slow waves recorded from the first optic ganglion and reported an average latency difference of 1.5 msec.

The response latency - log intensity curves for the on-maintained and on-off units (figure 3.10B) were derived from latency measurements taken from simultaneous records. The latency of the on-maintained unit was always shorter than that of the on-off unit, and the latency difference decreased to 1.5 msec. as the stimulus intensity increased. The dashed vertical lines in figure 3.10B represent asymptotes set by the threshold of each unit. Although not shown in figure 3.10, response latency - log intensity curves were also derived from simultaneously recorded on-off units and directional selective motion detection units (IIAin). The stimulus, in this case, was a sequence of moving striped patterns ($\lambda = 8^{o}$) subtending approximately 60 degrees and having increasing intensity levels. Since the IIAin unit had a lower threshold, its response latency - log intensity curve was not unlike that of the on-maintained unit relative to the on-off unit, except that at higher stimulus intensities, the IIAin unit had a slightly larger latency than did the on-off unit. On one occasion the medulla on-off unit was recorded simultaneously with the on-off unit using two

microelectrodes, and the on-off unit discharge preceded the discharge from the medulla on-off unit by 8 msec for the on response and 1 msec for the off response.

To ascertain the origin of spikes of the on-off and on-maintained units, experiments were performed which involved changes in the location of the microelectrode placement and surgical alterations of the optic lobe prior to recording responses. The intermediate chiasma can be partitioned into two parts; the extramedullar portion formed by pre-chiasmatic and chiasmatic fibers and the intramedullar portion of post-chiasmatic fibers. Most recordings of the on-off and on-maintained units were made from the peripheral intramedullar region. However, both classes of units were also recorded in penetration near the second optic ganglion. It was also possible to record without great difficulty both classes of units in the extramedullar region of the intermediate chiasma near the first optic ganglion. Several experiments were performed in which the microelectrode was inserted into the intermediate chiasma after the second and third optic ganglia were surgically removed. In such preparations, discharges from both the on-off and on-maintained units were observed. Apparently, removal of the second optic ganglion affected the on-off unit, for considerable light intensity was required to elicit an on-off discharge which usually consisted of only one or two spikes at initiation and cessation of the stimulus.

Anatomical studies [75, 77, 80] have revealed that the intermediate chiasma consists of bundles of axons ensheathed by glial cells. Each bundle of fibers links a cartridge in the first optic ganglion with a column in the second optic ganglion as schematically illustrated in figure 3.1. Within the extramedullar portion of the intermediate chiasma, each bundle is composed of two type I monopolar axons, two type II monopolar axons, two long visual fibers (superior and inferior central photoreceptor axons) and two centrifugal fibers. Bundles within the intramedullar portion of the intermediate chiasma consist of two large fibers (3-4μ) packed together with approximately ten medium to small fibers (.5-1μ). The two large fibers which are in close apposition throughout the chiasma were identified by Trujillo-Cenoz [80] to belong to the two type I monopolar cells of each cartridge. The photomicrograph in figure 3.11 of an oblique section through the intramedullar portion of the intermediate chiasma reveals the prominence of these two fibers and the periodic order of the second optic ganglion. The medium and small fibers of the bundle in addition to accounting for the fibers identified in the extramedullar portion of the intermediate chiasma also represent third order fibers originating from cell bodies of unipolar neurons concentrated in the intramedullar portion of the intermediate chiasma.

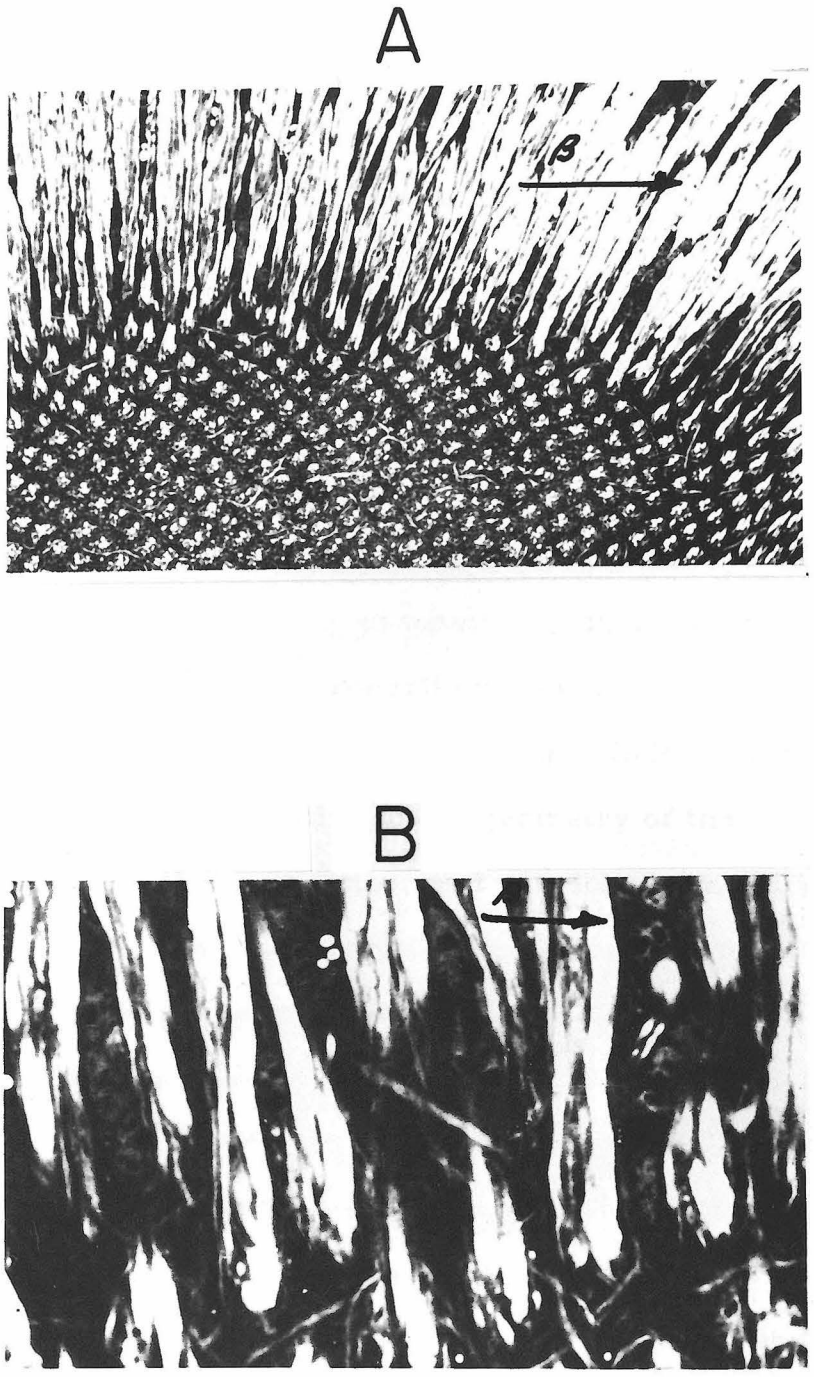

Figure 3.11 Photomicrographs of the intermediate chiasma as it enters the second optic ganglion (A) Oblique section revealing the regularly spaced chiasmic bundles (arrows) entering the second optic ganglion (B) Higher magnification of A. (Courtesy of O. Trujillo-Cenoz [80]).

CHAPTER IV

DIRECTIONAL SENSITIVITY AND RECEPTIVE FIELD ORGANIZATION

Introduction

In the last chapter, the temporal properties of the discharge behavior of the on-off and on-maintained units were presented and considerable temporal processing was found to take place between these units and the photoreceptor cells. Another important aspect of the information processing properties of these units is the way they respond to the spatial properties of the light stimulus. Questions pertaining to the shape of the receptive fields, the locations of the receptive fields relative to the geometry of the compound eye, the directional sensitivities, and possible forms of interaction between stimuli within the receptive fields are of prime importance in understanding the functional roles played by these units and how they are related to other electrophysiological and anatomical units.

This chapter describes the results of a series of experiments designed to determine the configuration of the receptive fields of the on-off and on-maintained units and their directional sensitivity for comparison with those established for other units. Also reported are the results of experiments utilizing light patterns of moving stripes for the purpose of evaluating the effect of motion on the organization of the receptive fields. Regions of antagonistic

interaction were found within the receptive field of the on-maintained unit, and the results of experiments examining this interaction are described. The chapter concludes with an account of some of the receptive field properties of other units discussed in the previous chapter.

Receptive Field Organization of the On-Off and On-Maintained Units

Several investigators [6, 7, 31] have reported on the size and shape of receptive fields of a variety of units recorded in the second and third optic ganglia. Although their measurements were valuable in determining receptive field shapes and for comparing the relative sizes of receptive fields when more than one unit were measured in the same way, the measurements do not allow a strict comparison with the results of others since sensitivity measurements were not used. It is important to specify receptive field size, particularly of first and second order units, in terms of their directional sensitivities, for this type of measurement is independent of the experimental conditions (viz., intensity of test light stimulus). The directional sensitivity of a photoreceptor is equivalent to its directional absorption function (i.e., the half directional sensitivity angle equals the acceptance angle). Consequently, directional sensitivity measurements are strictly comparable which makes it possible to contrast the directional sensitivity measurements made in this study with like measurements made elsewhere using different signals.

Before the directional sensitivities of the on-off and on-maintained units were established, however, two series of experiments were performed to determine the receptive field geometry of both units. The first series of experiments was performed using the reflecting sphere stimulus environment, and the stimulus program consisted of the sequential presentation of a 1.5 degree circular spot of "white" light for 460 msec. centered at each of the 77 grid points of an 11 by 7 grid having a 1.5 degree grid point spacing. The on-off and on-maintained units were recorded simultaneously, and the intensity of the spot stimulus was fixed to elicit a "respectable" response from the on-off unit yet not drive the discharge of the on-maintained unit into saturation. Figures 4.1 and 4.2 show the results of one such experiment. The raw data in figure 4.1 and the number of <u>on</u> and <u>off</u> discharges tallied in figure 4.2 for both units were arranged in an array corresponding to the location of the stimulus that evoked them, and contour lines were drawn in figure 4.2 to connect points of approximately equal magnitude of response (total number of <u>on</u> and <u>off</u> spikes).

There were several interesting features in these data. The on-off unit responded in its typical transient discharge form regardless of the position of stimulation within its receptive field. A total of eight receptive field geometry experiments were performed, and in all, the general receptive field configuration of the on-off unit was elliptical with its major axis tilted 10-20 degrees with respect

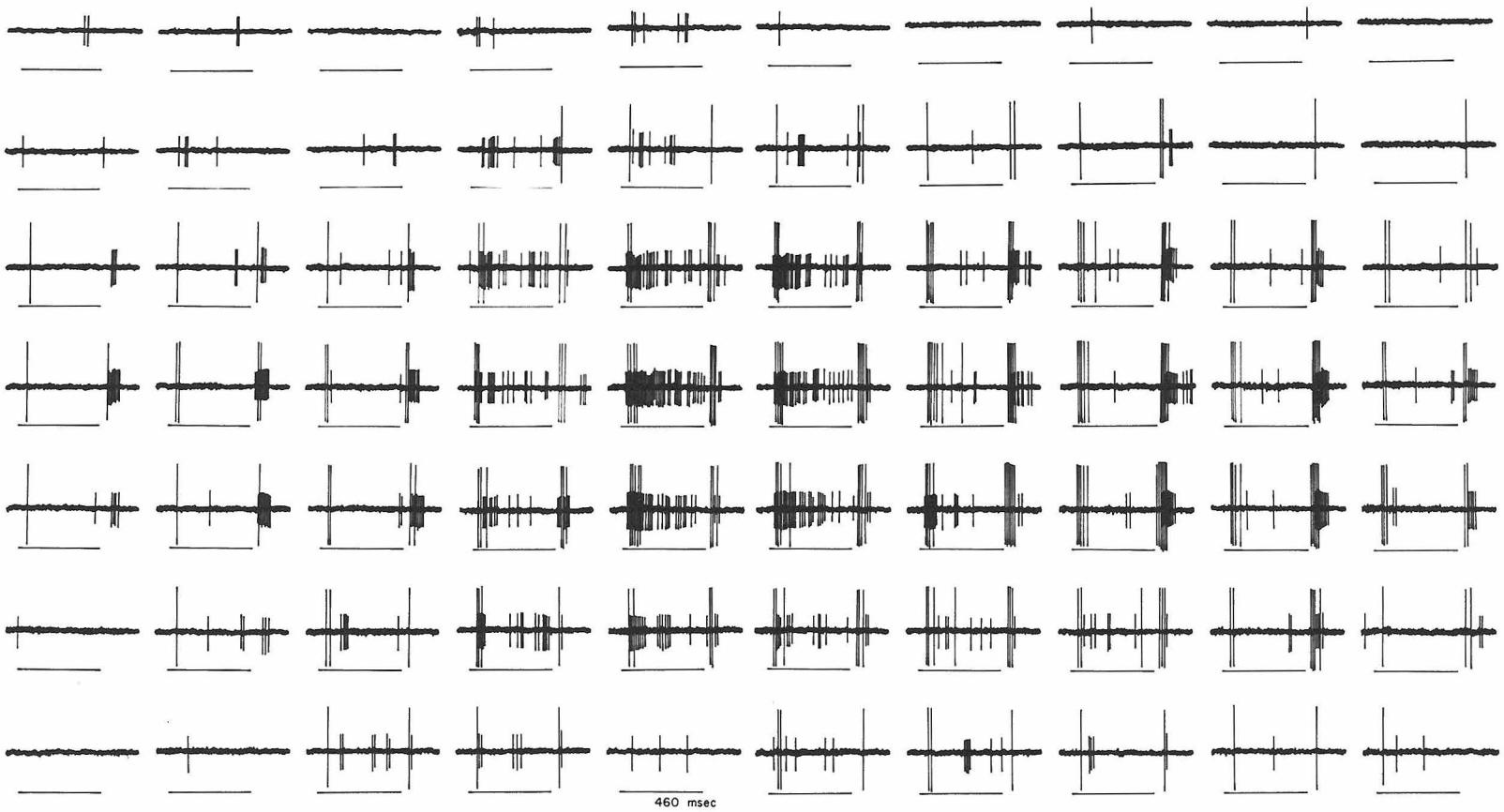

Figure 4.1 Simultaneous discharge of an on-off and on-maintained unit as a function of stimulus location. Each discharge was elicited by a 1.5° spot illuminated for 460 msec. The spot was sequentially placed at each grid point of a 7x11 grid (the right hand column has been omitted from this figure) with a 1.5° grid point spacing. The discharges are arranged in order corresponding to the position of the stimulus that evoked them.

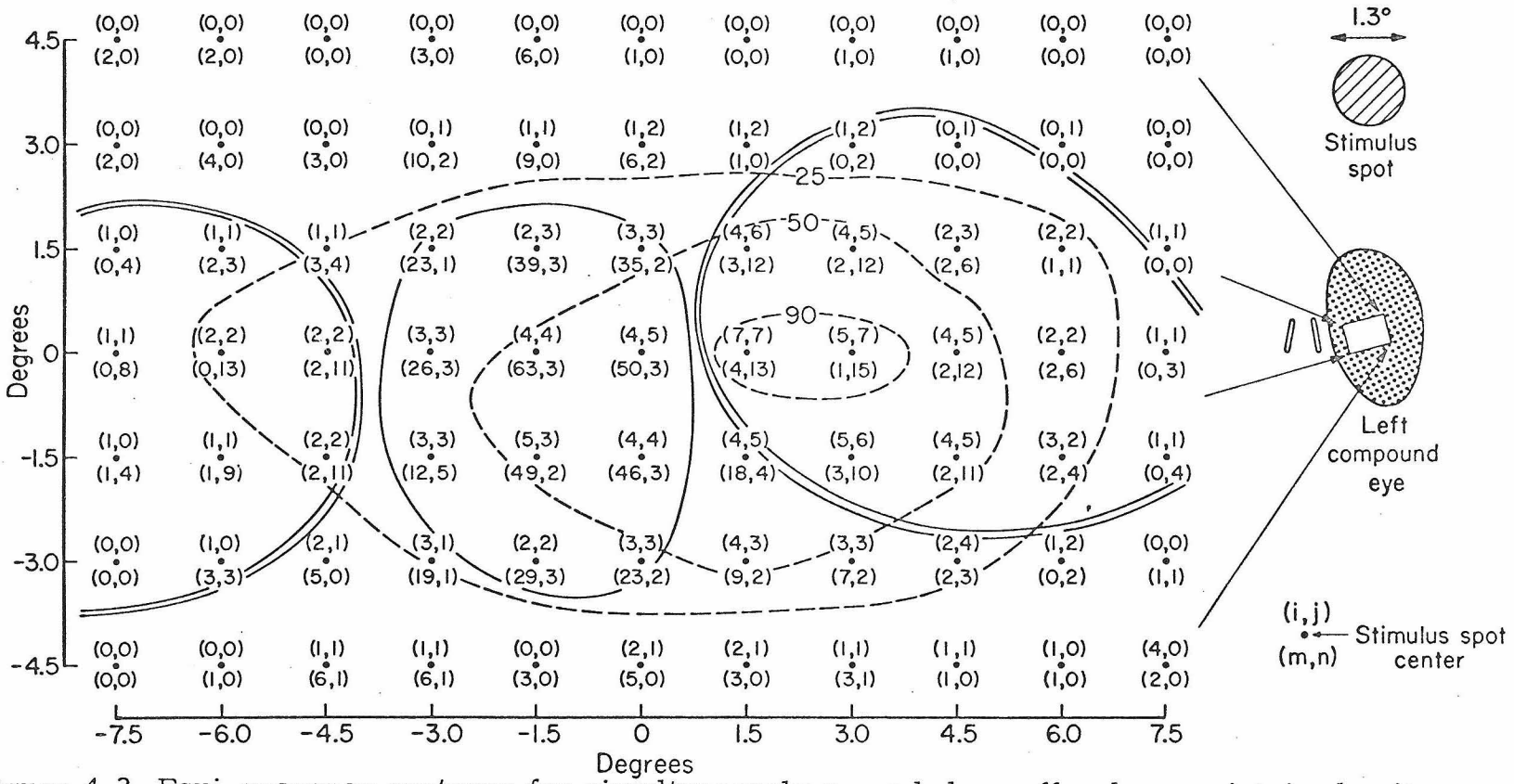

Figure 4.2 Equi-response contours for simultaneously recorded on-off and on-maintained units i = number of on discharges from the on-off unit, j = number of off discharges from the on-off unit, m = number of on discharges from the on-maintained unit, n = number of off discharges from the on-maintained unit. Dashed contours inclose receptive field from which on-off unit responses greater than the specified percentage of the maximum response could be elicited. Single contour roughly incloses the on region of the on-maintained unit. Double solid contours inclose the off regions of the on-maintained unit.

to the medial-lateral axis of the eye. Within the elliptical receptive field, the position of maximum sensitivity was usually not found to coincide with the center of the ellipse which gave the receptive field a skewed appearance as evidenced by the contours. In all cases, the skew was in the same direction (i. e., the receptive field extended farther medially from the center than it did laterally). It should also be noticed that the receptive field of the on-off unit approximately overlapped that of the on-maintained unit.

Whereas the discharge pattern of the on-off unit remained unchanged except in magnitude as different parts of its receptive field were stimulated, the discharge pattern of the on-maintained unit was dependent upon the part of the receptive field being stimulated. The raw data in figure 4. 1 and the contours in figure 4. 2 reveal two roughly circular regions on opposite sides of the center on region which when stimulated elicited an off discharge only. In all observations of the on-maintained unit, off discharge was elicited only from two specific areas on opposite sides of the on region along a line making a 10-20 degree angle with the medial-lateral axis of the eye. In other words, the major axis of asymmetry of the on-maintained unit receptive field corresponded roughly with that of the on-off unit receptive field. The on region from which the on-maintained response was elicited was also roughly oval and slightly smaller than the adjacent off regions, but its response dominated and characterized the unit. Taking into

consideration the spot size and the dominance of the on region, the separation between the centers of the on and off regions was 3-4 degrees. The PST histograms of the on-maintained unit in Chapter III were derived from on region stimulation only.

The second series of experiments was performed to determine how the on-off and on-maintained units responded to moving patterns of light and to obtain some idea of their half sensitivity angles based on their response to moving uniform striped patterns. However, an account of the experimental rationale of the experiment will be given before the experimental results are described. Consider the case of a photosensitive device which gathers light from different directions in 3-space according to

$$S(\theta, \phi) = \text{Exp} - 4\text{Ln}2\left[\left(\frac{\theta}{\alpha_\theta}\right)^2 + \left(\frac{\phi}{\alpha_\phi}\right)^2\right] \qquad (1)$$

where α_θ and α_ϕ represent the acceptance angles in the θ and ϕ directions, respectively. If a sinusoidal light intensity pattern moving with constant velocity (v) in the θ direction and represented by

$$I(\theta, t) = I\left\{1 + m\text{Sin } 2\pi(f_c t + \frac{\theta}{\lambda})\right\} \qquad (2)$$

where

m	=	contrast ratio
I	=	background illumination
λ	=	spatial wavelength of pattern (deg.)
f_c	=	contrast frequency (c/s)

and $$v = \lambda f_c \tag{3}$$

is presented to the photosensitive device, then the total light flux gathered by the device is the following:

$$F_\theta(t) = \frac{\pi \alpha_\theta \alpha_\phi I}{4 \text{Ln}2} \left\{ 1 + m\text{Exp}\left[- \frac{\pi^2}{4 \text{Ln}2} \left(\frac{\alpha_\theta}{\lambda}\right)^2 \right] \text{Sin}\, 2\pi f_c t \right\} \begin{matrix} \text{motion in the} \\ \theta \text{ direction} \end{matrix} \tag{4}$$

$$F_\phi(t) = \frac{\pi \alpha_\theta \alpha_\phi I}{4 \text{Ln}2} \left\{ 1 + m\text{Exp}\left[- \frac{\pi^2}{4 \text{Ln}2} \left(\frac{\alpha_\phi}{\lambda}\right)^2 \right] \text{Sin}\, 2\pi f_c t \right\} \begin{matrix} \text{motion in the} \\ \phi \text{ direction} \end{matrix} \tag{5}$$

It is theoretically possible to determine α_θ and α_ϕ by measuring the magnitude of the sinusoidal component of the light flux as a function of λ. This approach has been used by others [20, 26, 51, 52, 81] in modified form to determine properties of insect vision from measurements of optomotor torque or photoreceptor potential instead of total light flux. Since the experimental measurements (flight torque, photoreceptor potential, unit discharge rate) utilized were not the result of a linear transformation on the total light flux signal, the theory can not be strictly applied; however, it has been a useful first approximation measurement.

The experiments were performed using the reflecting sphere environment by alternately presenting a pattern of stripes of wavelength λ moving along the major axis of the receptive field then along the minor axis until a series of 12 stimulus presentations in each direction was completed. The duration of the stimulus was 2.6 seconds, and the pattern was circular and subtended 50-60 degrees of visual

field. The stimulus source was designed so that stripe edges always appeared at the same location when the stimulus was initiated which made it possible to average the responses without losing the desired oscillation component. Various pattern wavelengths between 3 and 20 degrees were used, and the speed of the pattern was always adjusted according to equation 3 in order to maintain a constant contrast frequency, f_c, equal to 3 $^{cycles}/_{sec}$.

The average discharge responses of the on-off and the on-maintained units to moving striped patterns of various spatial wavelengths are shown in figures 4. 3 and 4. 4. For each wavelength there are two average responses corresponding to motion directed along the major and minor axis of the receptive fields. The average responses corresponding to the two orthogonal directions (major, minor axes) of motion differed in magnitude, but no significant difference was found in the average response magnitudes for motion in opposite directions along either the minor or major axis. Three features of these responses were noteworthy. The magnitude of the average responses (average number of discharges elicited) along the major axis, especially for the on-off unit, were greater than along the minor axis which was a consequence of a greater degree of integration along this axis. Secondly, the average responses exhibited considerable oscillation, particularly for the on-maintained unit, in synchrony with the temporal intensity fluctuation of a point in the stimulus field. The magnitude of the response oscillations corresponded to the amplitude factor of the sinusoidal term in

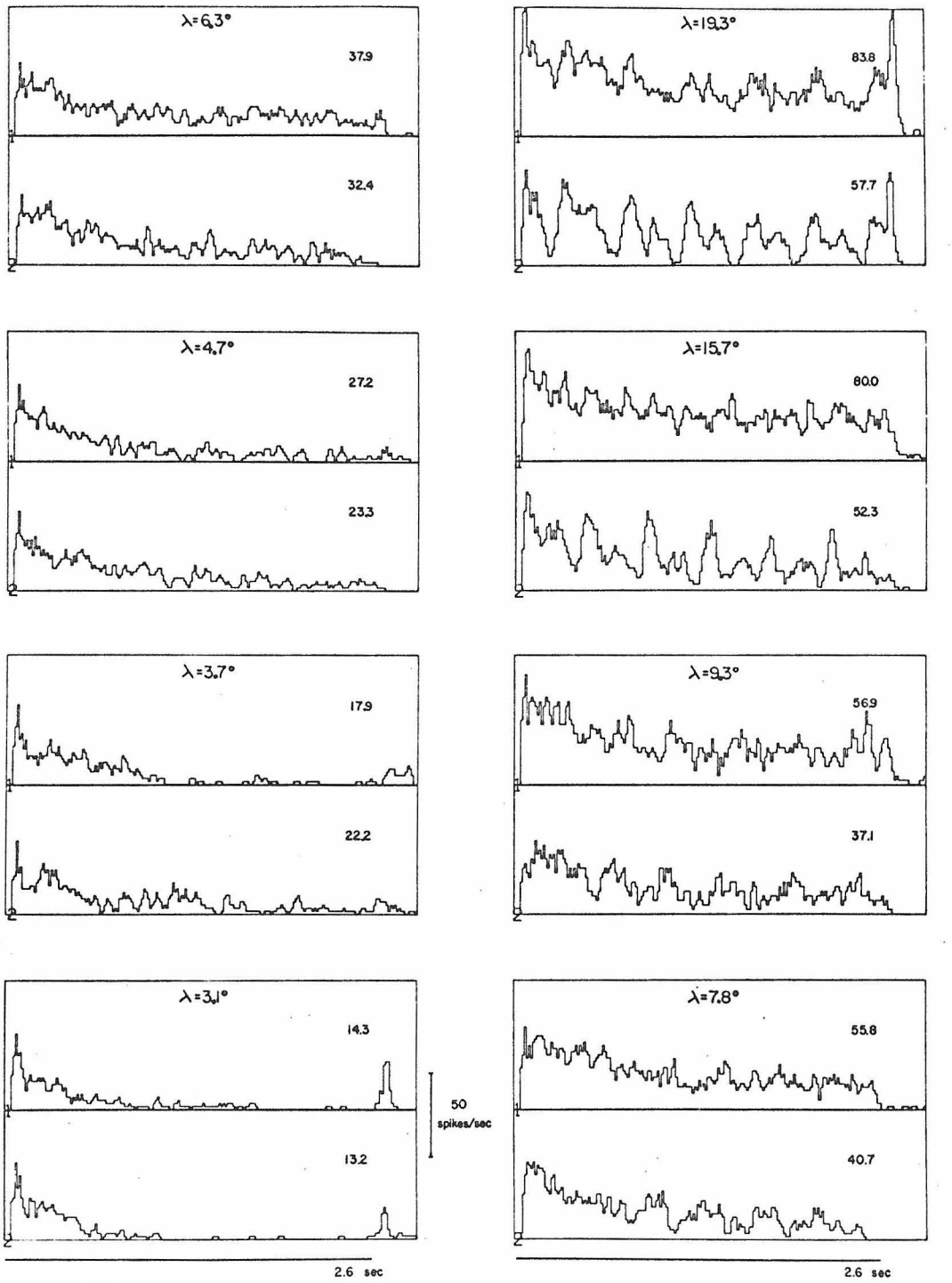

Figure 4.3 Average discharge pattern of an on-off unit to moving striped patterns of different spatial wavelength (λ). Upper PST histogram of each pair corresponds to motion directed along the major axis. Lower PST histogram corresponds to minor axis motion. The number associated with each histogram refers to the average number of spikes/stimulus. B.W. = 15 msec. f_c = 3Hz N = 12.

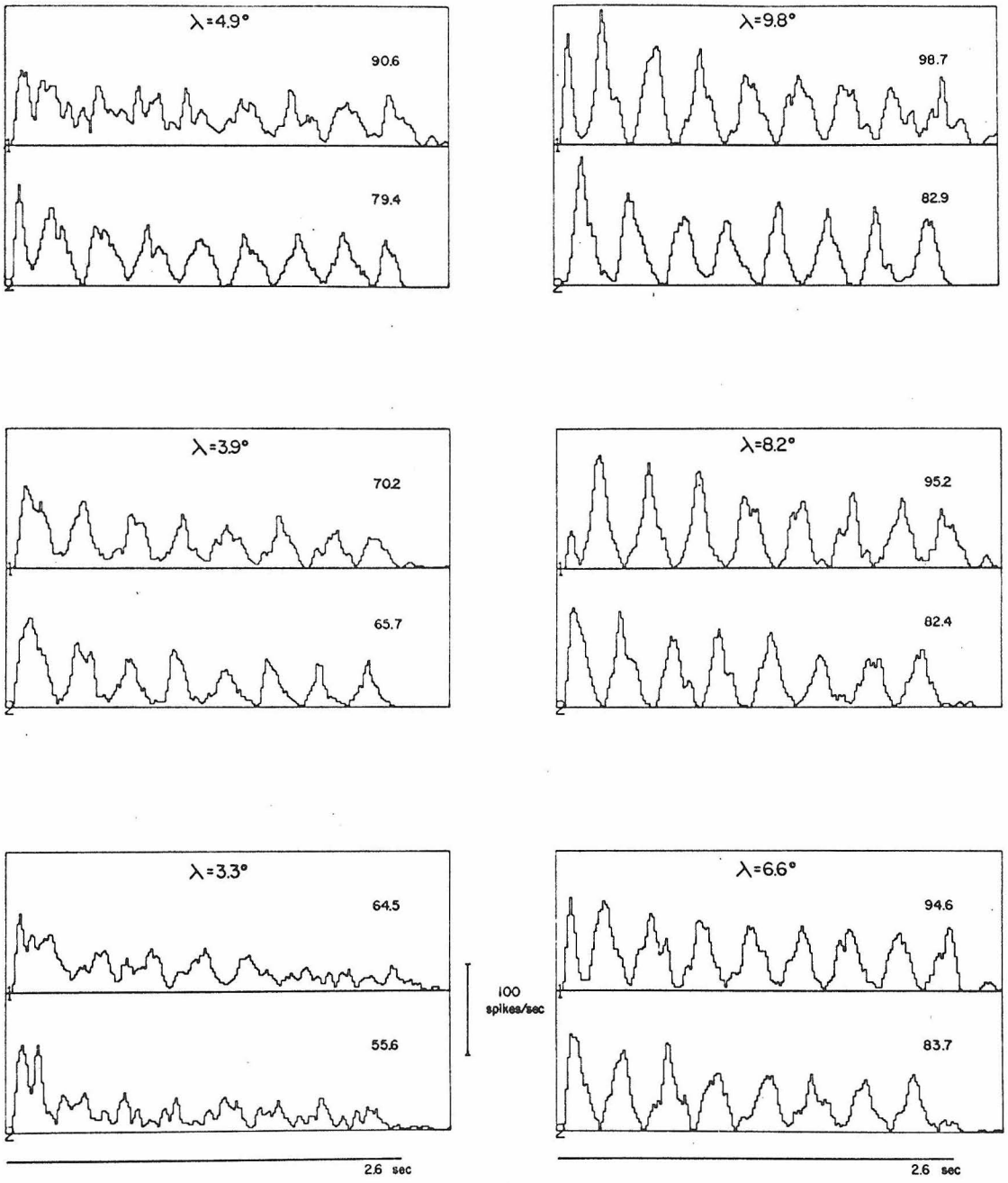

Figure 4.4 Average discharge pattern of an on-maintained unit to moving striped patterns of different spatial wavelengths (λ). Upper PST histogram of each pair corresponds to motion directed along the major axis. Lower PST histogram corresponds to minor axis motion. The number associated with each histogram refers to the average number of spikes/stimulus. B. W. = 15 msec. f_c = 3Hz N = 12.

equations 4 and 5 and were used to estimate the effective half angles of the receptive fields. Thirdly, when the wavelength was sufficiently small with respect to the receptive field half sensitivity angles ($\lambda < 7$ for on-off unit), the response oscillations attenuated so that only a relatively constant response remained. The magnitude of the constant response declined with smaller wavelengths which reflected the limits of acuity set by the half sensitivity angles of the photoreceptor cells. The potency of a moving intensity pattern to excite the on-off unit is revealed by the fact that the response magnitude to a moving 10 degree pattern exceeded that to a stationary diffuse stimulus of the same average intensity by more than a factor of four; whereas, the response magnitude of the on-maintained unit was elevated by less than a factor of two.

To illustrate these properties, consider the arbitrary model diagrammed in figure 4.5 which is not intended to have any specific physiological implications. An array of N photodevices each having a gaussian light gathering function with an acceptance angle of α are arranged so that an angle of $\Delta\theta$ separates the optical axes of adjacent photodevices. The light flux gathered by the k^{th} photodevice upon stimulation by a moving sinusoidal intensity pattern of velocity v and spatial wavelength λ is given by $f_k(t)$. The light flux signal from each photo-device enters a threshold device having a threshold of τ. The output, R(t), of this non-linear model is formed by making a weighted summation of the threshold device signals. Note that the magnitude of the threshold device signals is dependent upon

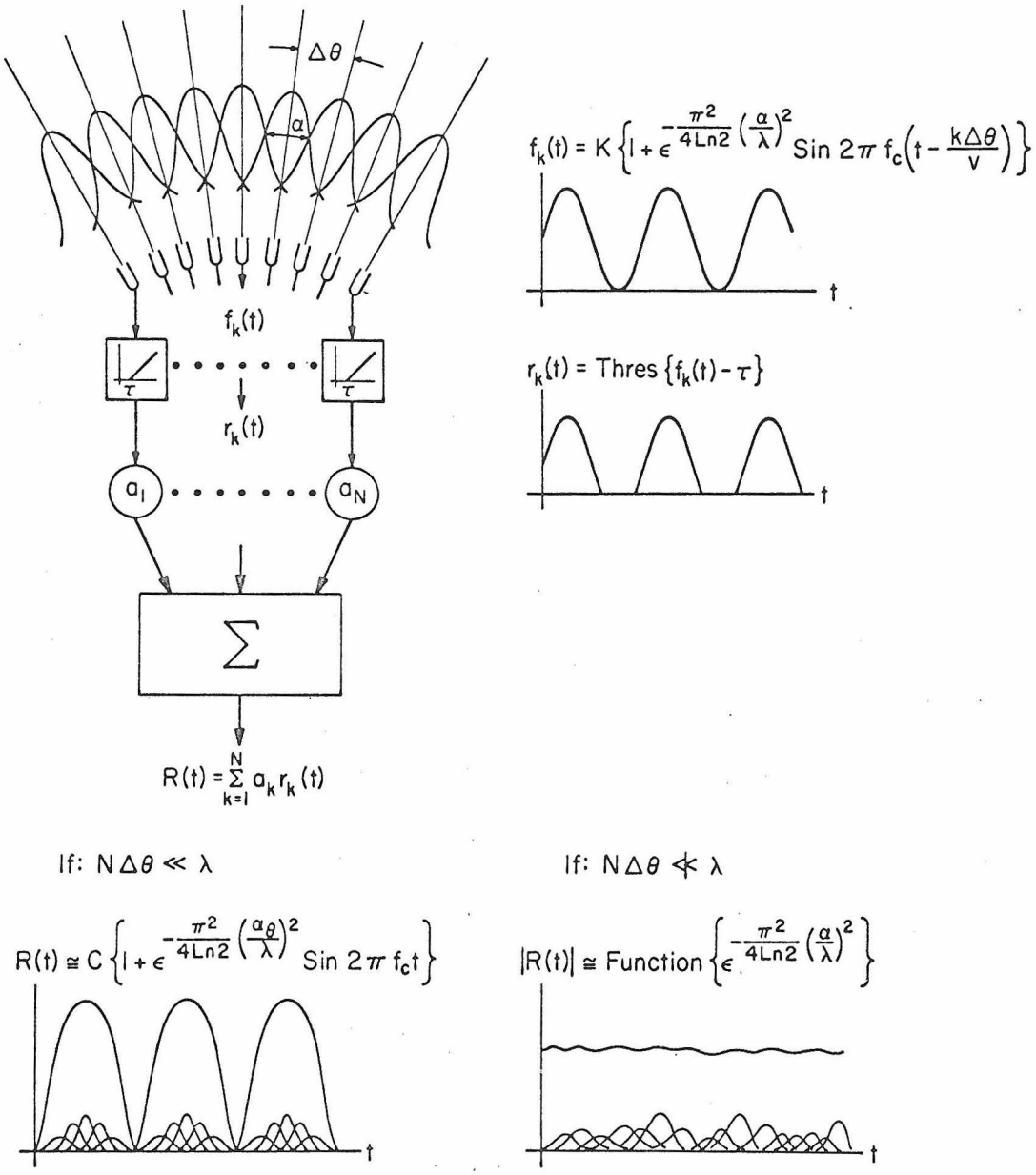

Figure 4.5 Diagram of the photodevice model $\Delta\theta$ = interdevice angle, α = photodevice acceptance angle, τ = threshold, f_k = flux function of k^{th} photodevice, $r_k(t)$ = response of k^{th} threshold device, a_k = k^{th} element summation weight, R(t) = model output signal, N = total number of photodevices summed, λ = spatial wavelength of sinusoidal intensity pattern moving at velocity (v), α_θ = acceptance angle of the model, $v = \lambda f_c$, C, K = constants.

$$K \text{ Exp } [-\frac{\pi^2}{4Ln2} (\frac{\alpha}{\lambda})^2] - \tau \ .$$

The output of this model is oscillatory (second feature of the data) when the maximum phase lag ($\frac{N\Delta\theta}{v}$) between the first and last photodevice signals is small compared to the period ($1/f_c$) of the sinusoidal light flux signal or, equivalently, the spatial wavelength (λ) is long compared to $N\Delta\theta$ (a first approximation of the effective acceptance angle α_θ of the model). In this situation, the individual component signals forming the output signal are essentially in phase resulting in an oscillatory output signal which to a first approximation can be described by

$$R(t) = C\left\{1 + \text{Exp} [-\frac{\pi^2}{4Ln2} (\frac{\alpha_\theta}{\lambda})^2] \ \text{Sin}2\pi f_c t\right\} \qquad (6)$$

The third feature of the average discharges can be illustrated by the model when

$$N\Delta\theta \not< \lambda$$

in which case the individual component signals summing to form the model output signal are out of phase and therefore sum to something approaching a constant. Since the magnitude of the individual components is dependent upon $\text{Exp}[-\frac{\pi^2}{4Ln2} (\frac{\alpha}{\lambda})^2]$, the magnitude of the model output signal is likewise dependent upon this factor which allows one to estimate the acceptance angle (α) of the photodevices by measuring the constant response magnitude as a function of λ. The first feature of the average discharge responses which represented a greater response magnitude for motion directed along the

major axis than along the minor axis is illustrated in this model by allowing N to take on a large value for a direction of motion corresponding to the major axis than it does when the direction of motion corresponds to the minor axis. Obviously, the magnitude of the model output signal is greater when more components are summed.

The model was useful in explaining the observations and in illustrating that information concerning the size of the receptive fields of photoreceptors and the on-off and on-maintained units can be derived from the average discharge responses to moving striped patterns. Estimates of the half sensitivity angle (α) of photoreceptors were obtained from the average discharge responses by plotting the normalized average number of spikes elicited during 2.6 seconds of stimulation against the spatial wavelength (λ) of the stimulus for the on-off and on-maintained units as shown in figure 4.6. These normalized response attenuation points were compared with the expected attenuation curves described by $\mathrm{Exp}[-\frac{\pi^2}{4\mathrm{Ln}2}(\frac{\alpha}{\lambda})^2]$, assuming gaussian shaped field with a half sensitivity angle of α, a few of which are plotted in figure 4.6. Considering there were several tenuous assumptions made in the reasoning, the response attenuation points (⊙, △) compared surprisingly well with the theoretical attenuation curve corresponding to a three degree half sensitivity angle. This agreed with the results of others [20, 51, 52] using optomotor torque measurements and can be interpreted to represent the approximate size of the limiting acceptance angle of the visual system serving these units. Estimates of the half sensitivity angles along

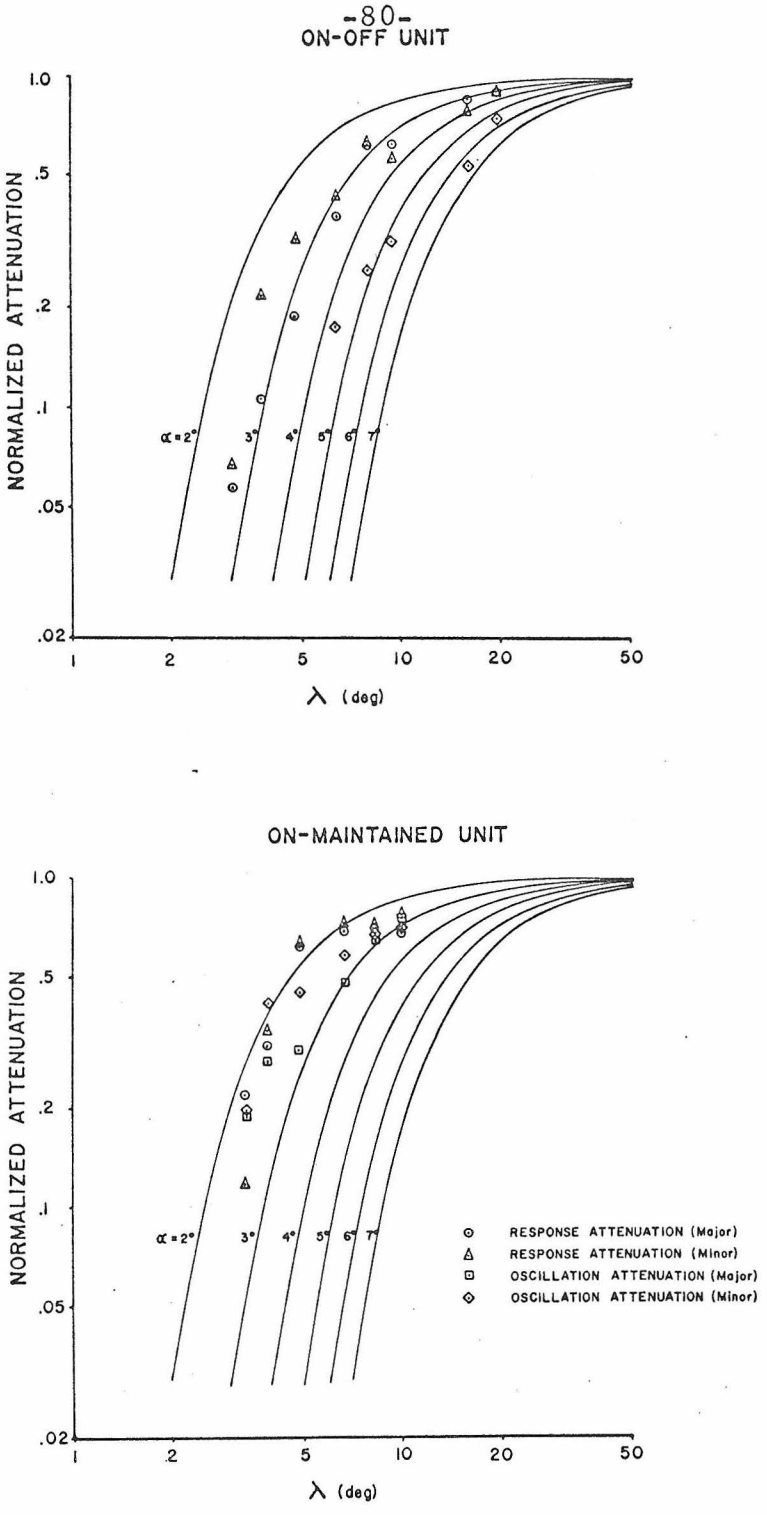

Figure 4.6 Response attenuation characteristics of on-off and on-maintained units as a function of spatial wavelength (λ). The family of curves represents the theoretical attenuation of a gaussian receptive field having half sensitivity angles of α degrees. Major and minor refer to direction of motion with respect to the receptive field axes.

the major and minor axes of the on-off and on-maintained units were obtained by comparing oscillation attenuation points (◇, ⊡) with those expected ($\text{Exp}[-\frac{\pi^2}{4\text{Ln}2}(\frac{\alpha_\theta}{\lambda})^2]$) as shown in figure 4.6. The oscillation attenuation points were derived from the average discharge responses by measuring the amplitude of the oscillatory component for each wavelength when possible and normalizing. Although oscillations in the average discharge responses of the on-off unit were small, a few measurements were possible as shown in figure 4.6. Discharge oscillation was clearly more prominent for striped patterns moving along the minor axis of the receptive field, and the corresponding oscillation attenuation points fitted reasonably well the attenuation expected from a half sensitivity angle of 5 degrees. Although the on-off unit of figure 4.5 and 4.6 did not exhibit significant response oscillations to major axis motion, other units did and their oscillation attenuation points fitted more closely to the attenuation curves predicted by a 7-8 degree half sensitivity angle. This type of analysis is particularly well suited for detecting the degree of spatial summation, and it clearly indicates the receptive field of the on-off unit is elliptical with its major axis roughly parallel to the medio-lateral axis of the eye. Since the receptive field size of the on-maintained unit was small compared to the spatial wavelengths used, all the average discharge responses were oscillatory, and the oscillation attenuation points for both directions of motion fitted well the attenuation curve expected from a 3 degree half sensitivity receptive field. The response of the <u>on</u> region dominated

causing the size of the receptive field along the major and minor axes to appear approximately equal, although asymmetry with respect to these two axes was indicated by a slightly larger response magnitude for motion along the major axis. Since the oscillation attenuation points of the on-maintained unit agreed reasonably well with response attenuation points from the on-off and on-maintained, units, the size of the on region of the on-maintained unit receptive field must approach the limit set by the photoreceptors.

Directional Sensitivities of the On-Off and On-Maintained Units

Directional sensitivity measurements were made so that receptive field sizes of the on-off and on-maintained units could be compared directly with receptive field sizes of photoreceptors reported by others [14, 39, 52, 72, 81, 83, 86]. The experiments were performed using the direct stimulating apparatus which allowed accurate control of the angular orientation and intensity of the stimulus. Sensitivity calculations required the measurement of the stimulus intensity necessary to evoke a criterion response as a single experimental variable was manipulated which, in this case, was the angular orientation of the stimulus along the medio-lateral axis (θ) or along the dorso-ventral axis (ϕ) of the compound eye. A set of response-log intensity curves, each corresponding to a particular value of the experimental variable, would provide the most general data from which to calculate sensitivities, for any criterion response could be selected requiring only trivial measurements of

the lateral displacements of the response-log intensity curves to determine the relative sensitivities. Unfortunately, large amounts of data were required because of the necessity to serially average discharge responses, and consequently the observation time was sufficiently long that non-stationarities in the data seriously deteriorated the accuracy of the measurements. A solution to this problem was to specify a criterion response and to simply determine the stimulus intensity necessary to evoke that response for each value of the experimental variable. In the case of discharge activity with no spontaneous discharge as the on-off, and on-maintained units, threshold response made a good criterion because it was well defined. Discharge threshold measurements were used in determining directional sensitivities; however, an additional method was also used which had the advantage of being less subjective and more quantitative. Furthermore, the stimulus levels used in the second method were typically two log units above threshold which provided a good check of the directional sensitivity measurements made at threshold. The second method was based on the assumption that the response-log intensity curves corresponding to each angular orientation of the stimulus were identical except for a shift along the log intensity axis. The assumption was found to be valid, and therefore the measurement of a single response-log intensity curve and the measurement of the response to a fixed stimulus intensity for each of the angular orientations of the stimulus was all that was required to calculate the directional sensitivities.

The experiments consisted of isolating a unit followed by rotating (θ) and tilting (ϕ) the preparation until the axis of the receptive field coincided with the optical axis of the immobile stimulus source. After measurements under dark adapted conditions were completed, the location of the receptive field with respect to the geometry of the compound eye was determined by placing a long focal length microscope along the optical axis of the stimulator and observing the position of the transmission pseudo pupils resulting from rear illumination of the opened head capsule. The recording method was highly selective for units having their receptive fields within region I;

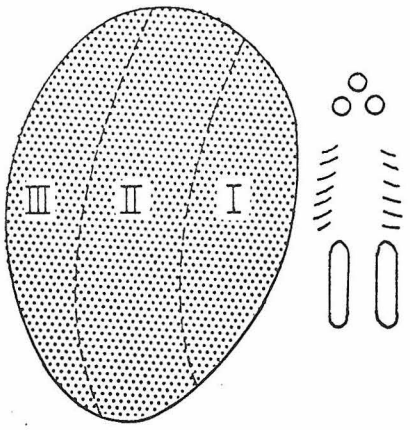

however, occasionally units having receptive fields in regions II and III were isolated and studied. Because of the limited amount of data from these other regions, nothing conclusive can be stated about the size of the receptive fields in these regions except that they tended to be slightly larger, particularly in region III.

The results shown in figure 4. 7 confirm the validity of the assumption implicit in the use of the second method of directional

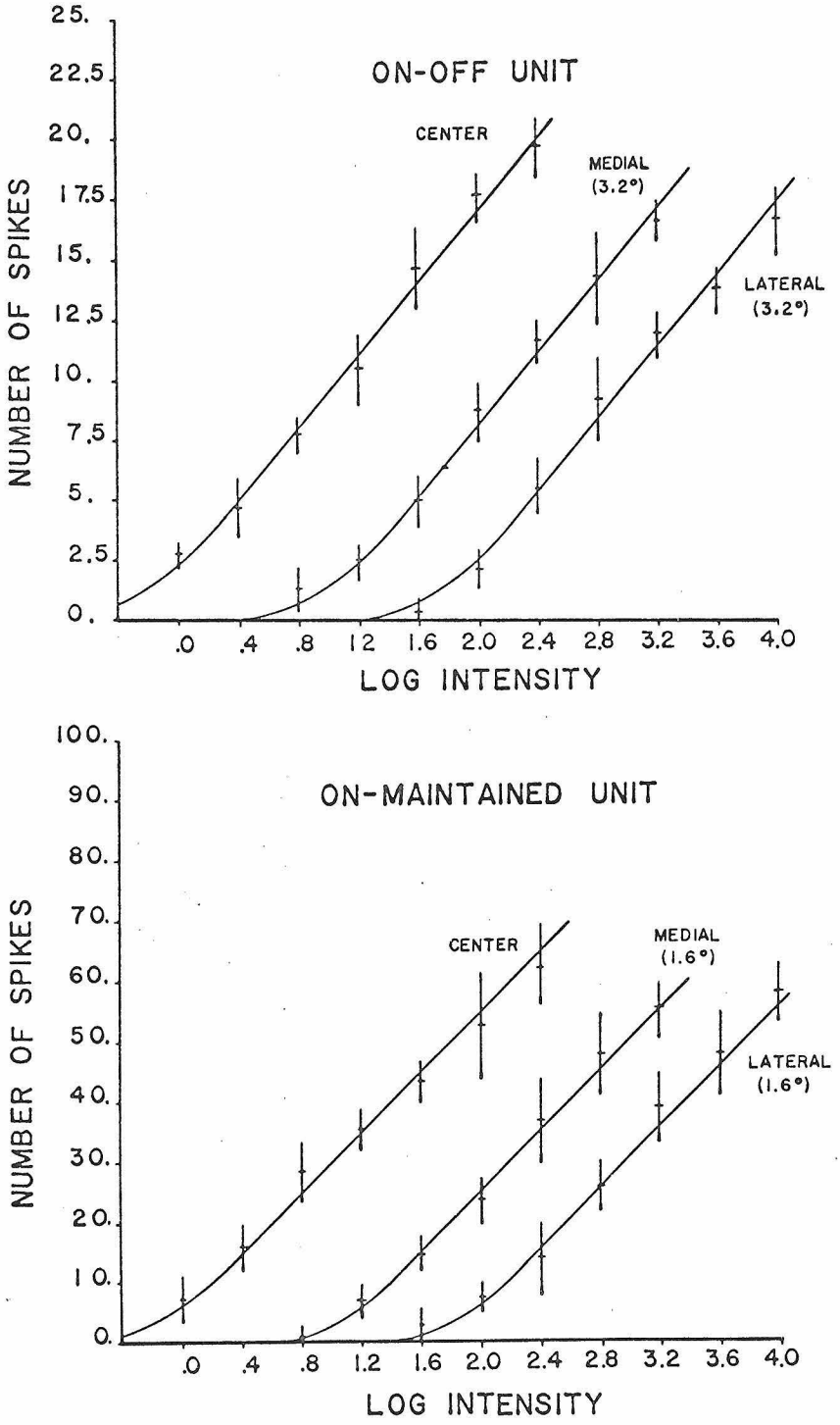

Figure 4.7 Typical response-log intensity characteristics of the on-off and on-maintained units for different angular orientations of the stimuli. The mean (and ± 1 S.D.) numbers of spikes elicited by 460 msec. light pulses delivered from the specified angular orientations are plotted against the stimulus intensity. The characteristics are arbitrarily placed along the log intensity axis. λ = 471 mμ. N = 5.

sensitivity measurement. The three response-log intensity curves corresponding to different angular orientations of the stimulus for both units were obtained by presenting the stimulus of lowest intensity successive from the three angular orientations followed by the next stimulus intensity level again presented successively from the three directions and so on until the run through the set of intensity levels was repeated 5 times (i. e., the intensity and direction of the stimulation were multiplexed). This program minimized the possible distorting influence of non-stationarities on the response-log intensity curves. For both, the on-off and on-maintained units, the response-log intensity curves corresponding to the three directions were parallel within the fluctuation of the data. The response-log intensity curves of the on-maintained units were measured from the on region only. Since the assumption could not be validated outside this region, this method was only applied to the on region of the receptive field (i. e., that from which an on-maintained discharge could be elicited).

Typical families of PST histograms for an on-off unit resulting from constant intensity stimulation from different directions along the θ and ϕ axis are shown in figure 4.8A, B (i. e., the second method of directional sensitivity measurement). The intensity of the monochromatic (λ = 471 mμ) stimulus was adjusted before the experimental runs to elicit a near threshold response from the two extreme directions of stimulation, and the direction of the stimulus was changed in steps of 1.9 degrees. Also shown in figure 4.8C, D

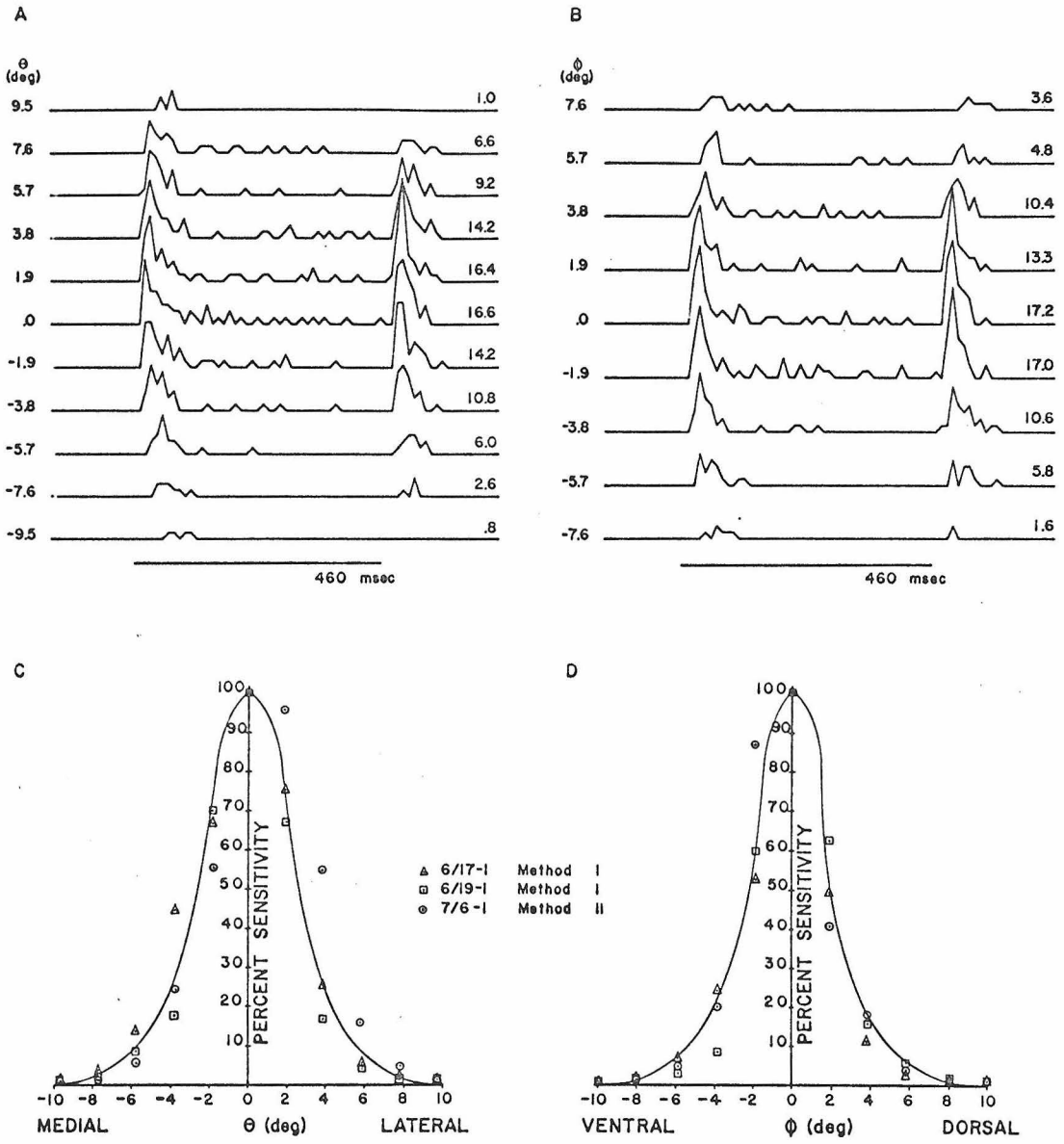

Figure 4.8 Directional sensitivities of three typical on-off units (A) Average discharges corresponding to different stimulus directions along the θ (horizontal) axis. (B) Average discharges corresponding to different stimulus directions along the ϕ (vertical) axis. Right hand column of figures refers to the average number of spikes/stimulus based on 5 trials. B.W. = 10 msec. λ = 471 mμ. (C) Horizontal directional sensitivity (D) Vertical directional sensitivity △, ⊡ - sensitivities derived from threshold measurements, ⊙ - sensitivities derived from the data in (A) and (B).

are the θ and φ directional sensitivities derived from the PST histograms and the θ and φ directional sensitivities derived from threshold determinations corresponding to the different stimulus directions in other units. The directional sensitivities obtained by these two methods were in good agreement and revealed a horizontal (θ) half directional sensitivity angle of 6 degrees and a 4.5 degree vertical (φ) half directional sensitivity angle.. The accumulated results from 26 on-off units studied in region I are expressed in table 4.1 and indicate the average horizontal and vertical half sensitivity angles to be 5.5 degrees and 4.3 degrees respectively which are in fair agreement with the half sensitivity angles found using moving striped patterns. The results obtained by the two methods are in good agreement, and the elliptical configuration of the receptive field of the on-off unit is manifested in the average half sensitivity angles. The horizontal directional sensitivity of the on-off unit was occasionally found to decrease more rapidly on the lateral side of the maximum sensitivity direction. This receptive field asymmetry was not an artifact introduced by the optics of the stimulating apparatus, for similar results were observed in the grid experiments which utilized a completely different stimulating design.

Typical on-maintained unit PST histograms are shown in figure 4.9 corresponding to horizontal (θ) and vertical (φ) changes in the direction of stimulation. Note the suggestion of an <u>off</u> discharge to stimulation from the extreme orientations along the θ axis. In addition, the directional sensitivity curves derived from the PST

		METHOD I	METHOD II
ON-OFF UNIT	HORIZ. (Θ)	5.57 ±.72°	5.47 ±1.0°
	VERT. (Φ)	4.45±.32°	4.20 ±.39°
ON-MAINTAINED UNIT	HORIZ. (Θ)	2.43 ±.28°	2.38 ±.57°
	VERT. (Φ)	2.58 ±.27°	2.60 ± .40°

Table 4.1 Average half sensitivity angles of the on-off and on-maintained units. Method I utilized threshold measurements, and Method II utilized responses elicited by constant intensity stimulation. Means and $\pm$ 1 S.D. are tabulated.

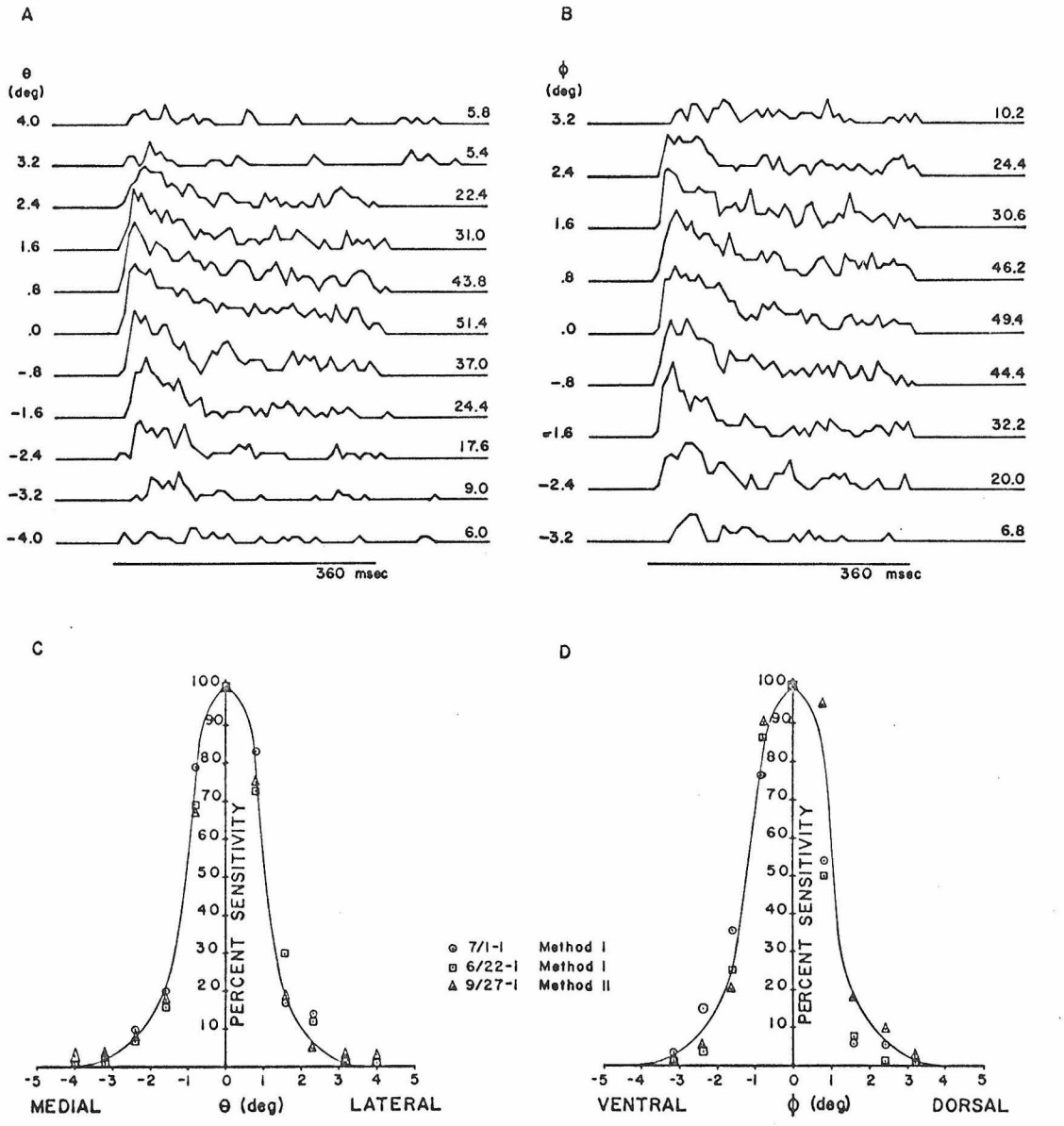

Figure 4.9 Directional sensitivities of three typical on-maintained units. (A) Average discharges corresponding to different stimulus directions along the θ (horizontal) axis (B) Average discharges corresponding to different stimulus directions along the φ (vertical) axis. Right hand columns of figures refer to the average number of spikes/stimulus based on 5 trials. B.W. = 10 msec. λ = 471 mμ (C) Horizontal directional sensitivity (D) Vertical directional sensitivity ⊙,⊡ - sensitivities derived from threshold measurements, △ - sensitivities derived from the data in (A) and (B).

histograms and from threshold determinations in two other units are shown. The accumulated results of directional sensitivity measurements from 16 on-maintained units in region I are summarized in table 4.1 and reveal average horizontal and vertical half sensitivity angles for the on region of 2.4 and 2.6 degrees respectively. The average half directional sensitivities indicated a roughly circular on region; however, the total receptive field of the on-maintained unit including the two off regions was clearly not circular. The directional sensitivities of the off regions were not determined, but judging from figure 4.1 they were slightly larger and of the same shape as the on region. Also, the maximum sensitivity of the off region was approximately 1 log unit lower than the maximum sensitivity of the on region.

Several investigators [14, 39, 52, 72, 83, 86] have studied the directional sensitivity of single photoreceptor cells in the compound eye of flies and have found half directional sensitivity angles ranging from 2 to 12 degrees. However, the most comprehensive study was made by Burkhardt et al. [14, 86] in which they found photoreceptor cells in region I to have circular receptive fields having an average half directional sensitivity angle of 3.3 degrees. Although the stimulus and recording equipment was not designed for intracellular potential recording experiments, the vertical directional sensitivity of several photoreceptor cells in region I were measured to provide direct comparisons with other measurements. The half directional sensitivity angles of the few photoreceptors studied agreed with those

found by Burkhardt et al., but it was found that the light intensity necessary to elicit a 20 mv photoreceptor depolarization exceeded that required to produce a saturated response from the on-maintained unit. Scholes [72] who first reported the positive slow potential in the first optic ganglion of flies found their horizontal half directional sensitivity angle to be approximately the same as that of photoreceptor cells. Similar measurements were made as shown in figure 4.10. The vertical half directional sensitivity angle of the positive slow potential recorded from the first optic ganglion was approximately 2.5 degrees, and the response changed only in amplitude as the stimulus direction was changed. Although the directional sensitivity of the hyperpolarizing slow potential was not measured due to the difficulty of recording the potential while changing the direction of the stimulus, it was believed to have a directional sensitivity comparable to that of photoreceptors. Shaw [74] reported that the horizontal half sensitivity angle of a similar response recorded from the first optic ganglion of the locust was approximately 4.5 degrees and the same as that of locust photoreceptors.

Interaction between Receptive Field Regions of On-Maintained Units

Only the on-maintained unit was found to have a non-homogeneous receptive field consisting of an oval on region flanked by two circular off regions. Receptive field organization similar to this has been observed in various units of the vertebrate retina with the major difference being the two different regions were concentrically

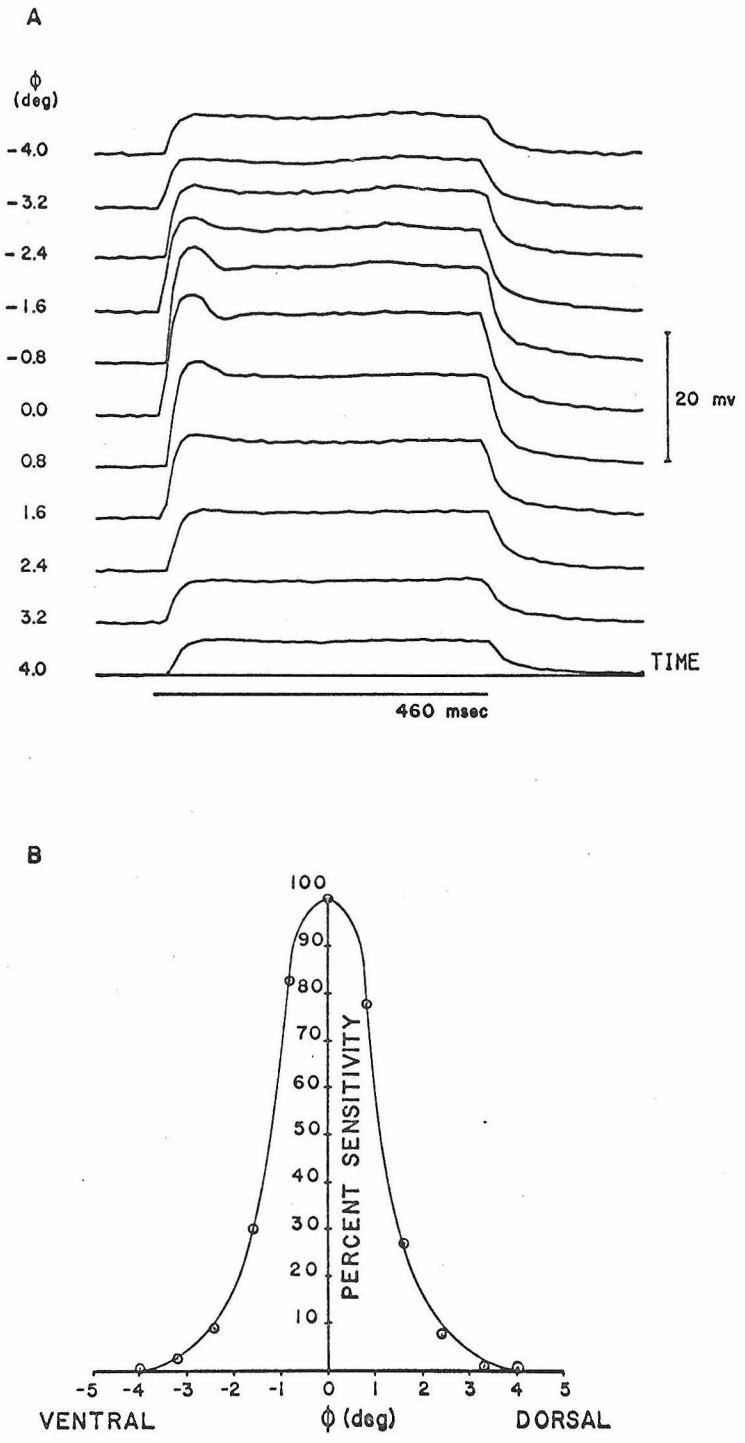

Figure 4.10 Directional sensitivity of typical positive slow potential (A) Evoked slow potentials corresponding to different directions of constant intensity stimulation λ = 471 mμ Sampling rate = 100 samples/sec. (B) Directional sensitivity calculated from the maximum polarization values in (A).

organized. Furthermore, the two regions of vertebrate retinal units interacted antagonistically. Lateral inhibitory interaction between the eccentric cells of the compound eye of Limulus has been extensively studied [30, 68], and it was found to be important in increasing acuity. Although lateral or surround inhibition was thought to be a ubiquitous sensory phenomenon, several attempts [31, 81] to demonstrate it in the compound eye of insects have failed. Based on the organization of the receptive field of the on-maintained unit disclosed by single light spot stimulation and the evidence provided by the anatomical work of Trujillo-Cenóz [77] suggesting possible interaction between adjacent cartridges of the first optic ganglion via the synaptic plexus, experiments utilizing two independent light sources were designed to test the possibility of interaction between the on and off regions of the on-maintained unit receptive field. The experiments were performed using the reflecting sphere environment by placing a 1.5 degree spot of light in the on region and another 1.5 degree spot in an off region while the two spots of light were gated in various temporal orders. It was readily apparent that the two regions exerted antagonistic effects upon each other, but due to the lower sensitivity of the off response, it was necessary to make the intensity of the spot stimulating this region at least 1 log unit greater than that used to elicit the center on-response in order to show significant inhibition of the on response. The results illustrated in figure 4.11 clearly indicate the nature of this interaction. PST histograms

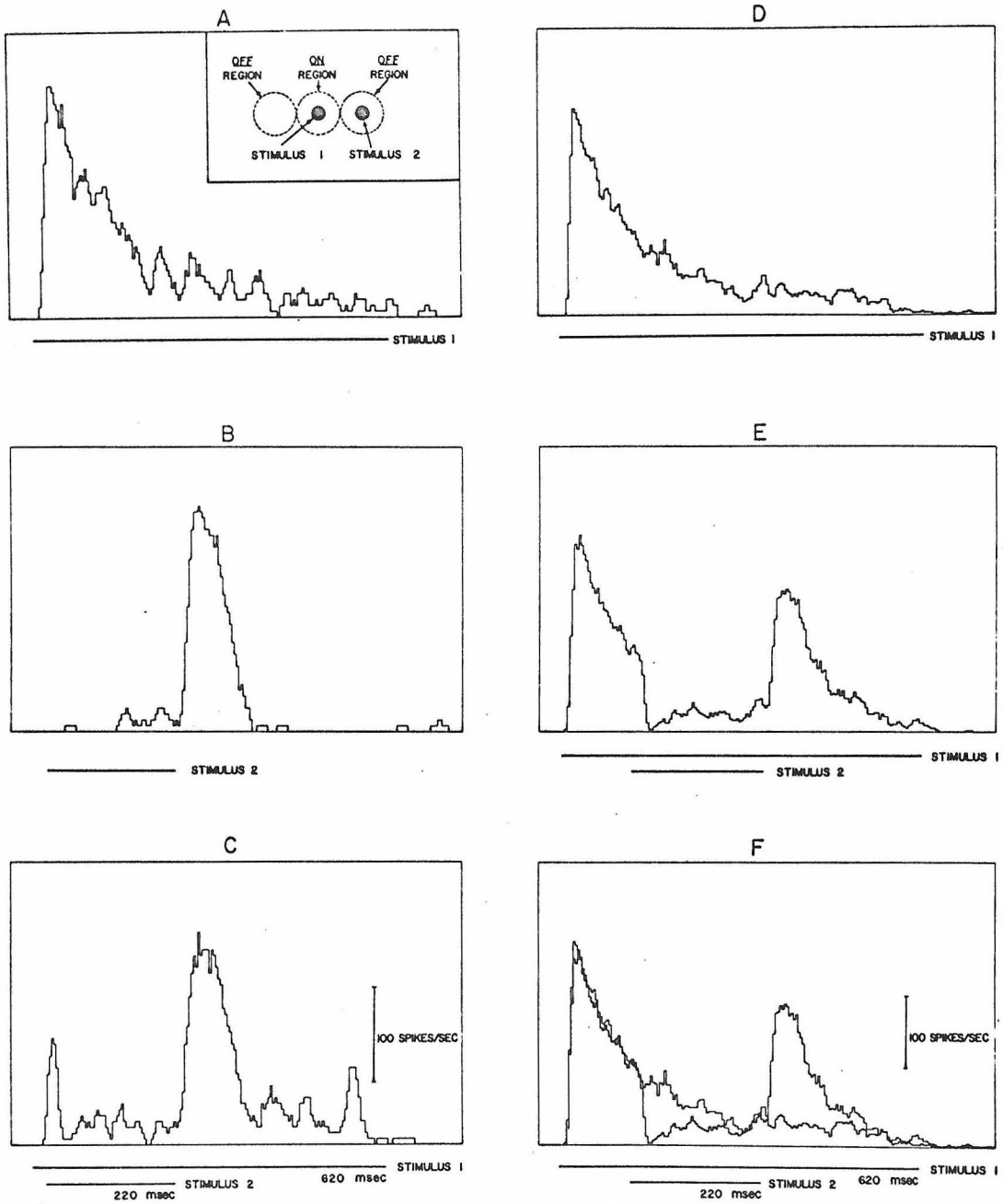

Figure 4.11 Inhibitory influence of the off region on the on region of the on-maintained unit. A-C and D-F are from different units. (A) Average discharge evoked by a 1.5° spot in the on region. The inset schematically describes the stimulus organization used in A-F. (B) Average discharge evoked by a 1.5° spot in an off region (C) Average discharge when both regions are stimulated in the temporal order shown (D) Same as (A) for another unit (E) Same as (C) except different temporal order (F) D and E are superimposed B.W. = 4 msec. $N_{A-C} = 8$, $N_{D-F} = 45$.

A and B show the average discharge behavior of a unit when the on- and off regions were stimulated separately. Note that there appeared to be some discharge during the presentation of the light pulse to the off region, probably resulting from scattered light into the more sensitive on region. The interaction is manifested in the average discharge behavior shown in the PST histogram C when both regions were stimulated in the temporal order indicated. Stimulation of the off region caused the on region discharge to be partially inhibited through the duration of stimulus 2, and cessation of stimulus 2 evoked an off response followed by an elevated discharge rate to stimulus 1 only. The PST histogram D reveals the average discharge behavior of another unit to on region stimulation only. The inhibitory influence of the off region on the on region is revealed by the average discharge behavior in PST histogram E when both regions were stimulated in the temporal order shown. The temporal magnitude of inhibition caused by sudden illumination of an off region could be estimated by subtracting the average interaction response from the average on response, and the resulting difference had a waveform very similar to the average discharge behavior to on region stimulation along. This is best visualized in F where PST histograms D and E have been superimposed.

In addition to the inhibitory effect of off region stimulation on the on discharge resulting from on region stimulation, there was a very specific inhibitory effect of on region stimulation on the off discharge resulting from off region stimulation. This inhibitory

effect is illustrated in figure 4.12. As long as the cessation of on region stimulation did not just precede the cessation of stimulation to an off region, an off discharge was elicited by off region stimulation. However, when the cessation of the on region stimulus just preceded the cessation of the off region stimulation as shown in records 4 and 5 of figure 4.12, the off response was totally inhibited. This type of antagonistic interaction was very specific in the temporal sense.

Based on the temporal specificity properties of the off response inhibition and the nature of the off response, the question was posed as to whether or not the membrane potential of the on-maintained unit was exhibiting some kind of rebound phenomenon which could explain these results. Further support for the rebound argument came from already existing data. Although it had been previously noticed that the on-maintained unit occasionally discharged after the cessation of on region stimulation as shown in figure 3.5, it was not considered significant. However, when considered in terms of a possible rebound mechanism, the discharges after cessation of on region stimulation took on significance. The after discharge, as it was called, was not manifested by all on-maintained units to the same degree, and a particularly good example of after discharge is shown in figure 4.13. The PST histograms were derived from on-maintained unit discharges elicited by a standard series of increasing intensity stimuli delivered to the on region. The on-maintained unit was observed simultaneously with

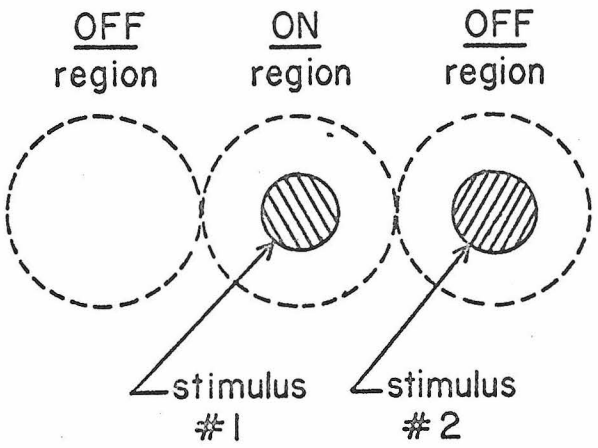

Figure 4.12 Temporal specificity of off discharge inhibition of the on-maintained unit. The two lines below each record represent the presentation of stimulus #1 and #2 which are defined above. The upper stimulus indication corresponds to stimulus #1 which had a duration of 400 msec. Stimulus #2 had a duration of 300 msec. Each of the nine records represents the typical discharge behavior of the on-maintained unit when the two stimuli are presented in the temporal order indicated.

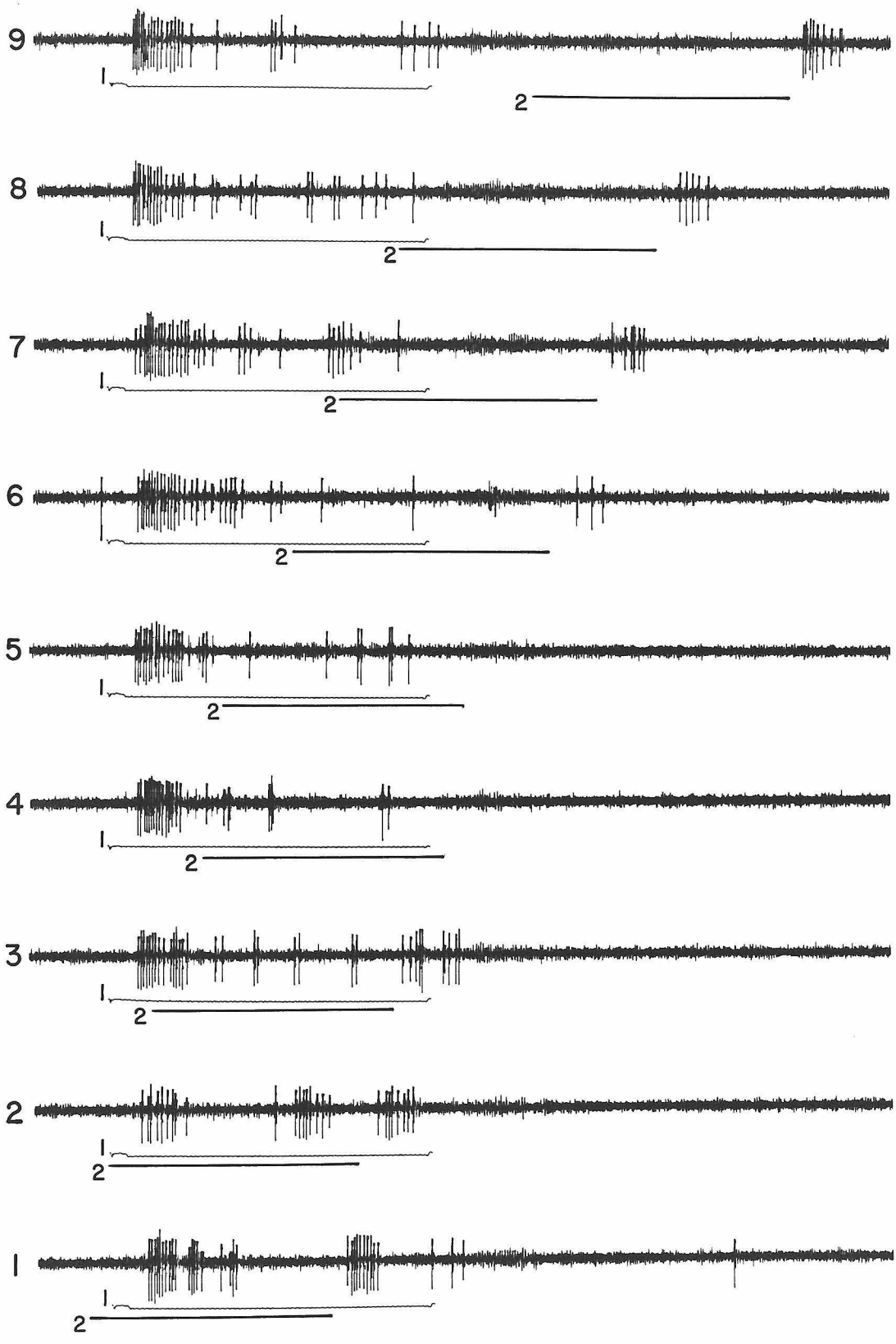
9
1
2
8
1
2
7
1
2
6
1
2
5
1
2
4
1
2
3
1
2
2
1
2
1
1
2

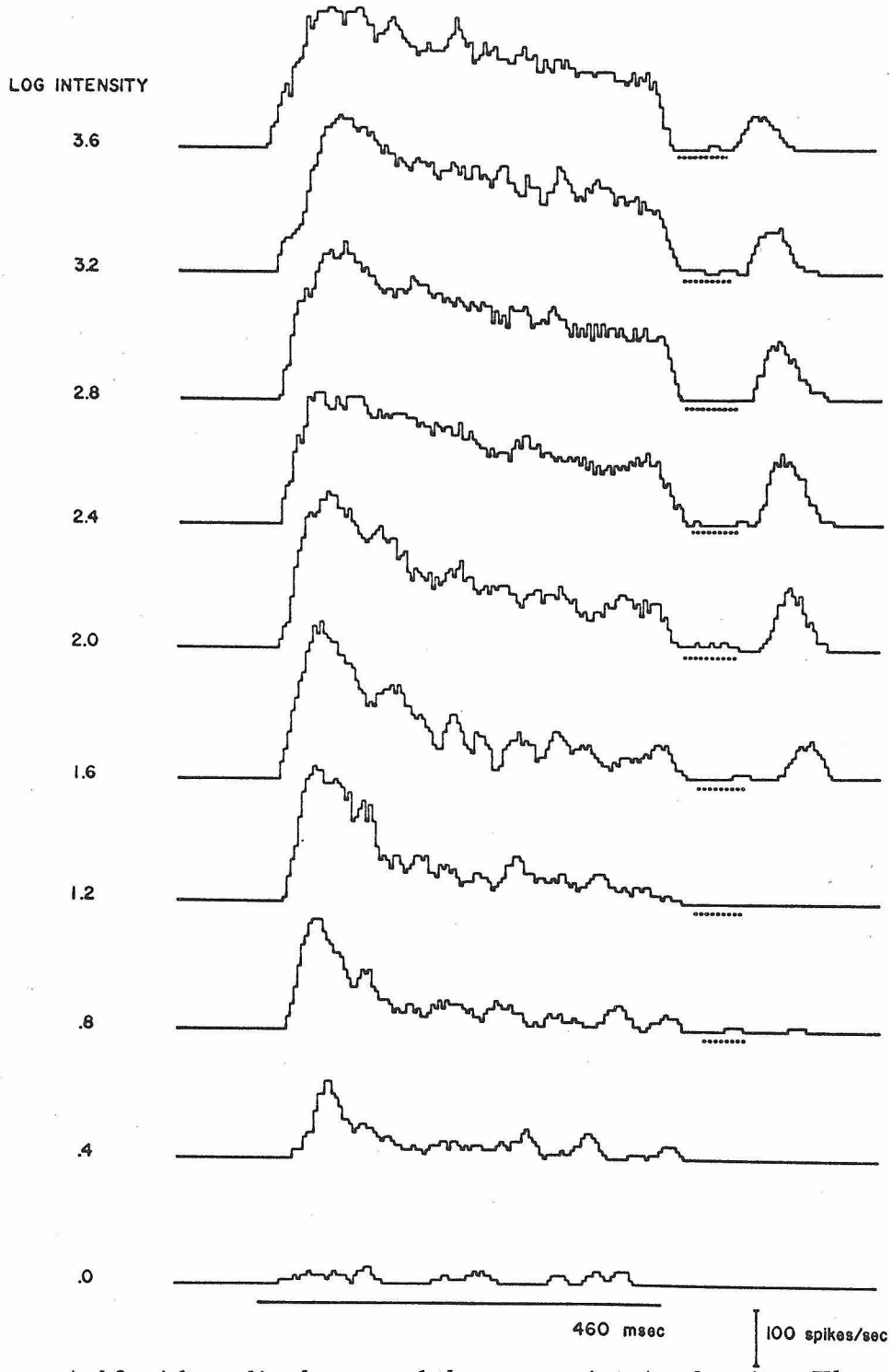

Figure 4.13 After discharge of the on-maintained unit. The stimulus was delivered to the on region for 460 msec. as indicated by the line below the set of PST histograms. The dashed lines represent the occurrence of an off discharge from a simultaneously recorded on-off unit. B.W. = 4 msec. λ = 471 mμ N = 7.

an on-off unit, and the occurrence of the on-off unit off response is indicated under each on-maintained unit PST histogram by a dashed line. The most important feature of the after discharge was its latency. The off discharges of the on-off unit and the off discharges of a properly stimulated on-maintained unit occurred approximately within the same time interval (dashed lines); whereas the after discharges occurred not before 90 msec. after cessation of the on region stimulus which was clearly later than the off discharges of the two units. Furthermore, the after discharge was not elicited by low stimulus intensity levels but only after the intensity became sufficiently intense.

To test further the possibility of a rebound phenomenon, an experiment was performed in which two identical 1 degree spots of light were placed adjacently in the on region. The delay between the onset of one spot of light, termed the condition stimulus and having a duration of .5 sec, and the onset of the other spot of light, called the test stimulus and having a duration of .1 sec, was varied systematically. The results shown in figure 4.14 indicated that when the onset of the test stimulus occurred shortly after the cessation of the condition stimulus (records 3, 4, and 5), the response normally exhibited by the test stimulus alone was inhibited. These results indicated that a period of inhibition (or depressed membrane potential) followed excitation of the unit which could be interpreted to result from a membrane potential rebound phenomenon as will be discussed later.

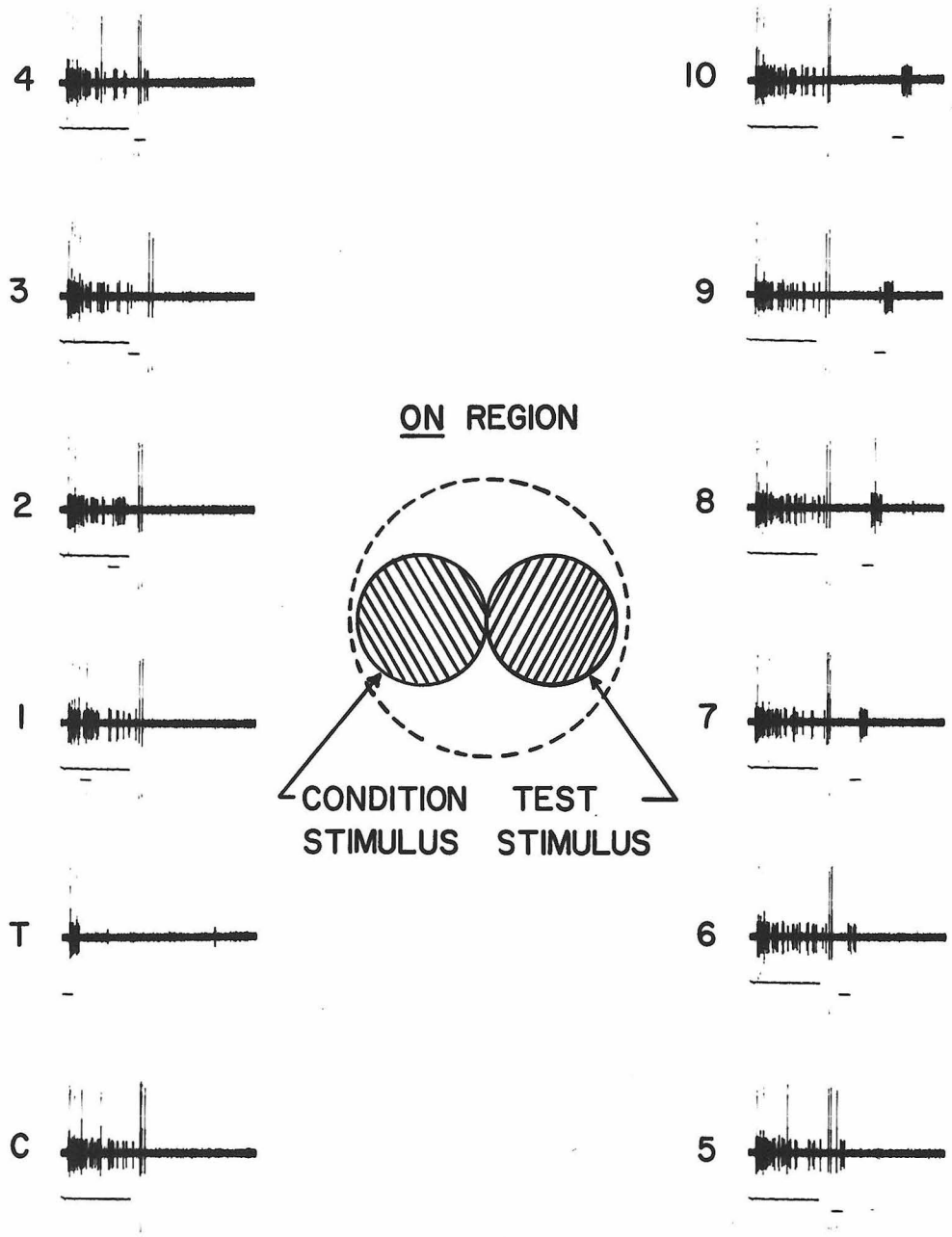

Figure 4.14 Temporal specificity of inhibition following the on discharge of an on-maintained unit. The lines below the records indicate the presentation of the condition (.5 sec.) and the test (.1 sec.) stimuli. The larger poorly reproduced discharge belongs to a simultaneously recorded on-off unit. The responses to the condition and test stimuli alone are shown in records C and T, respectively. Records 1-10 show typical discharge behavior when both stimuli are presented in the temporal order indicated.

Receptive Field Organization of the Medulla On-Off Unit

The receptive field of the medulla on-off unit was studied by eliciting a discharge with a 1.9 degree spot of light transiently presented at each grid point of a 7 by 11 grid having a 3 degree grid point spacing. In order to allow a direct comparison of the size and shape of the receptive field of the medulla on-off unit with those of other units, one microelectrode was used to observe the medulla on-off unit while another microelectrode, placed in the intermediate chiasma, simultaneously recorded the discharge of an on-off unit. Although several receptive field studies were made from single electrode observations, only one simultaneous observation was accomplished due to the difficulty of finding two units simultaneously with their relatively small receptive fields overlapped. The results of the single unit observation experiments agree with those of the simultaneous experiment illustrated in figure 4.15. The two sets of contour lines correspond to the two units and join field points having approximately equal response magnitudes measured in terms of total number of spikes elicited (interpolation between grid points was done by eye). The medulla on-off unit, like the on-off unit (intermediate chiasma), responded throughout its receptive field in a typical on-off discharge fashion without any indication of a more complex receptive organization as exhibited by the on-maintained unit. The response magnitude of the medulla on-off unit was greater than that of the on-off unit and over half of its discharge count was attributable to the off discharge which was previously shown to be

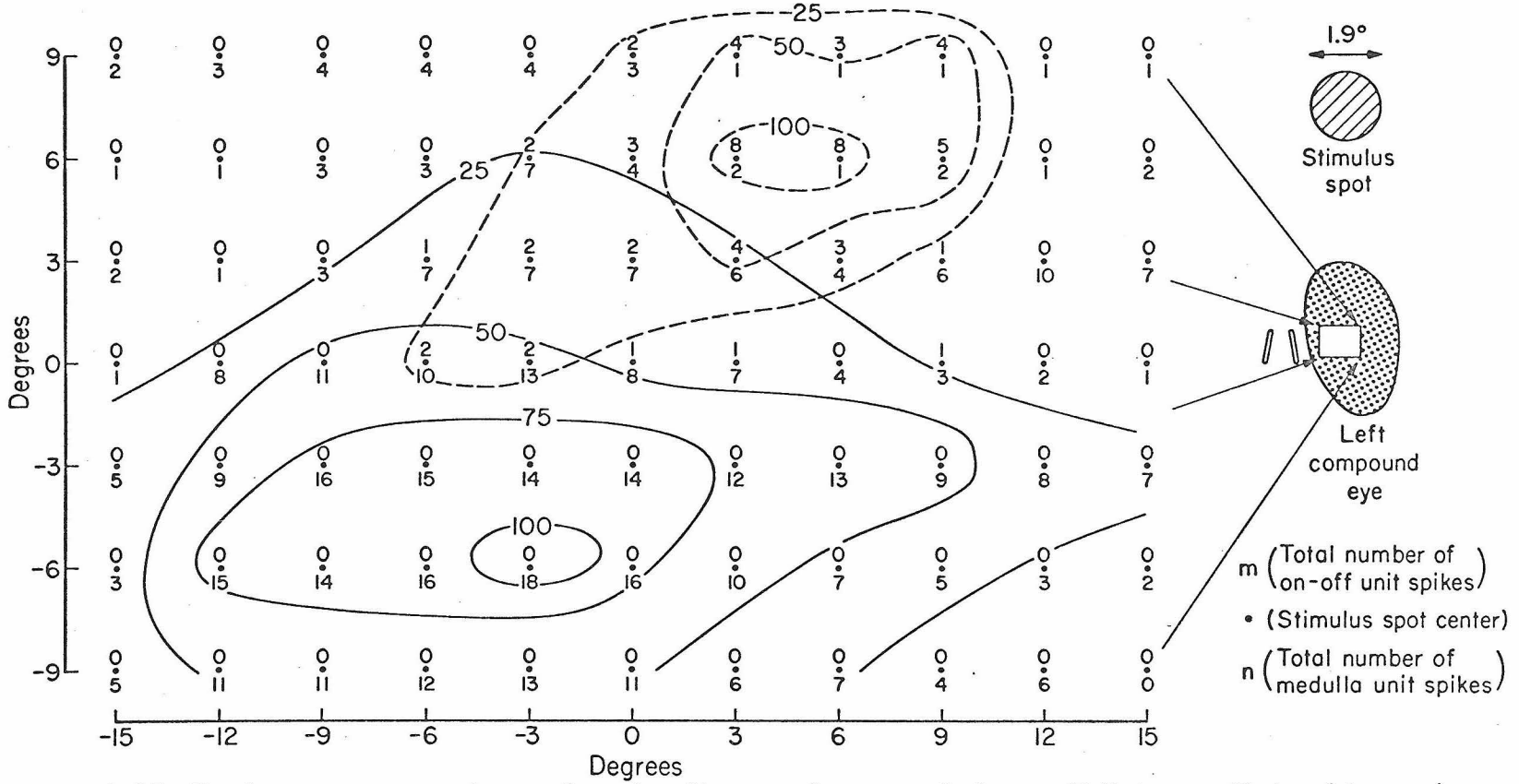

Figure 4.15 Equi-response contours for simultaneously recorded on-off (intermediate chiasma) and medulla on-off units. The numbers refer to the total number of on-off unit (upper) and medulla on-off unit (lower) spikes elicited by .5 sec. spot centered at the respective grid points. The contours inclose the receptive field from which responses greater than the specified percentage of the maximum response could be elicited.

——— medulla on-off unit contour ---- on-off unit contour

more prominent than the off response of the on-off unit. The contour lines of figure 4.15 revealed that the receptive field of the medulla on-off unit was larger than the receptive field of the on-off unit, and although directional sensitivity measurements were not attempted, it was judged on the basis of the relative sizes of the two half response magnitude contours, that the receptive field of the medulla on-off unit was at least twice that of the on-off unit (i.e., half directional sensitive of 10-15 degrees). Also revealed by the contours was the elliptical shape of the receptive field with its major axis having an angular orientation similar to that found for the on-off unit.

Moving light patterns within the receptive field of the medulla on-off unit were found to be the most potent stimuli; however, not all directions of motion elicited the same response magnitude. The results shown in figure 4.16 represent the average discharge behavior of the medulla on-off unit to motion of a striped pattern, having a 12 degree wavelength, in four directions along the major and minor axes of the receptive field. There was a transient response to the motion stimulus in all four directions caused by the sudden appearance of light within the receptive field followed by a slowly decaying discharge rate dependent upon motion. The movement generated response was considerably larger for motion directed along the major axis than for motion directed along the minor axis which presumably was due to the shape of the receptive field. However, a significant and consistent difference in the

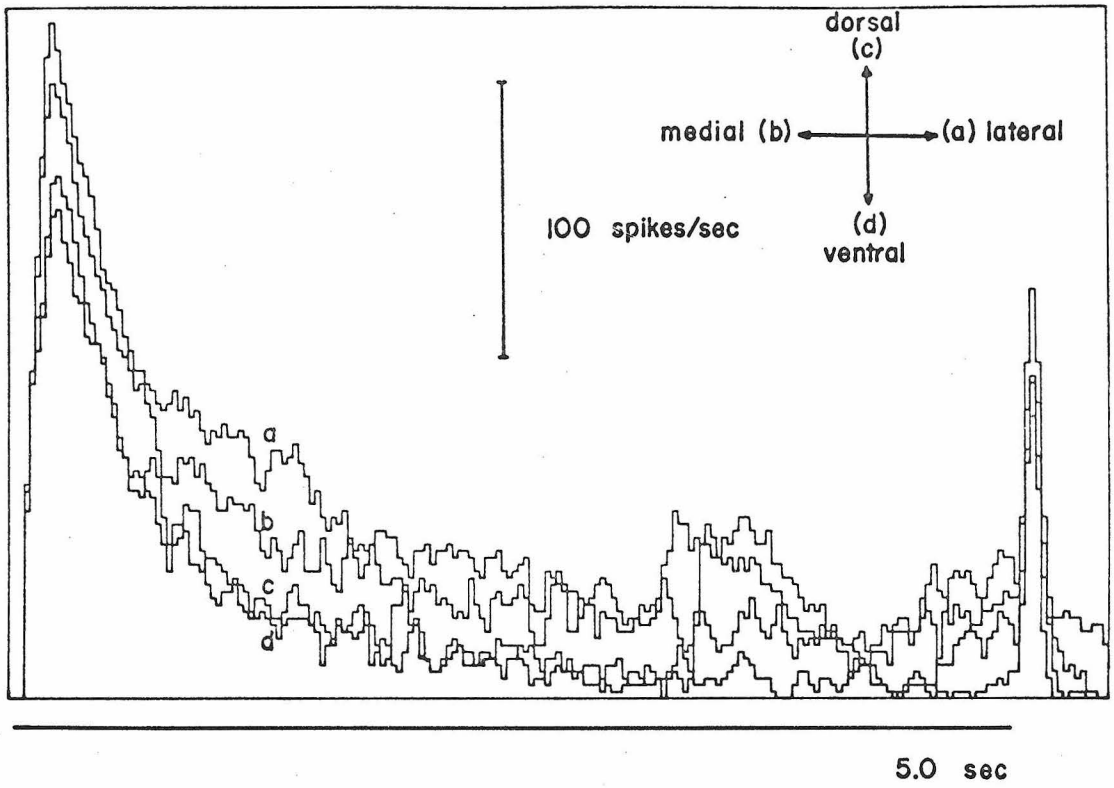

Figure 4.16 Dependence of the discharge of a medulla on-off unit on the direction of a moving striped pattern (a) Average discharge to lateral motion (342.8 $\pm$ 50.2 spikes) (b) Average discharge to medial motion (286.2 $\pm$ 48.2 spikes) (c) Average discharge to dorsal motion (185.4 $\pm$ 58.8 spikes) (d) Average discharge to ventral motion (188.4 $\pm$ 54.2 spikes). B.W. = 28 msec. N = 5 Spatial wavelength = 12° Contrast frequency = 3 Hz.

response magnitude was also found for motion in opposite directions along the major axis. Motion directed laterally along the major axis always generated a greater response magnitude which could not be readily explained in terms of gross receptive field geometry.

CHAPTER V

SPECTRAL AND POLARIZATION SENSITIVITY

Introduction

Considerable effort has gone into studies of color vision in insects since von Frisch [22] first established its existence in honey bees over fifty years ago. The majority of the studies utilized insect training techniques, light evoked behavior measurements (phototaxis, optomotor response) or light evoked gross electrical measurements (electroretinogram). Unfortunately, insect training experiments which are only successful with social, nesting insects as bees, wasps and ants, only provided information about the existence and degree of color discrimination and were incapable of providing information about the mechanisms of color discrimination. Experiments involving the measurement of light evoked behavior had the advantage of being applicable to more different species of insects, yet they suffered from many of the same shortcomings as did training experiments. In fact, most experiments of this type were useful only for determining the range of spectral radiation over which the animal was sensitive. Measurement of gross electrical events elicited by monochromatic light stimulation provided a considerably more powerful technique with which to attack the problems of insect color vision; however, the results by this method were often inconsistent largely because the origin of such measurements was multicellular and poorly understood.

Relatively recently the study of insect color vision has been placed on the cellular level. It proved possible to insert fine micropipettes into single photoreceptor cells [11, 67, 58, 59, 85] and to measure their intracellular potential change in response to flashes of light. This method of observation overcame most of the difficulties inherent in mass response methods and was applied in several recent studies [4, 5, 12, 13, 32] of insect color vision. In addition, microelectrodes have been used to record extracellular potentials from single units at different neural levels in a variety of insects. This method of cellular observation has recently been used to study the effects of spectral light on the discharge behavior of a class of higher order neurons in the fly [8].

The preceding two chapters have revealed some of the information processing characteristics of on-off and on-maintained units associated with temporal and spatial properties of light stimuli. The spectrum and polarization of light contain information which is also thought to be useful to insects. If the fly has developed visual mechanisms to process such information, then they would likely appear in the discharge behavior of the units of the first optic ganglion. This chapter deals with that subject and begins with a brief review of the evidence for color and polarization vision in flies, followed by an account of the experimental results pertaining to spectral discrimination mechanisms of the first optic ganglion as revealed by the discharge behavior of the on-off and on-maintained units to monochromatic stimulation. Also included is a description of the

effects of monochromatic light stimulation on the slow potential recorded from the first optic ganglion. The chapter concludes with an account of the light polarization sensitivity properties of these units.

Color and Polarization Vision in Flies

The spectral sensitivities of various light evoked behaviors in flies have been examined [18, 28, 37, 48] and the results were not entirely consistent owing chiefly to the variability of the behavior and the differences in behavior measurements made. Nevertheless, the results agreed on two characteristic properties. First, the visible spectrum for flies fell between 300 and 600 mμ which represented, approximately, a 100 mμ shift toward shorter wavelengths relative to the visible spectrum of humans. Secondly, spectral radiation in the vicinity of 350 mμ and 490 mμ was most effective in eliciting the behavioral responses examined.

Spectral sensitivity measurements utilizing the fly's electroretinogram, ERG, [2, 84] showed three sensitivity maxima located near 350, 500, and 620 mμ. The spectral sensitivity peak in the red (620 mμ) region has been a subject of some controversy [2, 13, 28, 48, 84], but the results of spectral sensitivity experiments on single photoreceptors [12, 13] and experiments on special mutant flies lacking the brownish-red screening pigments indicated that the red peak was an artifact caused by red light penetrating the screening pigments and exciting photoreceptors whose response contributed

to the measured ERG.

Burkhardt [12] measured the spectral sensitivity of individual fly photoreceptor cells by recording their membrane potential change resulting from monochromatic light stimulation. This method eliminated many problems associated with behavior and ERG derived spectral sensitivity measurements, but it was necessary to repeat the method on numerous single photoreceptor cells in order to establish, statistically, the spectral sensitivity of the retina. All photoreceptor cells had a narrow peak in their spectral sensitivity near 350 mμ and a broader peak in the region between 430 and 540 mμ. It was concluded that the population of photoreceptors investigated was not a homogeneous one but was composed of three distinct groups based on the distribution of the maximum sensitivities in the broad peak region. The predominant type, referred to as the green type, had its maximum sensitivity at 490 mμ while the other two types had their maxima at 470 and 521 mμ and were called the blue and yellow-green types, respectively. The proportion of the number of green, blue, and yellow-green type photoreceptors studied was 5:1:1 respectively, which fitted the hypothesis that within each ommatidium there were five green photoreceptors and one each of the blue and yellow-green variety. This situation only held for the ventral half of the compound eye, for the dorsal half appeared to contain exclusively photoreceptors of the green type. Each of the three classes of photoreceptors had a spectral sensitivity with two maxima, and in all three cases the ultraviolet (u.v.) maxima

were located at 350 mμ and had a sensitivity comparable to the maxima in the visible range. Selective adaptation experiments were performed to determine whether independent u. v. and visible pigments were present in each photoreceptor cell and responsible for the double peaked spectral sensitivities or whether a single pigment having a double peaked absorption characteristic was responsible. The results of the experiments revealed that adaptation of single photoreceptors was independent of the adapting wavelength. Burkhardt [12, 13] concluded that a u. v. receptor system did not exist in the compound eye of Calliphora erythrocephala, but that all photoreceptor cells contained pigments having two visually active absorption maxima.

Microspectrophotometric measurements were made on single rhabdomeres [44, 45, 46], and it was found that rhabdomeres belonging to photoreceptor cells no. 1-6 of each ommatidium possessed different spectral absorption properties than did the rhabdomere belonging to photoreceptor no. 7. The spectral absorption curves derived from photoreceptors no. 1-6 revealed a major absorption peak at 515 mμ and a minor absorption peak at 385 mμ; whereas, the spectral absorption curves derived from photoreceptor no. 7 had a major absorption peak at 476 mμ and a minor one at 400 mμ. These results indicated a clear correlation between anatomy and spectral absorption properties suggested by electrophysiological experiments. However, the details of the spectral absorption curves did not completely agree with the spectral sensitivity made by others, particularly

in the ultraviolet region. Whereas most spectral sensitivities derived from behavior, ERG, and intracellular potential measurements showed a significant peak near 350 mμ, the microspectrophotometric measurements found a surprisingly small absorption value (20%) at this wavelength.

Recently Bishop [6] and Kaizer [37] using different methods found no evidence of color vision in flies. Bishop observed the discharge behavior of selective motion detection units in the fly's third optic ganglion, which are thought to be intimately involved in the optomotor response mechanism, while providing a monochromatic stimulus (400-700 mμ). The resulting spectral sensitivity curves belonged to one class having a maximum near 500 mμ. Kaiser, on the other hand, studied the effect of spectral lights (325-600 mμ) on the optomotor response and found the spectral sensitivity to have a major peak at 490 mμ and a minor peak (50%) at 350 mμ.

In 1948 von Frisch [23] opened a new area of investigation in insect vision by demonstrating that honey bees could distinguish different quadrants of the sky in which the plane of polarization differed. Since then many arthropods have been found to behave as though sensitive to the plane of polarization [18, 36]. Furthermore, the ability of photoreceptors in several insects to transduce light polarization information was demonstrated [3, 11, 57, 72, 73] by showing that the amplitude of photoreceptor action potentials depended upon the orientation of the plane of polarized light.

Electronmicroscopic study [50] of the fine structure of arthropod rhabdomeres, which are thought to be the sites of the photochemical reaction, revealed it to consist of a matrix of microvilli such that all microvilli of a single rhabdomere were oriented in the same direction. It was proposed that the visual pigment molecules were specifically oriented within the microvilli and therefore were responsible for the observed polarization sensitivity. Support for this hypothesis came from microspectrophotometric measurements on single rhabdomeres using linearly polarized light. Dichroic absorption was observed from all rhabdomeres, and the direction of the E-vector corresponding to maximum absorption differed among the rhabdomeres of a single ommatidium. Recently it was found that the direction of the E-vector giving the maximum absorption within rhabdomeres no. 1-6 corresponded to the direction of the microvillar long axes. These results have supported the hypothesis originally suggested by Autrum and Stumpf [1] which proposed that opposite pairs of photoreceptor cells in a single ommatidium possessed sensitivity to a particular plane of polarization so that the total ommatidial signal was independent of the plane of polarization even though the individual photoreceptor signals were dependent. Exactly how flies utilize information contained in light polarization patterns is still unknown, but recently Kirschfeld and Reichardt [42] succeeded in showing that the optomotor flight torque could be modulated by revolving the plane of polarization of a moving striped pattern.

Spectral Sensitivity Measurements

Most evidence indicated that color vision in flies was absent or poorly developed. However, the existence of color vision is more difficult to disprove than it is to prove. If, in fact, flies did possess some form of color discrimination as suggested by the results of Burkhardt [12, 14] and Langer [44, 45, 46], then it should be expressed in the spectral response properties of second and third order neurons as was the case in some vertebrate retinas [17, 61, 89]. Experiments were therefore performed to determine the spectral response characteristics of the on-maintained and on-off units.

Three possible situations may occur with regard to the spectral response characteristics of each unit.

Situation I: The unit's discharge pattern depends upon the stimulus wavelength.

Situation II: Stimulus wavelength and intensity are completely interchangeable with respect to the discharge behavior of the units, but the units can be classified into different populations depending on their wavelength-intensity relationship (spectral sensitivity).

Situation III: Stimulus wavelength and intensity are completely interchangeable, and all observed units have the same wavelength-intensity relationship.

Situation I could only occur after signals ultimately derived from the action of different photopigment were mixed; otherwise the principle of univariance would be violated [62]. Interaction between signals derived from two or more different photopigments have been observed in vertebrate retinas [17, 61, 89] and certainly represented the first stages of signal processing in a system capable of color vision. Complete interchangeability of light intensity and wavelength in Situations II and III is tantamount to the principle of univariance which holds for all phototransduction processes having a single spectral absorption characteristic. If the spectral sensitivities derived from the family of response-log intensity relations corresponding to various wavelengths are not identical for all units observed (Situation II) but instead, fall into two or three distinctly different classes representing different populations of units, then color vision is likely mediated through these separate populations with discrimination mechanisms occurring at higher levels. However, if all units have the same spectral sensitivity (Situation III), then nothing conclusive can be said about color vision in flies, for this result does not satisfy a sufficient condition for the existence of color blindness.

All experiments described in this chapter were performed using the direct stimulating apparatus which was especially designed for accurate control of the stimulus intensity within the near ultraviolet-visible spectrum (300-700 mμ). The test of Situation I was to observe the discharge patterns of both types of units as the stimulus

wavelength was changed. Experiments were performed by observing the discharge behavior of both units to five repetitions of a series of nineteen different monochromatic stimulations between 325 and 575 mμ at a fixed neutral density wedge position. The average discharge behavior of typical on-off and on-maintained units are revealed by the PST histograms of figures 5.1 and 5.2. Although the intensity of stimulation at each wavelength was not ideally constant but depended on the transmission efficiency of the interference filters and the spectral emission properties of the xenon lamp, there were no obvious indications of wavelength dependent discharge patterns as would be expected in Situation I.

The results shown in figures 5.3 and 5.4 supported the same conclusion. These results were obtained from experiments in which three monochromatic (in this case λ = 471, 523, 349 mμ) light pulses were sequentially presented at each of six intensity levels. The PST histograms of figures 5.3 and 5.4 were computed from data of 5 trials and clearly indicated that the average discharge patterns of both units did not depend upon the stimulus wavelength in other than the trivial way of having greater or smaller instantaneous discharge rates which could be interpreted to mean that stimuli of different wavelengths were effectively more or less intense as revealed by the fact that the response-log intensity relationships for these wavelengths were superimposable by appropriate shifts along the log intensity axis. Therefore, the possibility of Situation I was eliminated since both units functionally obeyed the principle of univariance

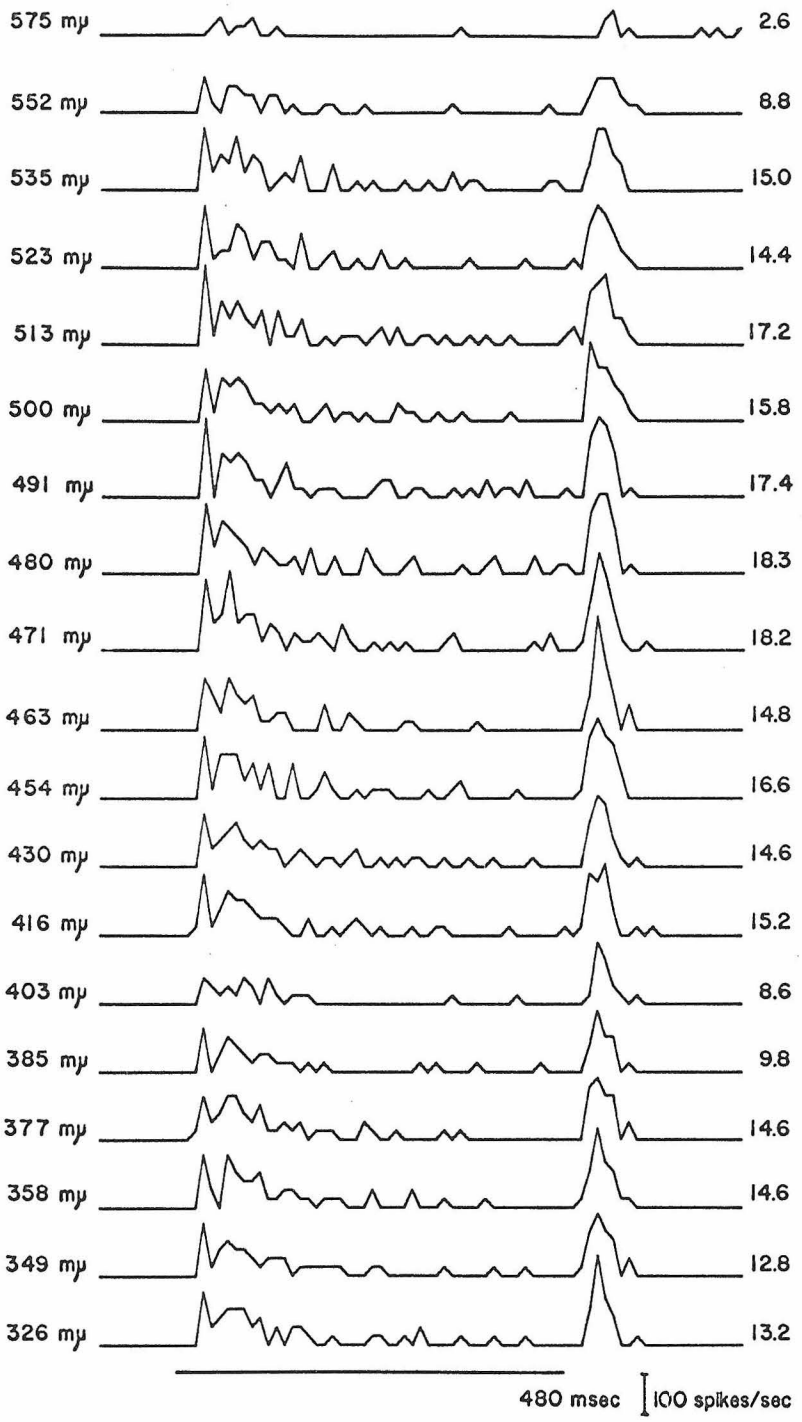

Figure 5.1 Multiple PST histograms of a typical on-off unit corresponding to monochromatic stimuli of different wavelengths. The lefthand column of figures refers to the stimulus wavelength, and the righthand column refers to the average number of spikes/stimulus based on 5 trials. B.W. = 10 msec.

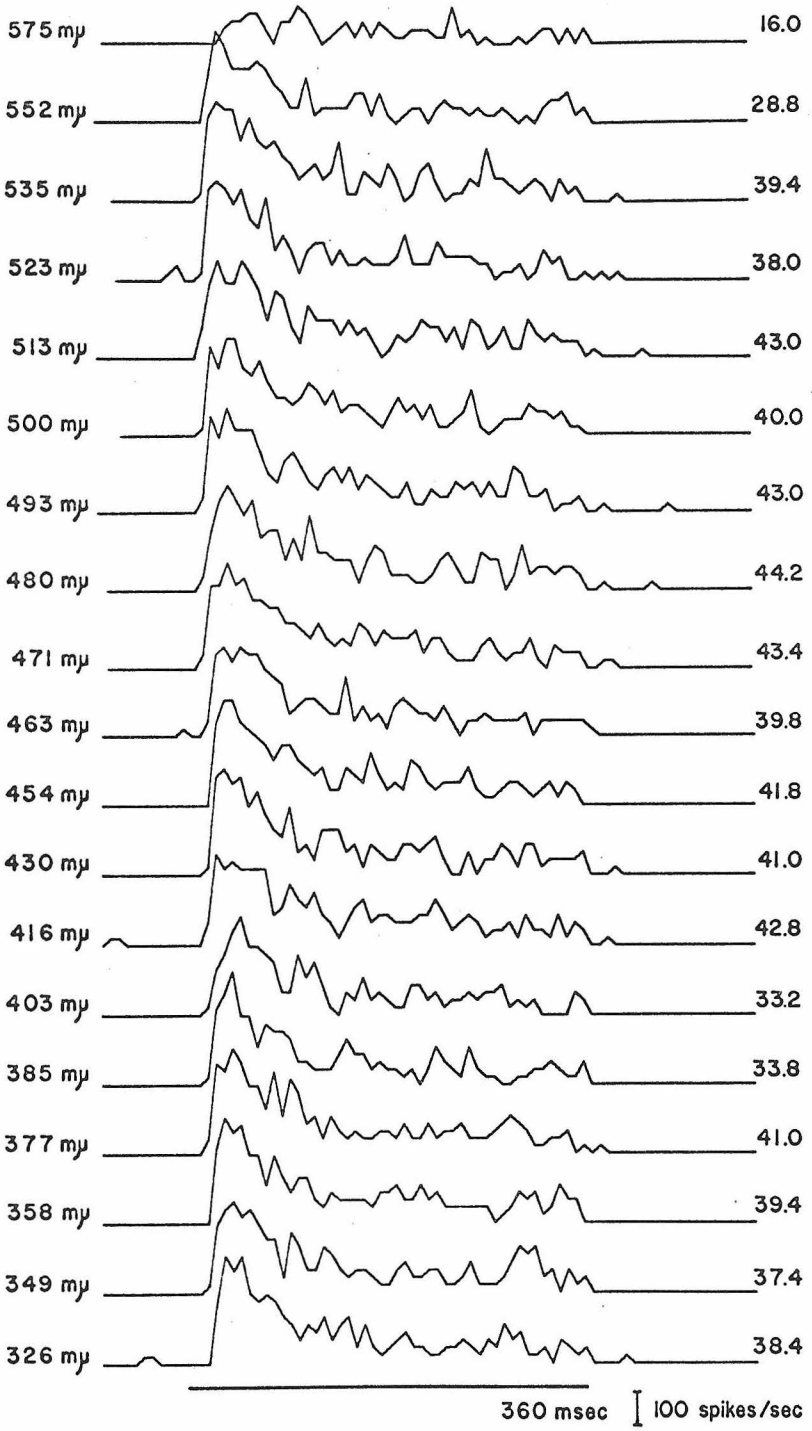

Figure 5.2 Multiple PST histograms of a typical on-maintained unit corresponding to monochromatic stimuli of different wavelengths. The lefthand column refers to the stimulus wavelength, and the righthand column refers to the average number of spikes/stimulus based on 5 trials. B. W. = 7.5 msec.

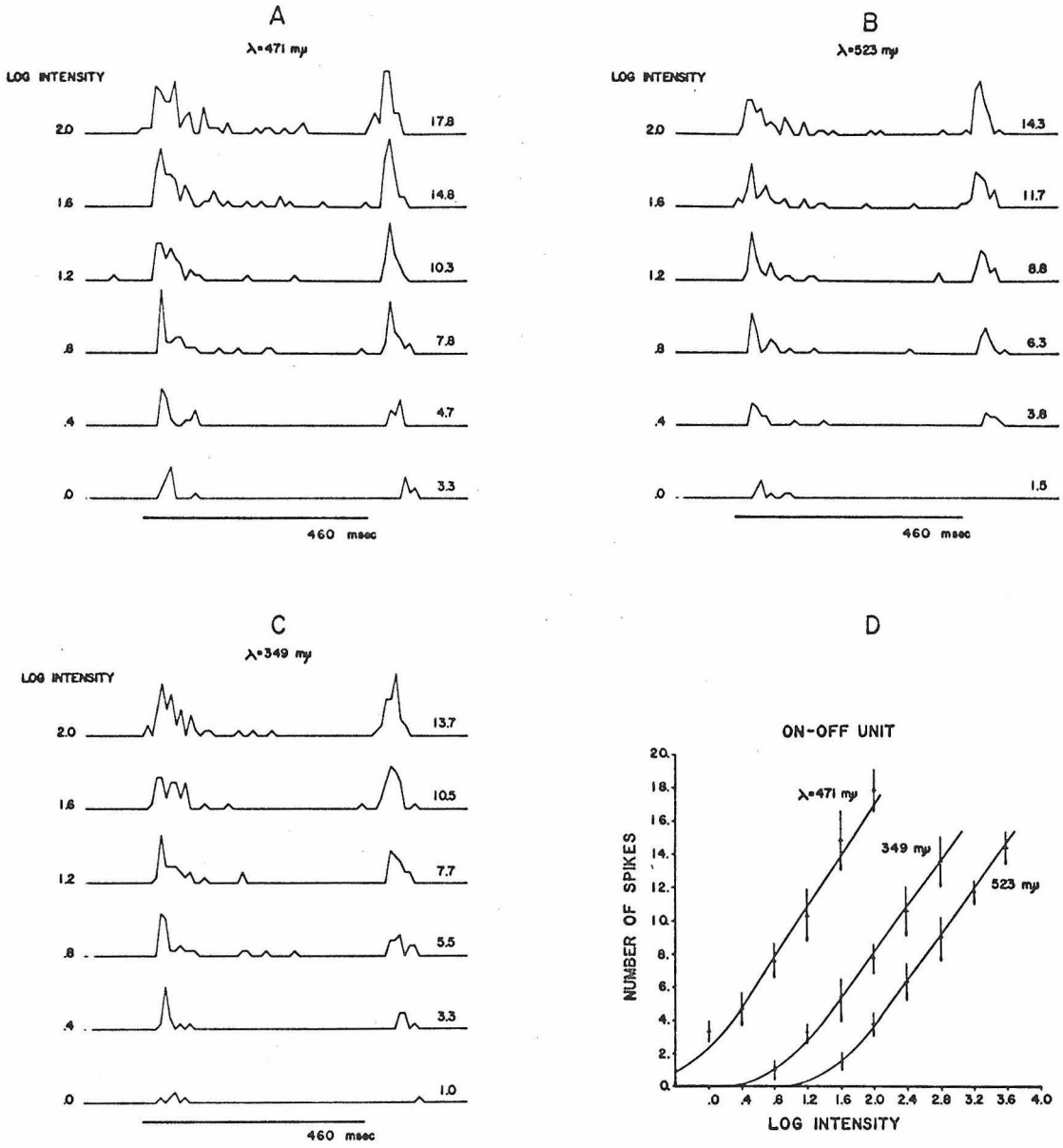

Figure 5.3 Dependence of the response-log intensity relation of a typical on-off unit on the stimulus wavelength (λ). (A) Log intensity series for λ = 471 mμ (B) Log intensity series for λ = 523 mμ (C) Log intensity series for λ = 349 mμ. Righthand column of figures refers to the average number of spikes/stimulus based on 5 trials. B.W. = 10 msec. (D) Response-log intensity relations based on data in A, B, and C. The curves have been arbitrarily shifted.

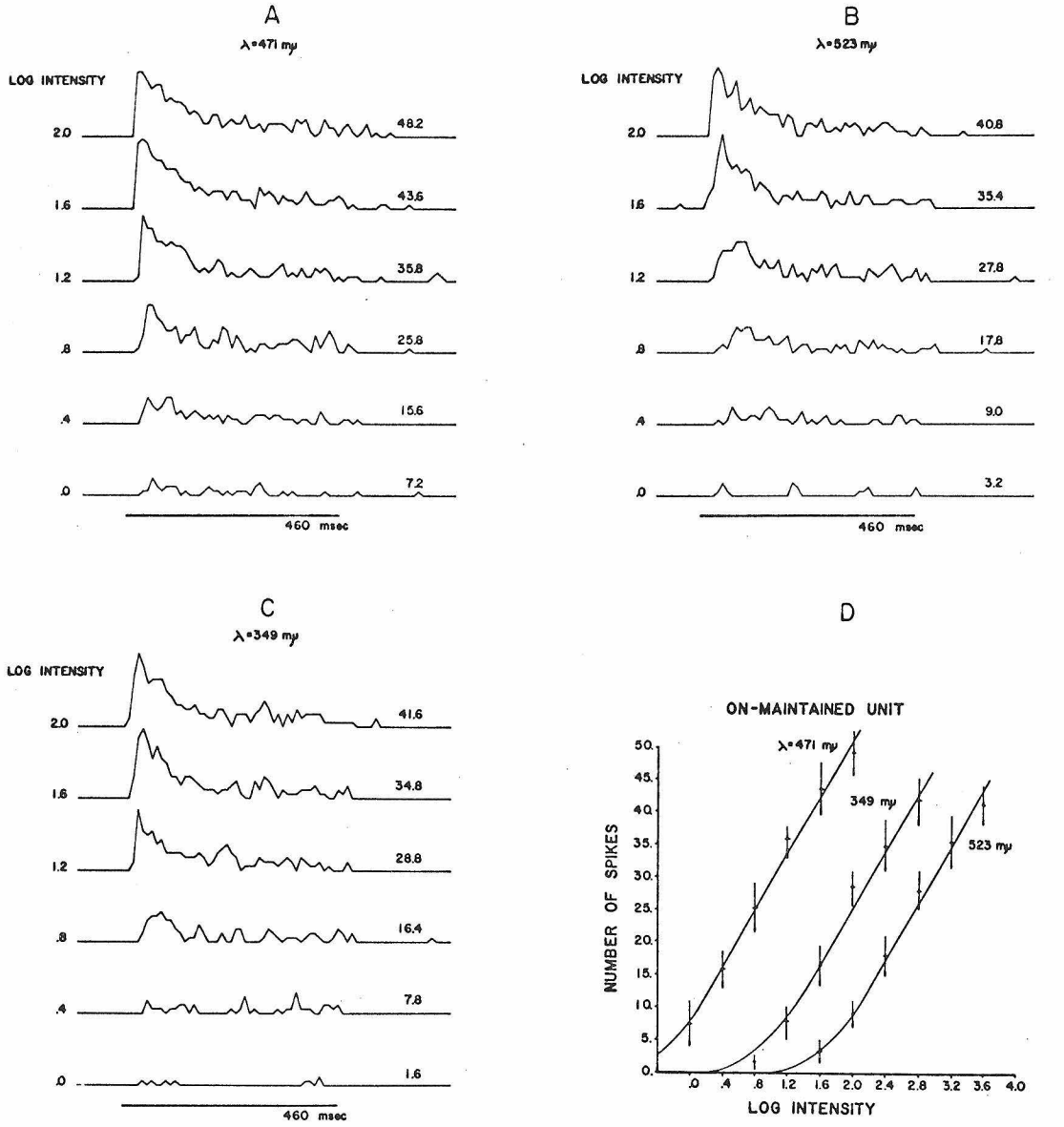

Figure 5.4 Dependence of the response-log intensity relation of a typical on-maintained unit on the stimulus wavelength (λ). (A) Log intensity series for λ = 471 mμ (B) Log intensity series for λ = 523 mμ (C) Log intensity series for λ = 349 mμ. Righthand column of figures refers to the average number of spikes/stimulus based on 5 trials. B.W. = 10 msec. (D) Response-log intensity relations based on data in A, B and C. The curves have been arbitrarily shifted.

which implied that a single photopigment was responsible for the responses observed, although the special case of the summation of signals derived from two or more different photopigments could exist.

To ascertain whether Situations II or III applied to these units, two different methods similar to those used in determining directional sensitivities were employed to measure spectral sensitivities of single units. Ideally the response-log intensity relation for each of the nineteen wavelengths should be determined, but due to the nature of discharge responses, averaging was necessary to provide sufficient accuracy (a few tenths of a log unit) in the measurement of the relative displacement of the family of response-log intensity curves. Unfortunately, such an experiment would require approximately 90 minutes to execute which was prohibitively long for several reasons, to say nothing of the hardship imposed on the experimenter. Fortunately, the principle of univariance could be applied to make the measurement feasible. Since the family of spectral response-log intensity curves were identical except for relative displacements along the log intensity axis, it was only necessary to accurately measure a single response-log intensity curve (usually corresponding to the wavelength eliciting the strongest response). After the template response-log intensity relation was determined, five or more repetitions of a series of sequential stimulations at 19 wavelengths between 326-575 mμ were made at a fixed neutral density wedge position predetermined so that the maximum

response did not fall within the saturation region of the response-log intensity curve. Occasionally the series was presented at equal quanta intensity level which required an appropriated adjustment of the wedge position for each wavelength. This was manually a much more difficult experiment to perform, but it had the advantage of immediately revealing the position of the maximum spectral sensitivity. From the spectral calibration of the light source and the template response-log intensity curve, it was a simple matter to determine the relative displacements of the family of response-log intensity curves and consequently the spectral sensitivity (method II). Utilizing the principle of univariance eliminated gathering redundant information and resulted in a feasible and relatively accurate method for determining the spectral sensitivity from spike discharge observations.

The other method (I) for measuring spectral sensitivity took advantage of the absence of dark discharge in both units. Therefore, the criterion response of a single spike was easily detectable which was not the case for units having dark discharge such as the selective motion detection units reported by Bishop [8]. Although threshold was well defined, it was not constant. Factors such as adaptation, deterioration of the preparation, and excitability changes, possibly mediated through centrifugal fibers, caused uncontrollable variations which corrupted spectral sensitivity measurements derived from a sequence of threshold measurements at different wavelengths. However, by sequentially measuring the threshold

difference between a standard wavelength, usually that having the lowest threshold, and all other wavelengths, most of the error associated with slow changes in the absolute threshold of the unit under study was eliminated. In bad cases, the absolute threshold (threshold of standard) was observed to change in the course of an experiment by as much as .6 log units. If the difference method was not used, the resulting spectral sensitivity would be seriously in error. This method was also used for determining the spectral sensitivity of the on-off unit in the light adapted state since the on-off unit did not respond to steady illumination.

The spectral sensitivities of 31 on-off units and 18 on-maintained units were calculated. Although most of these units belonged to region I of the compound eye, several units from regions II and III were recorded and analyzed, and in all cases, the spectral sensitivities were in agreement with those of region I units. Figure 5.5 shows the spectral sensitivities of three typical on-off units and three typical on-maintained units. Two of the three spectral sensitivities of both classes of units were derived from threshold measurements while the remaining one was calculated from the data of the first method (as in figures 5.1 and 5.2). The spectral sensitivities measured by the two methods were in good agreement, and the average spectral sensitivity of both types of units based on all results from both methods are shown in figure 5.6. The standard errors of spectral sensitivity for the on-maintained unit were slightly larger than those for the on-off unit due to the

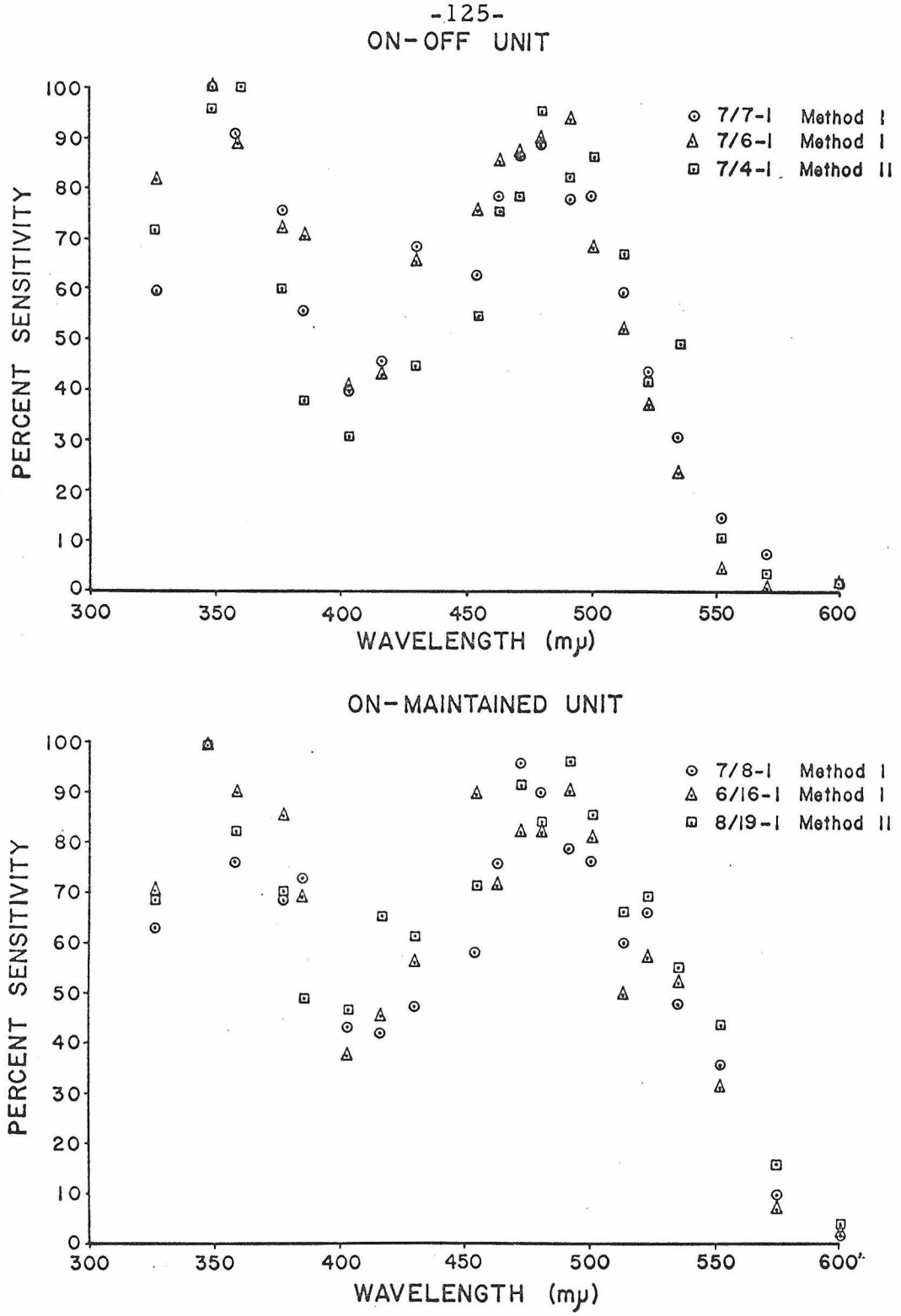

Figure 5.5 Typical spectral sensitivities of three on-off and three on-maintained units. Method I utilized threshold measurements, and method II utilized measurements of the average discharge to different spectral stimuli. (quantum basis)

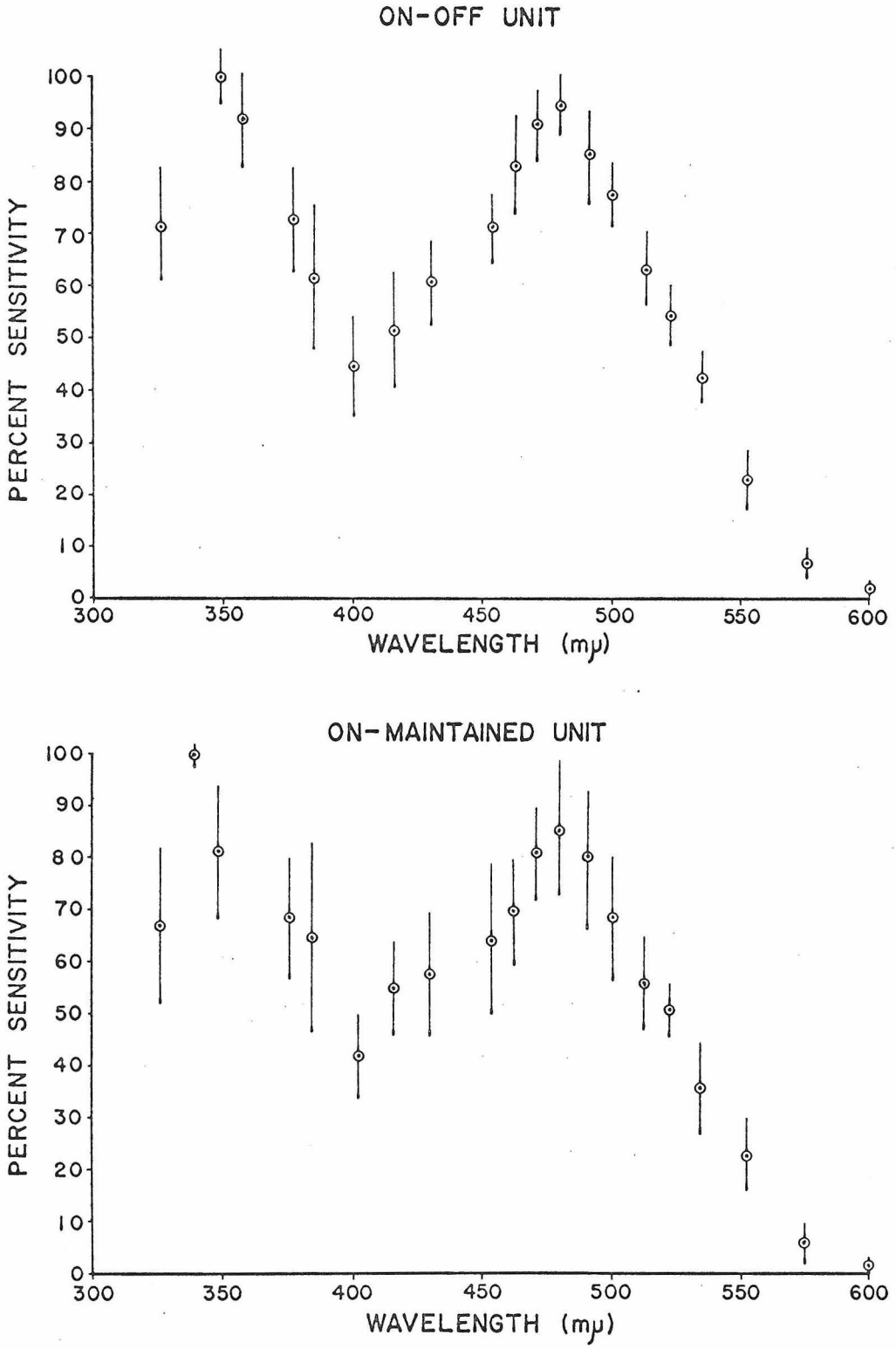

Figure 5.6 Average spectral sensitivities of the on-off and on-maintained units. The average spectral sensitivities (and $\pm$ 1 S.D.) are plotted. Spectral sensitivities are on a quantum basis.

fewer number of measurements and higher irregularity in its discharge response. The data are summarized in figure 5.7 by tallying in a histogram the locations of maximum sensitivity in the ultraviolet and visible regions of the spectrum. The peak in the ultraviolet region was relatively narrow which accounted for the small spread

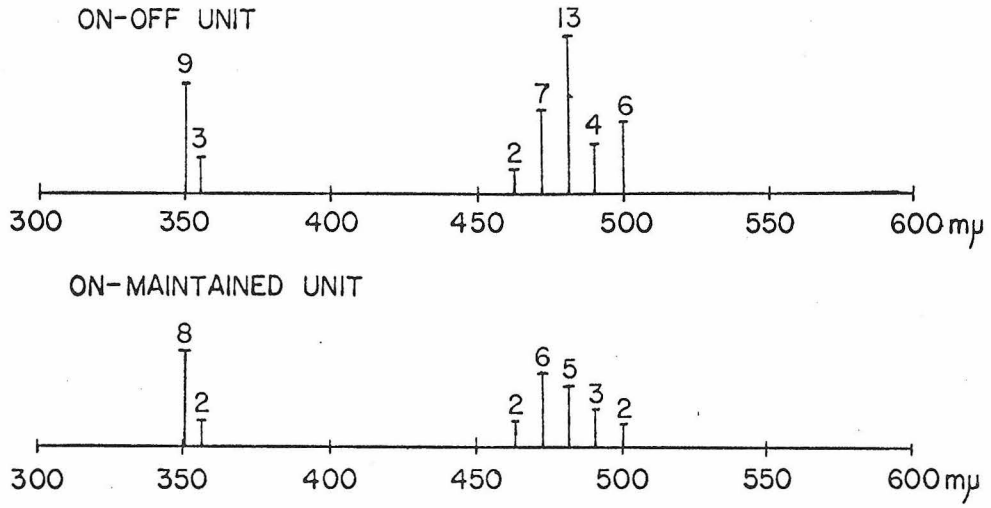

Figure 5.7 Histogram of the location of spectral sensitivity maxima. Since u.v. stimulation was unavailable for all measurements, the number of sensitivity maxima in the u.v. region does not equal that in the visible region.

in the locations of its maximum. On the other hand, the broader peak and the more closely spaced measurements in the visible region offered a better explanation of the scatter in the locations of maximum sensitivity than did the postulated existence of several different photopigments having closely spaced absorption maxima in the green region. Therefore, the spectral sensitivities of the on-off and on-maintained units sampled indicated that both units derived their input, ultimately, from photoreceptor cells containing one type of photopigment having a double peaked absorption curve with maxima at 350 mμ and 485 mμ (Situation III).

Further evidence supporting the conclusions reached from the spectral sensitivity measurements on the on-off and on-maintained units came from a limited study of the spectral sensitivity of positive slow potentials recorded in the first optic ganglion. Spectral sensitivity measurements were made on seven occasions while recording positive slow potentials (figure 3.8) from the first optic ganglion. Since it was not necessary to average slow potentials to enhance their signal to noise ratio, it was possible to record the spectral family of response-log intensity relations not possible from the discharge responses of on-off and on-maintained units. A wavelength dependent change in the waveform of the positive slow potential (or the hyperpolarizing slow potential) was never observed; only the magnitude of response was affected by the stimulus wavelength. The results of a typical experiment are shown in figure 5.8a in the form of a partial family of maximum response amplitude-log intensity curves corresponding to various stimulus wavelengths. The evoked positive slow potentials obeyed the principle of univariance previously established for the on-off and on-maintained units. The spectral sensitivities of all seven recordings were similar to that shown in figure 5.8b which was calculated from the family of response-log intensity curves, part of which is shown in figure 5.8a. Admittedly, the sample was too small to draw any conclusion about the spectral properties of these potential changes, but the limited results did support the conclusions reached from the spectral sensitivity study of on-off and on-maintained units.

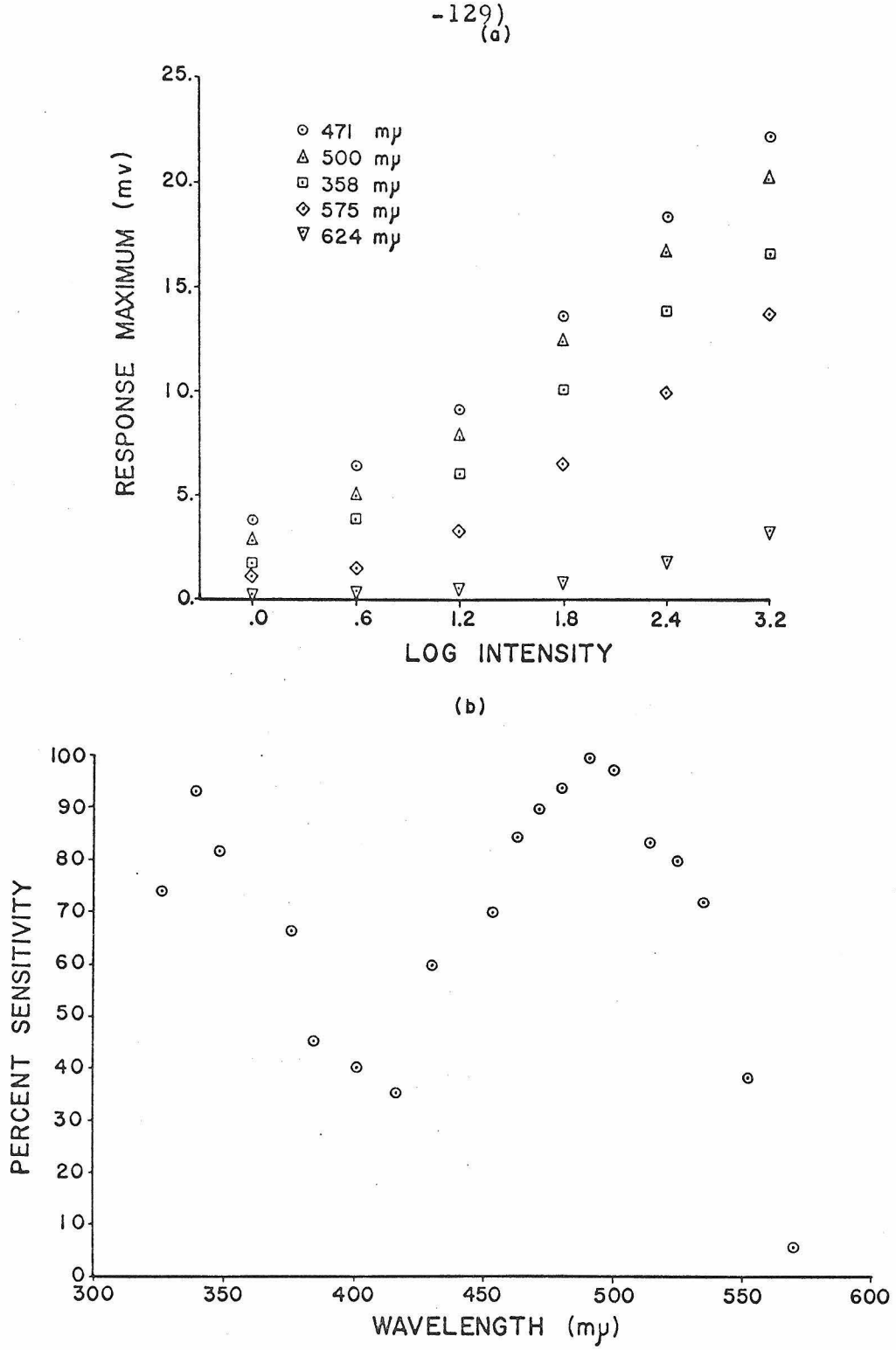

Figure 5.8 Spectral properties of the positive slow potentials recorded from the first optic ganglion (a) The maximum polarizations evoked by .5 second monochromatic pulses of light are plotted against the relative stimulus intensity. (b) Typical spectral sensitivity (partially derived from (a)) (quantum basis)

Although the previous results were consistent with the interpretation that the on-off and on-maintained units derived their input signals from photoreceptor cells containing a single type of photopigment molecule having two absorption peaks, it was also possible that two photopigments (ultraviolet sensitive, green sensitive) contributed signals to the on-off and on-maintained units in a manner which did not violate the principle of univariance. Such a situation was previously described by Goldsmith [27]. Goldsmith found that response-log intensity curves corresponding to different stimulus wavelengths derived from ERG measurements in dark adapted compound eyes of bees were superimposable by appropriate shifts along the log intensity axis which suggested that the ERG obeyed the principle of univariance. However, Goldsmith was able to show by selective spectral adaptation that at least two distinct photopigments (ultraviolet, green) were involved in the generation of the observed ERG. It was, therefore, logical to ask whether two photopigments (ultraviolet, green) were contributing to the dark adapted discharge response of the on-off and on-maintained units as suggested by the shape of their spectral sensitivities (figure 5.6). The problem was formulated in terms of the following three hypotheses:

Hypothesis I: Two populations of photoreceptor cells, one having an ultraviolet sensitive photopigment and the other having a green sensitive photopigment, contribute signals to the on-off and on-maintained units in such a manner that their dark adapted discharge properties suggest that

only a single photopigment having two absorption maxima is involved.

Hypothesis II: One population of photoreceptor cells, each containing a complement of an ultraviolet sensitive photopigment and a green sensitive photopigment, is responsible for the observed spectral sensitivity of the on-off and on-maintained units.

Hypothesis III: One population of photoreceptor cells, each containing a single type of photopigment which absorbs ultraviolet and green photons most efficiently is responsible for the observed spectral sensitivity of the on-off and on-maintained units.

In order to ascertain which hypothesis was correct, a series of experiments was performed based on the principle of selective spectral adaptation. Selective spectral adaptation has effectively been employed by others [12, 14, 27, 89] to solve similar problems of compound eye vision. The idea behind selective spectral adaptation as applied to the multi-photopigment question was essentially that if there were two (or more) populations of photoreceptors, based on their spectral absorption properties, which contributed to an observed signal (ERG, unit discharge, behavior), then an

appropriately chosen steady monochromatic adapting light would differentially attenuate the contribution of each population to the observed signal, and if only one population of photoreceptors existed, then differential adaptation would not be observed. Although the principle appears simple and straightforward, erroneous conclusions can be drawn if the limitations and assumptions of this method are not understood.

The method of selective adaptation depends entirely upon the mechanisms and sites of light adaptation about which little is known in the compound eyes of fast flying insects. Goldsmith [29] studied light adaptation in the compound eyes of honey bees by observing the ERG under different light adapted conditions. He found that light adaptation took place within a few seconds of the onset of a steady adapting light, but that dark adaptation was considerably slower. Furthermore, increment threshold measurements obeyed the Weber-Fechner Law, and the response-log intensity curves under different adapting conditions appeared identical except for shifts along the log intensity axis. By recording intracellular photoreceptor potentials in honey bees, Naka [60] also observed the nearly instantaneous time course of light adaptation but interpreted the shift of the response-log intensity curve along the log intensity axis upon the application of a steady background light as an apparent phenomenon rather than real. Instead, he showed that the presence of a steady adapting light merely shifted the dynamic range of the response along the dark adapted response-log intensity characteristic

which could be construed as a shift along the log intensity axis if the response was measured in terms of the stimulus evoked membrane potential change rather than the sum of this change and the initial potential change occurring when the steady background stimulus was initiated. He concluded that light adaptation in the honey bee was not mediated by lateral shifts of the response-log intensity curve but was a consequence of the initial transient phase of the photoreceptor response.

Considerably more is known about light adaptation in the vertebrate eye. Although it is surely an oversimplification, light adaptation can be considered to be of two types excluding purely mechancial methods as pupil constriction and shielding pigment movement. Bleaching type adaptation occurs when a significant portion of the total amount of receptor photopigment is bleached (made visually inactive) thereby decreasing the probability of photon capture which is manifested in a lower sensitivity. Field or neural adaptation occurs in the presence of a steady adapting light which can be interpreted as resulting from shifts of the operating point along the non-linear response-intensity curve thereby requiring a greater stimulus intensity to evoke a criterion response. Bleaching and neural adaptation have several distinguishing features. Whereas neural adaptation is effective for low as well as high background intensities, bleaching adaptation is effective only when a considerable portion of the photopigment molecules is bleached which requires high levels of background illumination. The time courses of both

types of adaptation differ with neural adaptation taking place almost instantaneously while bleaching adaptation requires minutes for completion. Although both types of adaptation are considered to occur primarily in the receptors, they may also occur in higher order neurons especially if bleaching type adaptation is defined in terms of transmitter depletion.

Based on the evidence provided by Naka [60] and Goldsmith [29], it appears that light adaptation in the bee compound eye is primarily of the neural type. The action of light adaptation on the response-log intensity characteristic of a photoreceptor can be mathematically described by equation 6 where

$$V_p = K \log_{10} (1 + \frac{I_b + I}{Id}) \qquad K = \text{constant} \qquad (6)$$

Id, the dark light intensity, locates the curve along the log intensity axis. In the absence of background light ($I_b = 0$), the relationship between the maximum photoreceptor depolarization (V_p) and the intensity (I) of a test stimulus is represented by curve A of figure 5.9a. If the photoreceptor was able to maintain its maximum depolarization, then in the presence of steady adapting lights (I_{b_1}, I_{b_2}), the response-log intensity relations would be represented by curves B and C. However, the photoreceptor depolarization is not maintained at its maximum but instead falls to a lower steady depolarization which is represented in figure 5.9a by vertical shifts of curves B and C to curves D and E. This description can be taken one step further by noting that if only the test stimulus evoked potential

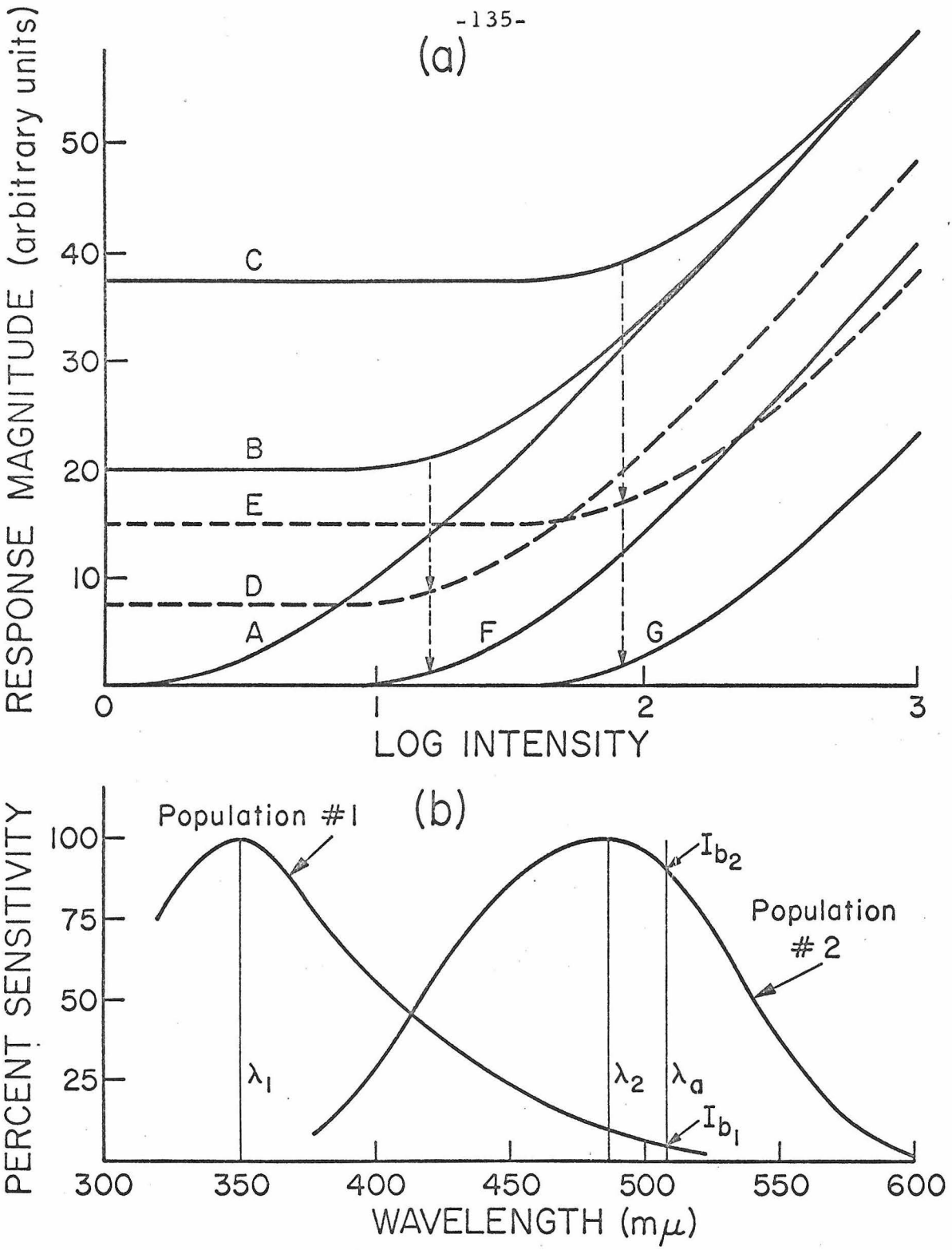

Figure 5.9 Selective spectral adaptation (a) Hypothetical photoreceptor behavior under adaptation conditions (b) Spectral sensitivities of two hypothetical photoreceptor populations.

changes are plotted against log intensity, as by Goldsmith [27], then curves F and G represent the response characteristics in the presence of steady adapting lights (I_{b_1}, I_{b_2}) and illustrate the apparent lateral shift of the response-log intensity relation under light adapting conditions.

Selective adaptation of a retina containing two populations of photoreceptors desensitizes one population more than the other if the wavelength of the monochromatic adapting stimulus is judiciously selected. Consider the situation illustrated in figure 5.9b. The wavelengths (λ_1, λ_2) of two monochromatic test stimuli are chosen to coincide with the wavelengths maximally absorbed by the two photoreceptor populations. For simplicity, the dark adapted response-log intensity relations for both populations are identical and are represented by curve A in figure 5.9a. In the presence of a steady monochromatic adapting light (λ_a) having effective intensities for both populations of I_{b_1} and I_{b_2}, the light adapted response characteristics for the two populations are given by curves B, D, F and C, E, G depending on your interpretation. Whereas the sensitivity of both populations in the dark are identical, under selective adaptation, both populations are desensitized by different amounts. Differential desensitization of the two photoreceptor populations by selective adaptation causes the contribution from one photoreceptor population to an observed signal which sums responses from both populations (e.g. ERG) to exceed that from the other population. This is manifested by unequal elevations of the observed signal

thresholds to the two test stimuli during selective adaptation. If only one population of photoreceptors exists in the retina, then selective adaptation would raise the threshold of the observed signal equally at both test wavelengths.

It was assumed that the mechanism of light adaptation in the fly was the same as that described for the bee. Therefore, a steady background light desensitized the photoreceptor cells rather than the photopigments which implied that selective adaptation would, at best, distinguish Hypothesis I from Hypotheses II and III. Under these circumstances, Hypotheses II and III were functionally indistinguishable and compatible with a system incapable of color discrimination. The important distinction, however, was between Hypothesis I and Hypotheses II and III (i. e., two populations of photoreceptors versus one population of photoreceptors), for if two populations of photoreceptors existed, then the basic requirement for color vision in flies would be established even though the evidence reported in this thesis did not indicate that color discrimination was mediated through the on-off and on-maintained units. It was also assumed that most of the observed desensitization resulting from the application of a steady background light occurred in the photoreceptors.

Fortunately, the on-off unit did not respond to steady background illumination, thereby making the discharge of a single spike a well-defined criterion response for selective adaptation experiments. The second light source and path, described in Chapter II,

supplied a steady monochromatic adapting stimulus of wavelength 508 mμ. The time course of light adaptation was found to be too rapid to measure and therefore consistent with the assumptions that adaptation in the fly was primarily neural and located in the photoreceptor membrane. Furthermore, dark adaptation was slow (order of three minutes), and the rate of dark adaptation was not constant but depended upon the intensity and duration of the light adaptation stimulus.

The two test stimuli used in the selective adaptation experiments had wavelengths of 349 and 491 mμ corresponding to the location of the spectral sensitivity maxima while the wavelength of the steady adapting stimulus was usually 508 mμ. Selective adaptation in eight units was studied, and in all, the difference between the thresholds of the two test stimuli in the dark was not significantly altered by the presence of steady monochromatic adapting stimuli having intensities up to approximately 2.5 log units above the dark adapted threshold intensity. The maximum intensity of the steady adapting stimulus raised the threshold of the unit by approximately 2.0 log units.

On several occasions the spectral sensitivities were measured (threshold method) during the presentation of steady monochromatic background light (λ = 501 mμ). The log spectral sensitivities of a typical unit measured in the dark and in the presence of a steady monochromatic background light are shown in figure 5.10. The steady background stimulus desensitized the unit by 1.6 log units

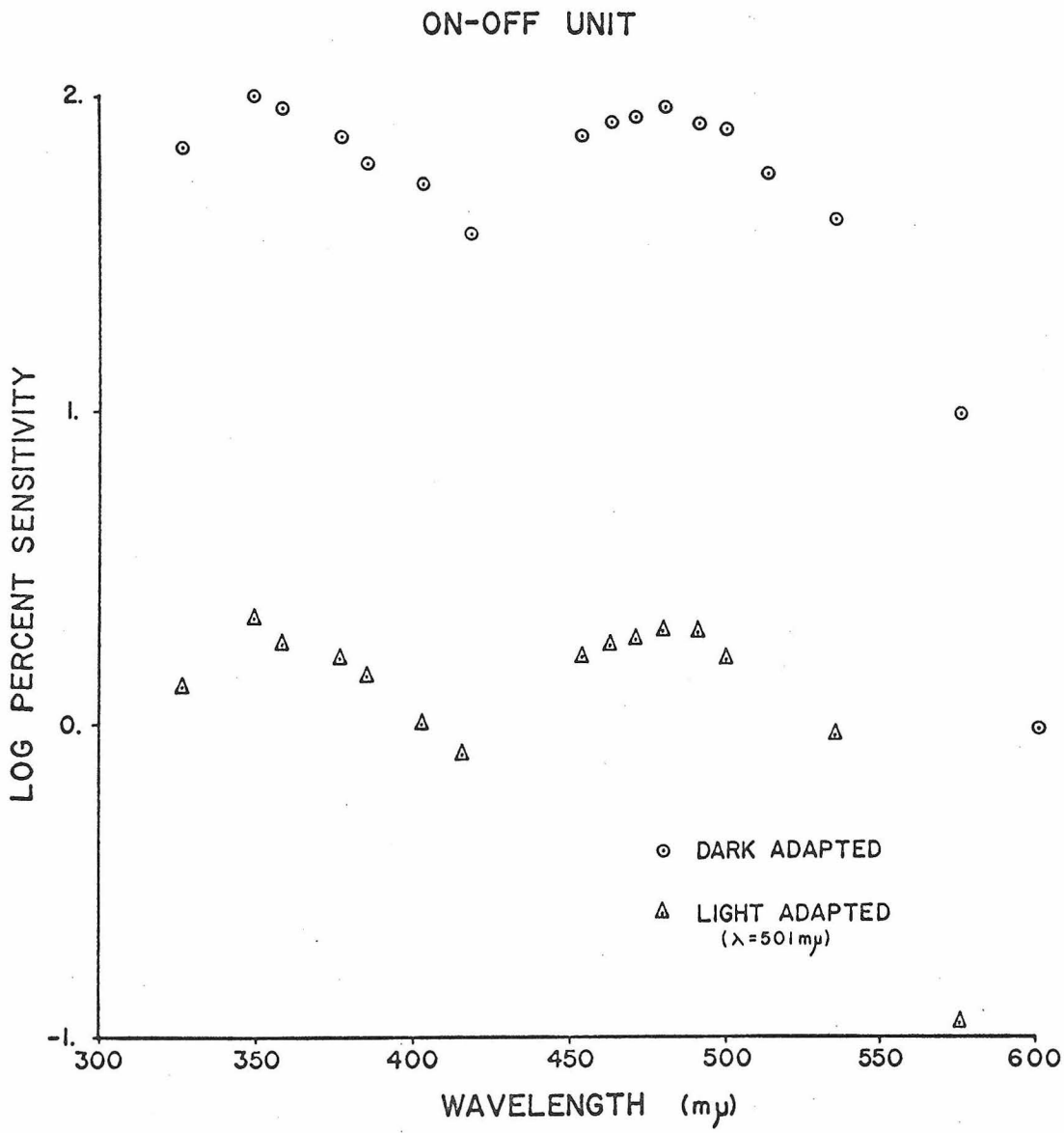

Figure 5.10 Effect of selective adaptation on the spectral sensitivity of the on-off unit ⊙ -spectral sensitivity of a dark adapted unit △ - spectral sensitivity of the same unit when adapted to a steady spectral light (λ = 501 mμ). Sensitivities were derived from threshold measurements (quantum basis).

without affecting the shape of the spectral sensitivity curve. Furthermore, it did not cause a Purkinje shift in the spectral sensitivity, although evidence for one has been provided by others [21,28]. The results of these experiments supported Hypothesis III that a single photopigment having a double peaked spectral absorption characteristic was responsible for the spectral properties of the on-off and on-maintained units.

Polarization Sensitivity Measurements

There were two main reasons for studying the effect of polarization on the discharge behavior of the on-off and on-maintained units. First, light polarization had been observed to influence photoreceptor activity and flight torque behavior which made it logical to study how polarization information transduced by the photoreceptors was processed by on-off and on-maintained units if at all. Secondly, observation of on-off or on-maintained unit sensitivity to the plane of polarization would provide information pertaining to the anatomical correlates of these units, for it was suspected that of all the fibers traversing the intermediate chiasma only the long visual fibers would demonstrate polarization sensitivity.

The experiments were performed with the direct stimulating apparatus, and the plane of polarization was controlled manually by revolving the polarizer shown in figure 2.3. The units were recorded while repeatedly presenting a series of twelve .5 second pulses of monochromatic light (λ = 491 mμ) each of which had a different plane

of polarization separated by multiples of 30 degrees. Neither the on-off or on-maintained unit demonstrated any sensitivity to the plane of polarization. Threshold measurements at different polarization orientations were made without any evidence of a preferred orientation. Experiments were also performed in which a steady monochromatic light (λ = 491 mμ) was presented to the eye while its plane of polarization was rapidly rotated. Again neither unit appeared to sense the change in the plane of polarization.

CHAPTER VI

FUNCTIONAL INTERACTIONS

Introduction

It was possible to observe the discharge behavior of single units in the first, second, and third optic ganglia. Therefore, the question of how the activity of one unit affected the activity of another unit (functional interaction) immediately arose. Similar questions have often been posed before, but it was not until computers became practical laboratory tools and the development of statistical methods for analyzing simultaneously recorded spike trains that such questions could be answered quantitatively. The recent discovery [19] that inward motion detection units in the right and left third optic ganglia are mutually inhibitory is a particularly good example of functional interaction revealed by crosscorrelation analysis. It was virtually impossible to detect this functional interaction from the discharge patterns of both units without crosscorrelation analysis.

Directional selective motion detection units, medulla on-off units, on-maintained units and on-off units were simultaneously recorded in various combinations and their functional interactions are described in this chapter. Also included is a discussion of the limitations of the crosscorrelation analysis as revealed by the present application of the technique.

Functional Interactions

The crosscorrelation $R_{AB}(\tau)$ of unit B with respect to unit A is an estimator of the probability of a "B" discharge at time τ given an "A" discharge at time zero for $\tau > 0$ and the probability of an "A" discharge at time $|\tau|$ given a "B" discharge at time zero for $\tau < 0$.

$$R_{AB}(\tau) \approx \text{Prob ("B" discharge } t = \tau / \text{"A" discharge } t = 0) \quad \tau > 0$$

$$R_{AB}(\tau) \approx \text{Prob ("A" discharge } t = |\tau| / \text{"B" discharge } t = 0) \quad \tau < 0$$

$$= R_{BA}(-\tau)$$

Depending upon the type of structural interaction existing between the two units under study, the crosscorrelogram may take on any of several characteristic signatures [67, 54]. Unilateral excitation or inhibition is the easiest signatures to identify due to the elevated or reduced probability of discharge on one side of zero in the crosscorrelogram. The mutual inhibition between inward motion detection units in opposite optic lobes of the fly was manifested in the crosscorrelogram by valleys of reduced discharge likelihood on both sides of zero. Other types of functional interaction include combinations of excitation and inhibition and common influence through another unit or units. Unfortunately, each type of interaction does not have a unique crosscorrelogram signature which seriously limits the usefulness of the technique in cases of complex interactions.

Although crosscorrelation analysis is claimed to be a powerful tool for assessing the functional interaction between two units, it

has some serious limitations which were revealed by its application to simultaneously observed on-off, on-maintained, medulla on-off, and directional selective motion detection (IIAin) units. Experiments were performed in which an on-off or on-maintained unit was recorded by one microelectrode in the intermediate chiasma while a IIAin unit was recorded by another microelectrode in the contralateral third optic ganglion. The purpose of the experiments was to ascertain the role of the on-off and on-maintained units in the mechanism of directional selective motion detection. Crosscorrelograms should be computed from the TOE's of two units while in the absence of stimulation, otherwise the crosscorrelations are confounded with common stimulus effects. Although IIAin units were spontaneously active, the on-off and on-maintained units were not which made it necessary to apply a stimulus. The stimulus was a striped pattern ($\lambda = 6°$) moving in the preferred direction and repeatedly presented for 3 seconds every 7 seconds. In order to minimize the common stimulus component in the crosscorrelogram between IIAin units and on-off or on-maintained units, the stimulus was centered on the receptive field center of the chiasma unit and subtended only about 10 degrees. Typical correlations of IIAin units with on-off and on-maintained units are shown in figures 6.1 and 6.2. Correlograms A and B in each figure represent autocorrelations of the two units involved, and correlogram C represents the crosscorrelations. Crosscorrelogram (a) was computed from the original TOE data sets, whereas crosscorrelogram (b) was computed from modified TOE

data sets resulting from shifting the TOE's belonging to the IIAin unit by the stimulus period (7 sec.). Shifting [67] has the effect of eliminating true interaction components from the resulting crosscorrelogram while preserving the common stimulus induced components. In this way, the significance of a feature in the unshifted crosscorrelogram could be tested by computing the shifted crosscorrelogram. As revealed in figures 6.1 and 6.2, a positive correlation existed between the IIAin unit and the on-off and on-maintained units, but the correlation was small in magnitude and centered about zero. Several correlation runs revealed no correlation, and for those that did, it was always centered near zero and not a common stimulus artifact since the positive correlation was eliminated by shifting. These results indicated that the activity of both the on-off and on-maintained units influenced that of the IIAin unit which was expected from gross anatomical considerations, but that the interaction was small and impossible to interpret. These examples demonstrate that crosscorrelation analysis is ineffective when the two units under study are not pre-postsynaptic pairs [54]. The great success of crosscorrelation analysis applied to different combinations of directional selective motion detection units can be attributed to their spontaneous activity and to their anatomical "closeness," neither of which exists for combinations of chiasma units and directional selective motion detection units.

Experiments were also performed in which medulla on-off units and chiasma on-off units were simultaneously recorded, but

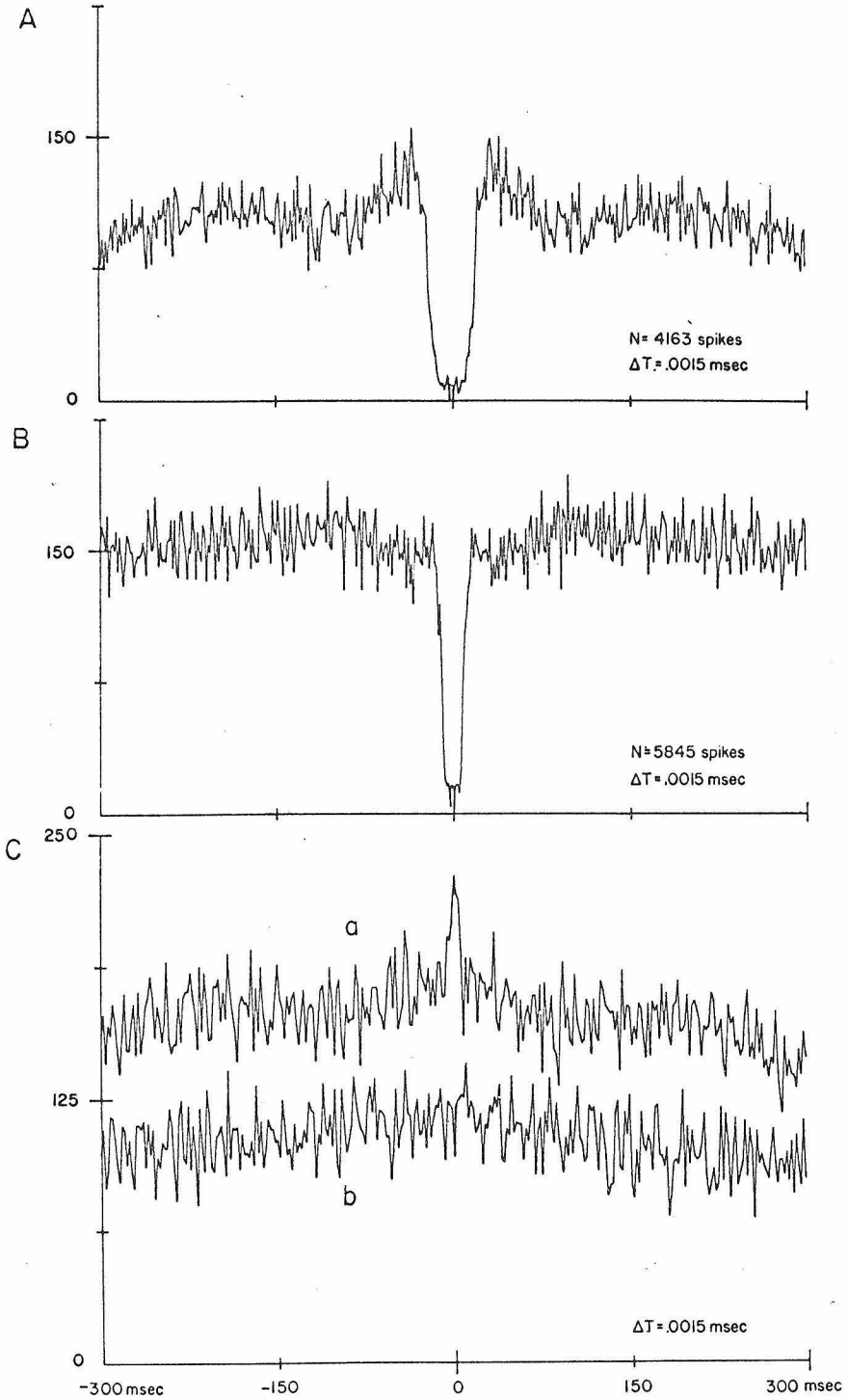

Figure 6.1 Correlation of a directional selective motion detection unit (IIAin) with an on-off unit (A) Autocorrelation of the on-off unit (B) Autocorrelation of the IIAin unit (C) Crosscorrelation of the IIAin unit with the on-off unit (a) Normal crosscorrelation (b) Shifted crosscorrelation Stimulus: repeated presentation of a striped pattern moving in the preferred direction Ordinate: number of coincidences Crosscorrelation (b) was shifted downward for clarity.

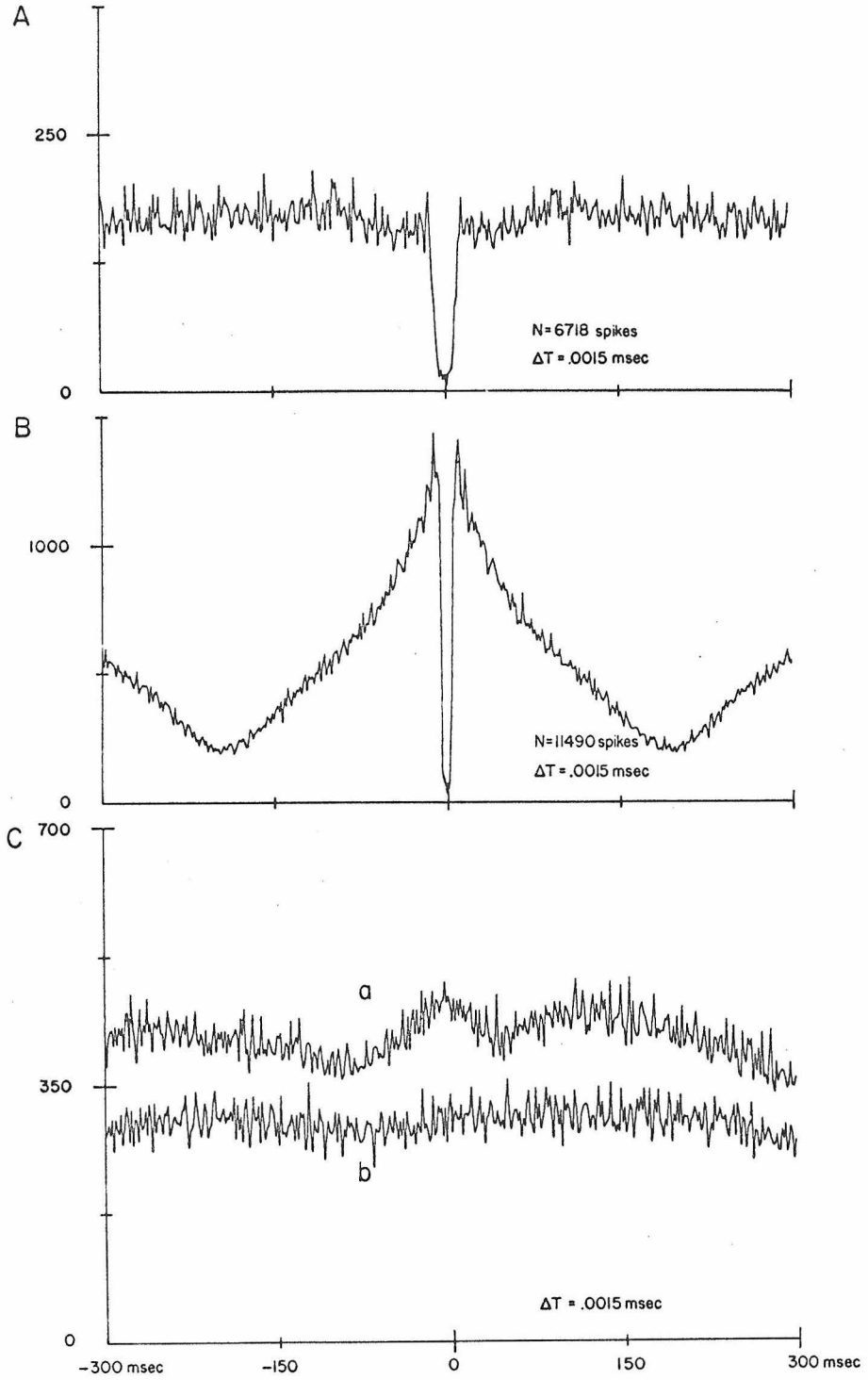

Figure 6.2 Correlation of a directional selective motion detection unit (IIAin) with an on-maintained unit (A) Autocorrelation of the IIAin unit (B) Autocorrelation of the on-maintained unit (C) Crosscorrelation of the IIAin unit with the on-maintained unit (a) Normal crosscorrelation (b) Shifted crosscorrelation Stimulus: repeated presentation of a striped pattern moving in the preferred direction Ordinate: Number of coincidences Crosscorrelation (b) was shifted downward.

only one recording was made when the receptive fields of both units overlapped (figure 4.15). Since neither unit was spontaneously active, a moving striped pattern was presented to the union of the two receptive fields. In this case, the stimulus was constantly applied until the desired number of TOE's was generated. The correlations of these two units are shown in figure 6.3, and the crosscorrelogram (a) is characterized by an elevated correlation within 15 msec on both sides of zero. Several bursts occurred during the record, and it was suspected that they were responsible for the positive correlation. However, the positive correlation remained after the bursts were eliminated from the records (crosscorrelation (b)). Removing the bursts did eliminate a positive correlation having a wide spread which is not apparent in the crosscorrelograms a and b since the maximum lag is too short. Such a wide positive correlation results when the discharge rates of both units are correlated as they are during a burst. The true positive crosscorrelation occurring within $\pm$ 15 msec. was larger than that of the previously described examples (figures 6.1, 6.2), but it was not strong or easily interpreted. The medulla on-off units were recorded from the vicinity of the serpentine layer of the second optic ganglion, and it is entirely possible that they represented fourth or higher order units.

As it was not difficult to simultaneously record on-off and on-maintained units with a single microelectrode, their correlations were studied. These units are obviously anatomically "close", but

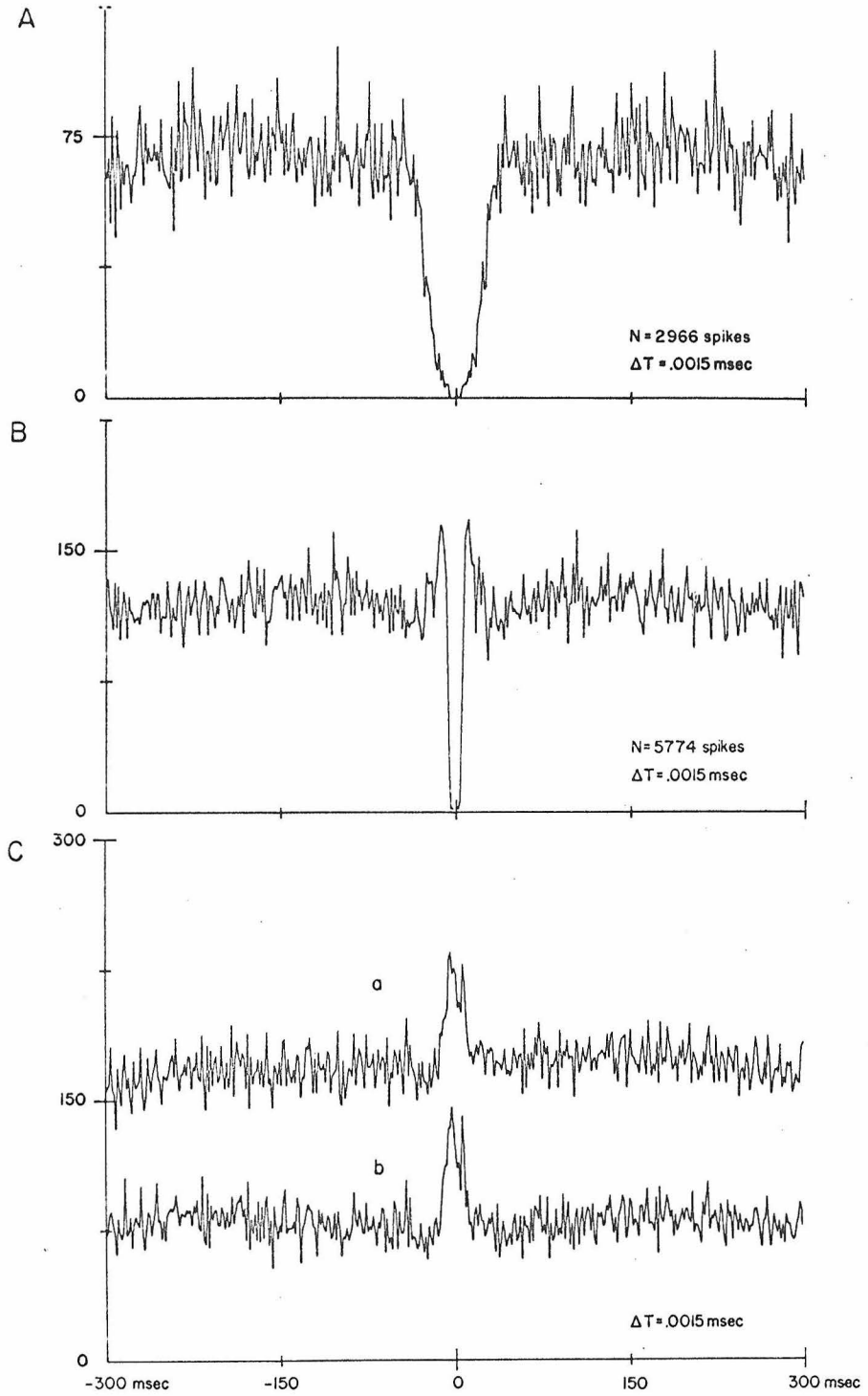

Figure 6.3 Correlation of a medulla on-off unit and on-off unit (A) Autocorrelation of the on-off unit (B) Autocorrelation of the medulla on-off unit (C) Crosscorrelation of the medulla on-off unit with the on-off unit (a) Normal crosscorrelation (b) Crosscorrelation with burst discharges removed. Crosscorrelation (b) shifted downward for clarity. Stimulus: continuous motion of a striped pattern $\lambda = 8^{o}$. Ordinate: number of coincidences.

their crosscorrelation revealed no indications of functional interaction other than that resulting from the common stimulus. It is possible that both units do indeed interact as suggested by their discharge properties described in the preceding chapters, but that their interaction is via slow potentials and not manifested in the crosscorrelogram. If one unit directly influences another unit via slow potentials, the discharges of both units could conceivably be independent, and only their discharge rates would be correlated.

In summary, strong functional interaction was not demonstrated between the chiasma units and other readily observed units in the second and third optic ganglia. Presumably, the weak correlations resulted because the units were separated by at least one interneuron.

CHAPTER VII

DISCUSSION OF RESULTS

Introduction

A major portion of the work described in the previous chapters was directed toward answering questions about the visual information encoding properties of the on-off and on-maintained units recorded from the intermediate chiasma. In addition, effort went into ascertaining the anatomical origin of the electrical signals observed. Therefore, the results pertaining to the spatial, temporal, spectral, and polarization information processing properties of these units and their significance will be discussed, followed by a discussion of the possible anatomical correlates of the on-off and on-maintained units. The chapter will conclude with a discussion of the role of these units in the mechanism of directional selective motion detection.

Mode of Information Transmission

Several investigators [6, 56, 72] have expressed surprise not to discover any evidence of spike potentials in the retina or first optic ganglion of the compound eye of flies, and justifiably so, for it is hard to imagine slow potentials passively transmitting information to the second optic ganglion over the relatively long intermediate chiasma (approximately 200μ). However, slow potentials appear to be a major mode of signal transmission in the outer plexiform layer of the vertebrate retina]38, 88] and in some

compound eyes [56, 72, 85] where only short communication distances are involved. The observation of discharge potentials in the intermediate chiasma and the demonstration that the discharges are centrally directed, show that some information is transmitted across the intermediate chiasma by spikes. The site of impulse generation is not known, but based on the apparent absence of spike potentials from the first optic ganglion (except for the two instances of deteriorated spike observations described in Chapter III) and their existence in the intermediate chiasma, it is attractive to hypothesize that spike potentials are generated near the inner margin of the first optic ganglion. The question of the mode of information transmission is not entirely settled, for only two types of units (on-off and on-maintained units) have been observed in the intermediate chiasma, and judging from neural anatomical evidence, at least six different centripetal fibers associated with each cartridge exist in the intermediate chiasma. Two of these fibers belong to the superior and inferior central photoreceptor cells which must transmit their signals the farthest since they originate in the retina and terminate in the second optic ganglion. If they do support impulse traffic, as it appears they must, then this property would differentiate them from photoreceptor cells 1-6 which are believed to be incapable of generating spike potentials. It is entirely possible that the central photoreceptors are, in this respect, analogous to the eccentric cells found in some arthropod compound eyes.

Spatial Information Processing

The shape of the receptive field, of the on-off unit is elliptical, and for all cases observed in this study, the major axis of the receptive field was found to roughly coincide with the medio-lateral axis of the compound eye. The best available data pertaining to the size and shape of fly photoreceptor receptive fields come from the work of Burkhardt et al. [12, 14] in which the photoreceptors of Calliphora in region I of its compound eye were found to have approximately circular receptive fields with an average half sensitivity angle of 3.3 degrees. Obviously, substantial spatial integration occurs between the photoreceptors and the on-off unit. Each cartridge in the first optic ganglion receives primary excitation from six photoreceptors belonging to six different ommatidial and having identical optical axis which suggests that the size of the "receptive field" of each cartridge is roughly the same as that of the photoreceptors forming each cartridge. Assuming that the positive slow potential recorded from the first optic ganglion reflects cartridge activity as Scholes [72] suggests, then the close agreement between the half sensitivity angle values derived from photoreceptor potential and positive slow potential measurements supports this belief. Therefore, an on-off unit associated with one cartridge must partially integrate the activity from neighboring cartridges. Apparently the summation is more extensive along the medio-lateral axis. Although it is not manifested in all horizontal directional sensitivity measurements, in many cases, there appears

to be another form of receptive field asymmetry. It is best demonstrated by the equi-response contours of figures 4.2 and 4.15 in which the contours are more closely spaced on the lateral side of the receptive field center. This represents a more abrupt response efficiency change as the stimulus moves laterally from the field center than when it moves medially. The functional aspects of spatial summation must have their anatomical counterpart and will be discussed later.

The receptive field organization of the on-maintained unit is more complicated than that of the on-off unit due to the presence of three receptive field regions defined in terms of the type of discharge their stimulation elicits. In terms of response magnitude (total number of spikes elicited), the center on region clearly dominates, but if the total receptive field including both antagonistic off regions is considered, the over-all shape is roughly elliptical with a major axis orientation identical, within observational errors, to that of the on-off unit receptive field. The 2.5 degree half directional sensitivity angle of the center region is comparable to that of the photoreceptors and indicates that the on region response reflects the activity of a single cartridge. Although directional sensitivity measurements were not performed on the off regions, their size as indicated in figure 4.1 appears to be slightly larger than the size of the center on region. The off region centers are displaced (medially and laterally) relative to the on region center by 3-4 degrees. This exceeds the interommatidial angle (2.5

degrees) in this region of the eye [86], but since the boundary of the off region is displaced from the on region center by approximately the interommatidial angle, it is likely that the off regions are, in part, mediated by the cartridges medially and laterally adjacent to the one serving the on region.

Concentrically organized receptive fields in which the center and annulus regions are mutually antagonistic are commonly observed in second and higher order units of the vertebrate retina [38, 43, 65, 88]. A similar, though much simpler, receptive field organization is found in the compound eye of Limulus. Like the concentrically organized vertebrate receptive field, it is possible to define a surround region of the eccentric cell receptive field which when stimulated suppresses or entirely inhibits the response evoked by center region stimulation. Whereas, both regions of the vertebrate receptive field when stimulated elicit characteristic discharge patterns, only stimulation of the center region of the Limulus receptive field will evoke a discharge. The function of the more complicated vertebrate receptive field organization is still unknown, but the surround inhibition organization of the eccentric cell receptive field is believed to be a manifestation of a neural mechanism responsible for increasing the acuity of the compound eye. Several efforts [31, 56, 81] to demonstrate surround inhibition in the organization of receptive fields in the compound eyes of other insects have not met with much success. The demonstration of antagonism between the two off regions and the on region of the

on-maintained unit receptive field clearly indicates that a modified form of surround inhibition exists in flies and possibly other flying insects. The receptive field organization of the on-maintained unit in the fly differs from that of the eccentric cell of Limulus in two ways. First, the center on region is not antagonized by an annulus shaped region but rather by two roughly circular regions located on opposite sides of the on region. Second, stimulation of the antagonistic regions elicits an off discharge, and in this respect, the organization resembles that of the vertebrate retina. The functional importance of this type of organization remains uncertain. The inhibitory influence of the two off regions on the on region does narrow the on region along the medio-lateral axis, and this type of acuity enhancement may be more pronounced at higher intensity levels than those used. The functional importance of the different discharge patterns derived from the stimulation of the on and off regions is as uncertain as it is in the vertebrate retina; however, it may be involved in the mechanisms of on-off response generation as discussed later.

Temporal Information Processing

Most every visual system (and for that matter, sensory system) of fair complexity has developed temporal transformations for generating on-off responses from simple maintained receptor responses. Usually, this mechanism occurs early in the sequence of information transformations because of the importance of such a

temporal abstraction to subsequent stages of information processing. The visual system of the fly makes this particular transformation in the first optic ganglion, and it is difficult to observe units from subsequent optic ganglia which do not exhibit some form of on-off discharge.

Most of the invertebrate photoreceptor responses studied to date are similar in that they are monophasic with temporal characteristics not substantially different from those of a low-pass filter response to the stimulus. Studies [61, 85] of single photoreceptors in the compound eyes of flies have revealed that their response to a pulse of light consists of two components. The tonic component accounts for the steady state depolarization of the photoreceptor membrane while the phasic component accounts for the transient membrane depolarization following the onset of the light pulse. Both components are graded but the phasic component exhibits a pseudo-threshold behavior in that it does not approach significant magnitudes until the stimulus is sufficiently intense. At high stimulus intensities, the phasic component is often twice as large as the tonic component.

The temporal properties of the slow potentials (especially the positive slow potential) recorded from the first optic ganglion are in several respects similar to those of the photoreceptors. The monophasic positive slow potential exhibits a phasic and tonic component, but the phasic component is surprisingly much less prominent than it is in the case of the photoreceptor response.

The source of the positive slow potential is unsettled. Though Scholes [72] who first reported it in Musca domestica refers to it as a cartridge response, he implies that it is of intracellular origin. His belief was based upon the large size of the potential, its latency (1-2 msec.) with respect to photoreceptor responses, and the observation that the response could be elicited by individually stimulating each of six ommatidia arranged in the characteristic trapezoidal pattern. For an intracellular potential to satisfy the properties Scholes observed, it would most probably originate from the type I monopolar cells. However, the absence of impulses is most disconcerting, and Scholes speculates about the possibility of impulse-free transmission. Mote [56] studied the same response in another dipteran and came to the conclusion that the slow potentials were recorded extracellularly and reflected activity in a directly coupled low resistance pathway between the photoreceptor cells and sites in the first optic ganglion. Although the study of the positive slow potential reported in this thesis was limited, it was concluded that the potential was extracellular due to the absence of an abrupt membrane potential change and the ease with which the recordings were made. The most likely source of an extracellular slow potential in the first optic ganglion is from the densely packed photoreceptor endings. If this is the case, then the results described by Scholes can be explained if the recording micropipette is coupled extracellularly through a low resistance pathway to only the six photoreceptor axons of a single cartridge which is a likely possibility

since the photoreceptor axons of each cartridge are in close proximity and are isolated from the photoreceptor axons of adjacent cartridges by epithelial glial cells. This interpretation also explains the linear summation of responses from each of the six photoreceptors which Scholes observed and pondered. Although the time course of positive slow potentials are similar to that of photoreceptors, the potentials appear to have undergone some temporal smoothing possibly occurring during their passive spread from the photoreceptor layer to the first optic ganglion. Even so, it is difficult to explain the marked attenuation of the prominent phasic component of the photoreceptor response entirely in terms of low pass filtering.

Although the hyperpolarizing potential recorded from the first optic ganglion is monophasic, it does not exhibit a significant phasic component and is characterized by an extremely noisy waveform for low intensity stimulation. The noisy nature of the hyperpolarization often appeared to be associated with discrete events such as spikes or photon absorptions, though the latter seems unlikely. It was concluded, in accordance with Shaw [74], that the potential was intracellularly recorded, and from an anatomical standpoint, the cells most likely penetrated in the first optic ganglion are the epithelial glial cells which surround each cartridge. The epithelial cells resemble the Müller cells in the vertebrate retina and are intimately associated with the photoreceptor axons through captate projections which are projections of their

plasma membrane into small invaginations of the photoreceptor axon membrane. The exact source of the hyperpolarizing potential can be ascertained by dye injection, and future studies of the functional organization of the first optic ganglion should include this objective.

The average discharge pattern of the on-maintained unit when only the on region is stimulated is similar in time course to the positive slow potential and to the photoreceptor potential. It is characterized by quiescence in the dark and a phasic and tonic component during illumination of the on region. Like the positive slow potential, the phasic component is relatively small in comparison to that of the photoreceptor potential. Another feature of the average discharge pattern is the slow attenuation of the maintained discharge rate until it eventually reaches a steady discharge rate. This is particularly marked for low intensity stimuli and possibly results from some sort of discharge adaptation mechanism, or since the stimulus intensity level required to produce a discharge is several log units lower than that required to evoke a detectable positive slow potential, the excitation delivered by photoreceptors at this low intensity level may in fact have a time history resembling the average discharge behavior. The maintained discharge rate in the presence of steady illumination of the on region conceivably encodes the illuminance level in this region. Because of this, information pertaining to the direction of luminosity changes can be conveyed by the on-maintained unit which is not true of the on-off unit.

The off discharge elicited by stimulating either of the two off regions of the on-maintained unit is particularly interesting in view of the unusual organization of the receptive field. This discharge appears to be involved in the synthesis of the on-off discharge and can be satisfactorily accounted for in terms of the dynamics of the unit and the interaction between units in the first optic ganglion. Stimulation of either off region by a light pulse of sufficient intensity evokes a discharge of high temporal resolution occurring shortly after cessation of the stimulus. Although the off response has a smaller number of discharges than the on response and its threshold is higher by approximately one log unit, it is a significant response because its temporal resolution makes the discharge rate modest.

Occasionally, it was possible to record, either simultaneously or serially, two on-maintained units having their receptive field centers separated by only a few degrees. In some of the simultaneously recorded cases, a spot of light in the center of the receptive field of one unit evoked a typical on discharge from that unit and an off discharge from the other unit. These observations along with the finding that the angular separation between the center of the on region and the boundary of the off regions was approximately the interommatidial angle, suggest that the receptive fields of adjacent on-maintained units along the medio-lateral axis are arranged so that the on region of one unit of an adjacent pair is overlapped by by an off region of the other unit. This is represented diagrammatically in figure 7.1A. Since this schematic representation of the

receptive field organization of three adjacent on-maintained units (a, b, c) forms the basic structure of the model to be used to explain the neural behavior of a system of on-off and on-maintained units, it is wise to point out that this represents a simplification, for the off regions undoubtedly encompass the on regions of several adjacent on-maintained units instead of just one as shown in figure 7.1A and subsequent figures. The simplification is minor and was made to clarify the treatment. The configuration shown in figure 7.1A implies that inhibition of an on discharge resulting from illumination of either off region as in figure 4.11 is mediated through the channel (photoreceptor-cartridge) adjacent to the one mediating the on response. Since the time course of the inhibition (figure 4.11F) resembles the time history of the on discharge, the inhibition is likely of the backward type as illustrated in figure 7.1B. This arrangement of inhibition between neighboring visual channels has been observed and extensively studied in the compound eye of Limulus [30, 68], and the theoretical aspects of this type of interaction have been exhaustively analyzed using linear mathematics [82]. A network of elements as this possessing mutual backward inhibition exhibits two properties not existing in a network organized with forward inhibition, and they are: disinhibition and interaction between elements separate by more than the extent of backward inhibition. Observation of disinhibition would provide support for the backward inhibition hypothesis but such experiments were not performed.

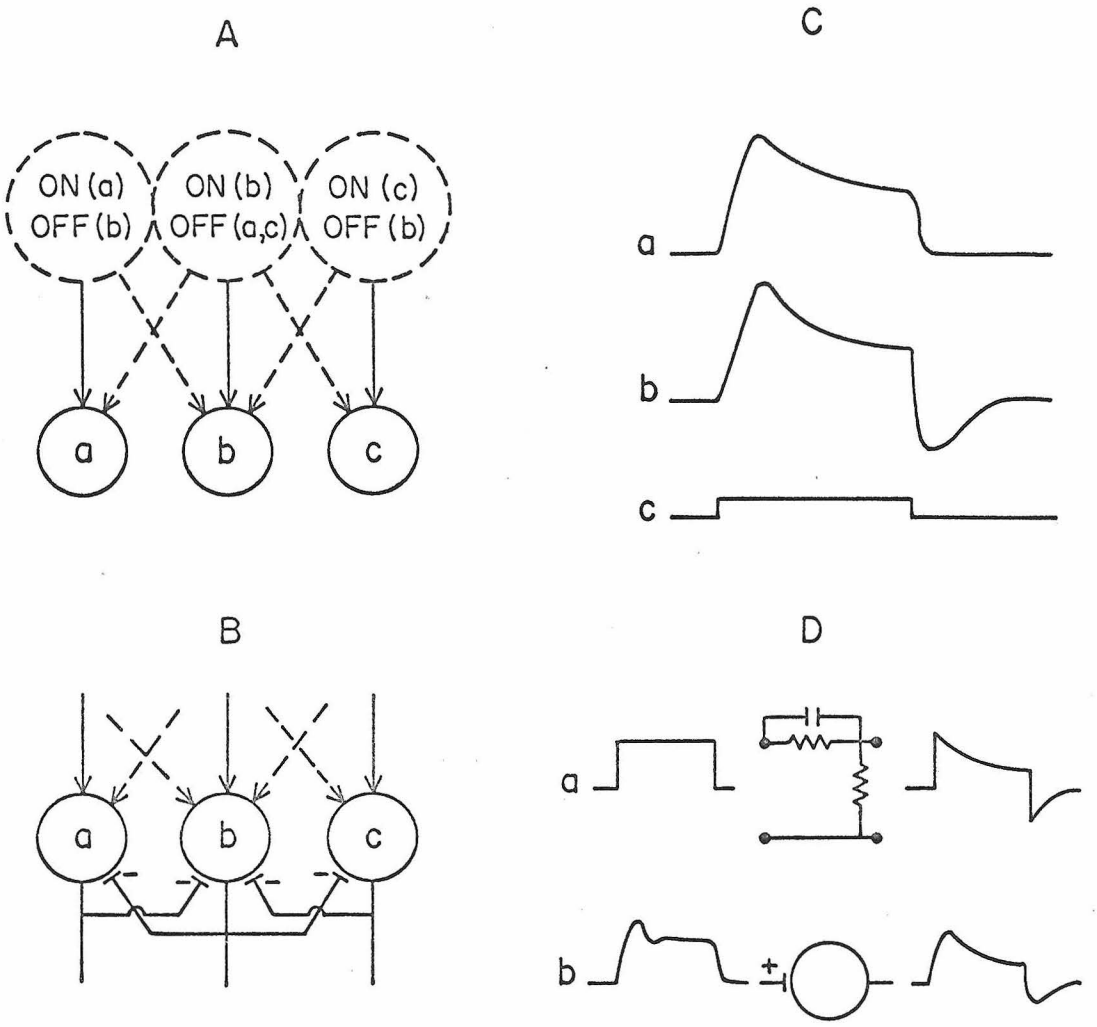

Figure 7.1 Schematic representation of the structural and temporal organization of a system of on-maintained units (A) Simplified organization of the receptive fields of three adjacent on-maintained units (a, b, c). Solid connecting lines represent paths of on region influence, and dashed connecting lines represent paths of off region influence. (B) Mutual backward inhibition between adjacent on-maintained units (C) Hypothetical behavior of the on-maintained unit membrane potential (a) Average discharge behavior (b) Hypothetical membrane potential behavior (c) Stimulus presented to the on region (D) Simple electrical analog of on-maintained unit membrane. (a) Input-output relation of the electrical analog (b) Input-output relation of the hypothetical on-maintained unit membrane.

The dynamic behavior of the system of units can be studied by analyzing the temporal aspects of the off discharge inhibition phenomenon and the time history of the discharge modes of the on-maintained unit. As illustrated in figure 4.12 inhibition of the off discharge is temporally very specific in that partial or complete inhibition occurs only within 200 msec. after the cessation of on region stimulation. This type of temporal specificity suggests that the membrane potential of the on-maintained unit may undershoot its dark value immediately after the cessation of on region stimulalation. Since the on-maintained unit does not exhibit a dark discharge, it is impossible to ascertain the membrane potential behavior following cessation of on region illumination since no discharge occurs. In order to determine the membrane potential behavior after cessation of on region stimulation and to ascertain whether excitation of the adjacent channel and the resulting off discharge are necessary to elicit the inhibition, the experiment of figure 4.14 was performed. It was found that cessation of one stimulus spot delivered to the on region of an on-maintained unit partially or completely inhibited the on discharge elicited by another stimulus spot delivered to the on region when the second stimulus was presented within 200 msec. after cessation of the first stimulus. The results reveal that on discharges as well as off discharges can be inhibited following the cessation of stimulation of the on region or, in other words, following cessation of excitation of the on-maintained unit. These results strengthen the belief that the membrane potential of

the on-maintained unit undershoots its final value immediately following cessation of on region stimulation or equivalently following the cessation of a membrane depolarizing influence. Therefore, the expected membrane potential change resulting from a pulse of light delivered to the on region of an on-maintained unit is expected to appear as illustrated in figure 7.1C. Kaneko and Hashimoto [38] have observed this type of membrane potential behavior from single neurons in the inner nuclear layer of fish retina. Further support for this interpretation comes from the demonstration of after discharge. After discharge can be viewed as resulting from a rebound of the membrane potential after its undershoot phase. In the extraordinary example of figure 4.13, the membrane potential rebound apparently exceeded the threshold and spikes were produced. Normally, this is a very minor effect and occurs only at high levels of stimulus intensity if at all. Note that a suggestion of after discharge appears in figure 3.5 as well.

It is clear that following excitation of the on-maintained unit a short period of inhibition occurs, but the neural mechanism for this is uncertain. Several possible mechanisms can be formulated, all of which can be classified into the two categories of unit genic and system genic mechanisms. The most appealing mechanism, though there are no compelling reasons other than simplicity, accounts for the inhibition phenomenon entirely in terms of the dynamics of the unit exhibiting the phenomenon. In other words, the dynamics of that unit are such that membrane potential will

hyperpolarize after the cessation of a depolarizing influence even if the unit is isolated from the system. For clarification, the membrane potential behavior of an isolated on-maintained unit is interpreted as being analogous to the behavior of the R-C circuit shown in figure 7.1D. Given the dynamic behavior of isolated on-maintained units and system structure as described, it is possible to derive the system behavior to arbitrary inputs. The important spatial and temporal behaviors of the system are summarized in the diagram in figure 7.2. The diagram illustrates the behavior of a system of three on-maintained units to a pulse of light delivered to the on region of the middle (#2) on-maintained unit. As shown, stimulation of the on region of unit #2 is equivalent to off region stimulation for units #1 and #3. The stimulus causes the membrane potential of unit #2 to be biphasic about its resting level with a hyperpolarization phase following the cessation of stimulation. Since there is no dark discharge, the threshold for spike generation exceeds the dark membrane potential, and therefore, the discharge evoked by stimulation does not directly reveal the hyperpolarization phase. Although the system behavior is not greatly altered if spike discharges are assumed to be the mode of signal communication through the lateral channels, it is simpler and, in some respects, more reasonable to assume that slow potentials are the vehicle of interaction. Furthermore, such an assumption has anatomical support as will be discussed later. The membrane potentials of units #1 and #3 are influenced by the membrane potential of unit #2 through the backward

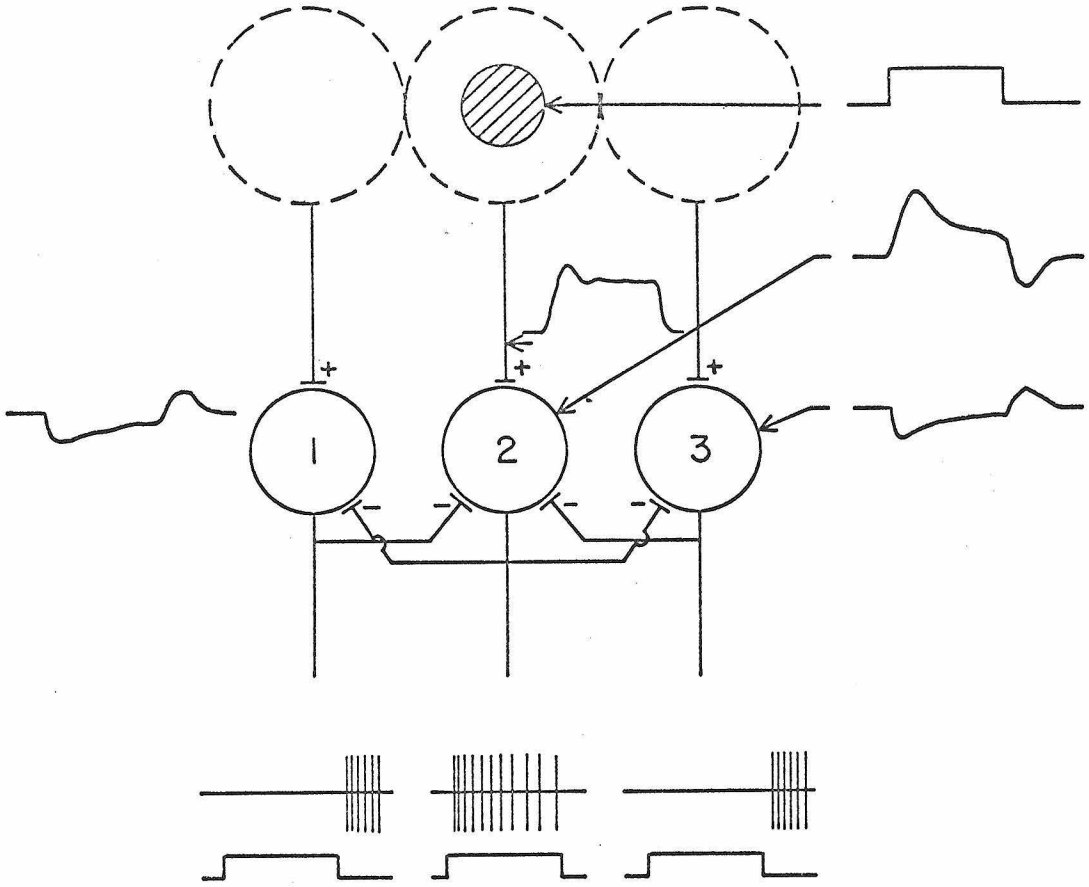

Figure 7.2 Proposed behavior of a system of on-maintained units A light pulse is applied to the on region of unit #2 and the smooth curves represent the expected slow potential behavior at the indicated locations. The proposed discharge behavior is illustrated below each unit.

inhibition pathways, and they take the form of the membrane potential of unit #2 except for being inverted and smaller. The hyperpolarization of units #1 and #3 is, of course, not manifested in their discharge patterns unless they are already discharging due to stimuli delivered to their on regions as was the case in the experiments of figure 4.11. However, their depolarization phase corresponding to the hyperpolarization phase of unit #2 may exceed the spike threshold level thereby producing a purely off discharge. This explains the generation of the off discharge resulting from the stimulation of the on regions of the neighboring units along the medio-lateral axis. All other temporal and spatial discharge properties of the on-maintained unit can be explained in terms of this system of units having the described dynamics and structural organization. The synthesis of this system of units was determined entirely from considerations of the functional behavior of single on-maintained units, and the system organization will later be compared to the anatomical structure of the first optic ganglion.

The average discharge pattern of the on-off unit is fundamentally unlike either of the two slow potentials observed in the first optic ganglion. Like the on-maintained unit, the on-off unit does not possess a dark discharge, and in contrast, it does not support a maintained discharge during steady stimulation. Based on its discharge properties, the on-off unit can be interpreted as abstracting information about the rate of change of light flux within its receptive field without regard to the direction of flux change.

Sensitivity of the on-off unit to positive and negative rates of flux change makes a moving pattern consisting of positive and negative intensity gradients a particularly potent stimulus for eliciting on-off unit activity. Whereas pulses of stationary light spots were the most effective stimuli for the on-maintained unit, moving intensity patterns were the most effective stimuli for the on-off unit due to its temporal discharge characteristics and to the spatial summation within its receptive field. Although moving patterns were the most effective stimuli, the on-off unit did not exhibit a preferred direction of motion as did the directional selective motion detection units found in the third optic ganglion. It did, however, have a preferred axis of motion resulting from the elliptical shape of the receptive field.

One of the fundamental questions still unanswered in the field of sensory visual physiology pertains to the ubiquitous mechanism of on-off discharge generation. On the basis of the discharge behavior of the on-off unit, it is possible to formulate a model which accounts for the generation of the on-off discharge and incorporates the structure and function of the system of on-maintained units just described. The size and homogeneity of the on-off unit receptive field indicates that more than a few of the primary channels described in regard to the system of on-maintained units are contributing to the on-off unit and that it integrates localized on-off activity. Judging from its temporal and spatial discharge properties, the on-off unit appears to be of higher order than the on-maintained unit

which is supported by the fact that its response latency exceeds that of the on-maintained unit.

The difficulty in formulating a mechanism for the on-off response is in accounting for the off response. At first glance, the solution appears simple. The on-off unit simply sums the discharge activity of several on-maintained units some of which will be exhibiting an off discharge while others exhibit an on discharge to a spot of light. Such a formulation is appealing from several standpoints, but although it adequately explains the on-off response elicited by small spot stimulation, it fails to account for the on-off discharge elicited by a spot encompassing the entire receptive field. Under such stimulus conditions, all on-maintained units contributing to the on-off unit would exhibit only on discharge, and therefore, an off response from the on-off unit would not occur. Obviously, the off response of the on-off unit is not derived from the off discharge of on-maintained units; however, the hyperpolarizing phase of the on-maintained unit membrane potential following cessation of the stimulus, occurring even for large spots, may contribute in some way to the off response of the on-off unit.

On a few occasions, two on-off units having their receptive field centers displaced by just a few degrees were simultaneously observed which suggests that the on-off units are organized in a periodic fashion as the on-maintained units. This belief was incorporated into the model diagrammed in figure 7. 3a which also includes

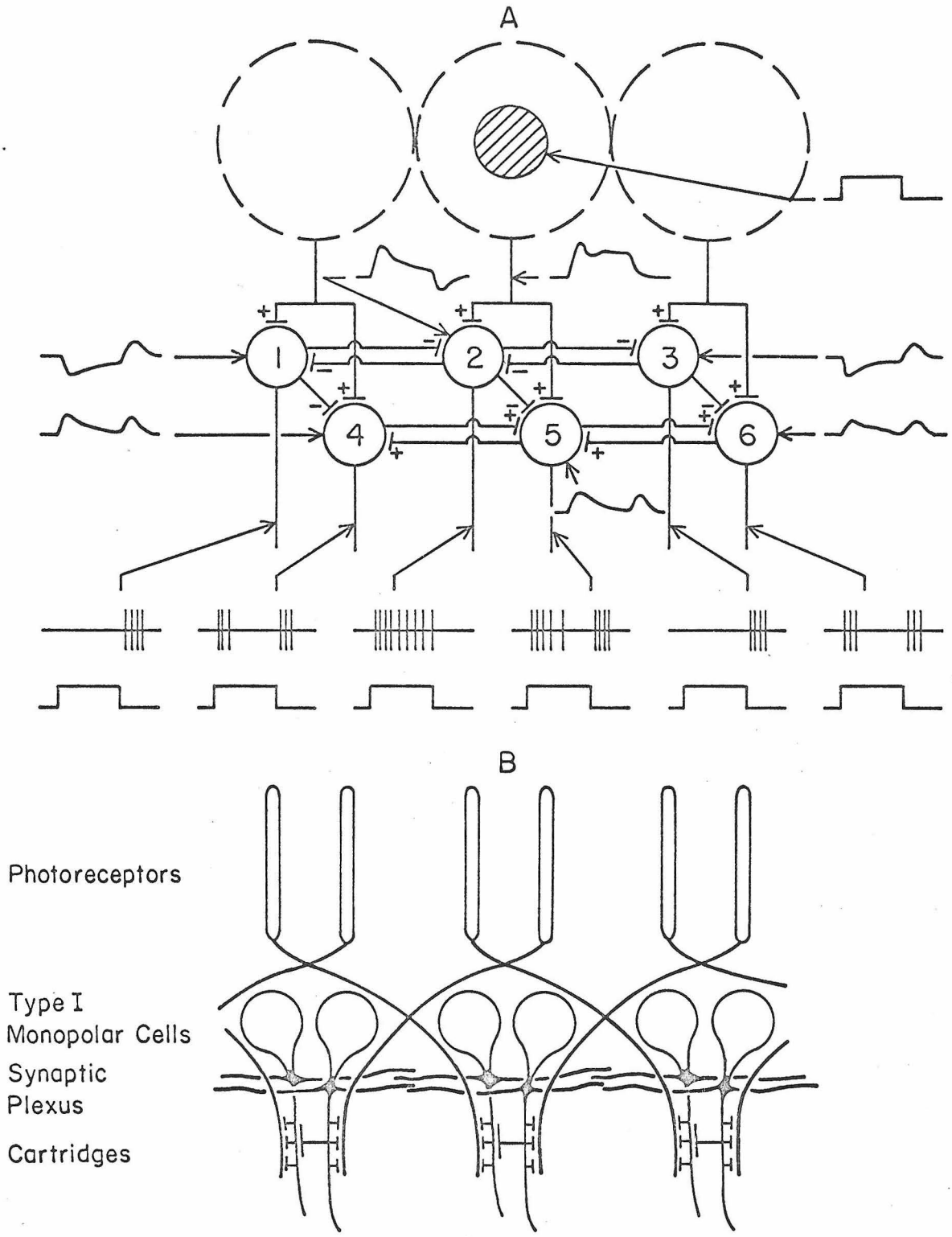

Figure 7.3 (A) Behavior of the proposed system of on-off and on-maintained units (B) Schematic diagram of the relevant neural anatomy of the first optic ganglion.

the structural and functional aspects of the system of on-maintained units. The diagram illustrates three adjacent on-off units each associated with a companion on-maintained unit. Justification for the particular structural configuration comes from the functional properties of single on-off units. Because of the size and homogeneity of the on-off unit receptive field, each on-off unit (4, 5, 6) is shown to have an excitatory influence on its neighboring on-off units. Since the on-off unit exhibited a higher threshold and less discharge to a pulse of light than did the on-maintained unit, inhibition is believed to be acting on the on-off unit, and this is represented in the model by the inhibitory influence of each on-maintained unit on its companion on-off unit. The behavior of each unit is shown for the case in which a pulse of light is presented to the on region of on-maintained unit #2 as in figure 7.2. Note that the behavior of the system of on-maintained units is not altered by the addition of the on-off units.

Presentation of the stimulus causes excitatory and inhibitory influences to be exerted on on-off unit #5. The dynamics of the primary excitatory and inhibitory influences are such that the excitatory influence has a faster initiation and a slower termination than does the inhibitory influence. Admittedly, this is a rather arbitrary specification, but it was found through simulation studies that the behavior of the modelled on-off units was very sensitive to difference in time course between the primary excitatory and inhibitory influences. Following the onset of stimulation, the excitatory influence

initially exceeds the inhibitory influence, but during steady state the two influences cancel. Furthermore, the observed prolongation of the on discharge of the on-off unit at high stimulus intensities can be accounted for if it is assumed that the steady state excitatory influence exceeds the inhibitory influence at high stimulus intensities. Following cessation of the stimulus, the off response of on-off unit #5 results from the excitatory influence having a slower termination than the inhibitory influence and from the inverted inhibitory phase of on-maintained unit #2. This, in principle, explains the generation of the on-off response when the stimulus is placed in the center of the receptive field. The lateral excitatory pathways between adjacent on-off units account for the generation of the on-off response when the stimuli are not centered within the receptive field (i. e., for the extent of the receptive field). In contrast to the simpler formulation, each on-off unit in this model exhibits on-off behavior when the entire receptive field is stimulated since the on-off mechanism is localized at each unit. Although this relatively simple model contains some arbitrary properties, its behavior is compatible with the known mechanisms of cellular interaction and accounts for all the observed spatial and temporal discharge properties of the on-off and on-maintained units. The anatomical correlates of this model will be discussed later.

Spectral and Polarization Information Processing

Since von Frisch [23] demonstrated the existence of color

vision in honey bees, there has been considerable interest in the spectral sensitivity properties of the compound eyes of many different species of arthropods. Relatively recently, the problem of color discrimination by the compound eye has been approached at the cellular level with considerable success. The most impressive study was made by Autrum [4] on worker and drone honey bees in which he found, as predicted from the behavior study of Daumer [16], three populations of photoreceptor cells with maximum spectral sensitivities at 340, 430, and 530 mμ, respectively. Similar studies have been performed on a variety of arthropods, and in all studies, including two on dipterans, it has been possible to demonstrate two or more populations of photoreceptors.

Using electrophysiological methods, Burkhardt [12] found three types of photoreceptors in the compound eye of Calliphora erythrocephala having their maximum spectral sensitivities at 455 mμ (blue), 490 mμ (green), and 540 mμ (yellow-green). In the housefly, Musca domestica, Langer [44, 45, 46] found, using microspectrophotometric methods, that photoreceptor cells 1-6 maximally absorbed light having a wavelength near 515 mμ while photoreceptor cell 7 (and presumably cell 8) maximally absorbed light having a wavelength near 470 mμ. Although the results of both studies are not in complete agreement, both suggest that flies possess the necessary types of photopigments for color discrimination. If color discrimination is actually mediated through these photoreceptor populations, then evidence of it should appear at higher

levels of the nervous system, but spectral sensitivity studies of directionally selective motion detection units [8] in the third optic ganglion and of the optomotor reaction [37] have not revealed evidence of color discrimination. This, however, does not exclude its existence, for the responses studied were very specialized, and color discrimination is likely unimportant. In contrast, the units carrying information across the intermediate chiasma would be expected to possess the spectral properties necessary for color discrimination, if it, in fact, does exist. Furthermore, most of the units crossing the intermediate chiasma are of second order, and it seems likely, judging from the situation in vertebrate retinas possessing color vision, that special transformations on the spectral information carried by the photoreceptors would be made by these second order units. This seems particularly necessary in the fly's case, for the receptor populations do not differ greatly.

As described in Chapter V, for color discrimination to be mediated by the on-off and on-maintained units, the units must either belong to different classes based on their spectral sensitivity (Situation II), or demonstrate that more than one class of photoreceptors are contributing to their activity (Situation I). Neither of these situations was found to apply. All units studied of both the on-off and on-maintained varieties possessed the same spectral sensitivity which was characterized by two roughly equal sensitivity peaks located near 350 mμ and 485 mμ. These results like those of the higher order responses do not entirely exclude the possibility

of color discrimination in the fly, for other channels across the intermediate chiasma besides those described in this thesis must exist.

Although there are differences between the spectral properties revealed in this study and those revealed by the two photoreceptor studies, they can be partially reconciled. If the ultraviolet (u. v.) sensitivity differences are momentarily disregarded, the results differ only in the number of photoreceptor classifications and the location of their maximum sensitivity or absorption. Burkhardt's claim of three photoreceptor classifications based on the location of the visible region sensitivity peak is open to question, for the classification differences are subtle (requiring statistical tests to verify their significance), the spectral sensitivities in the visible region are broad, and the state of adaptation was not well controlled. His data could be reinterpreted, in light of Langer's results, such that the common green cells be identified with photoreceptors 1-6 and the blue cells with the photoreceptors 7 and 8 while yellow-green cells be regarded as aberrant green cells. However, Langer found the maximum absorption of photoreceptors 1-6 to occur near 515 mμ, but this is a small quantitative difference possibly due to the method of measurement, for other features of the spectral absorption measurements appear shifted toward longer wavelengths. The observation that all on-off and on-maintained units displayed a spectral sensitivity peak near 485 mμ, shows that the on-off and on-maintained units derive their spectral characteris-

tics from photoreceptors 1-6.

The most interesting feature of the spectral sensitivities of the on-off and on-maintained units is their high sensitivity to ultraviolet light. The sensitivity of insects to u. v. radiation has been demonstrated on numerous occasions [18, 28, 84] using behavioral or mass response measurements. With the exception of photoreceptor studies, this study represents the first spectral sensitivity study of single units in the fly employing u. v. stimulation. The relatively narrow sensitivity peak with its maximum near 350 mμ is in complete accord with Burkhardt's observation that all three classes of photoreceptors exhibit a significant u. v. sensitivity. Whereas the relative magnitude of the u. v. sensitivity varied between the different classes of photoreceptors, it was constant and comparable to the green sensitivity in both the on-off and on-maintained units. Although it seems certain that flies are extremely sensitive to ultraviolet stimulation, Langer's [44, 45, 46] microspectrophotometric measurements and Kaiser's [37] optomotor response measurements do not reveal a prominent u. v. sensitivity even though they do exhibit the green sensitivity. The reasons for the inconsistencies are unknown, but they serve to demonstrate the difficult nature of spectral sensitivity measurements, particularly in the u. v. region.

The form of the dark adapted spectral sensitivity of the on-off and on-maintained units suggests that two photopigements (u. v., green absorbing) are involved. If two photoreceptor populations

(u. v., green sensitive) are contributing excitation to the on-off and on-maintained units, then selective adaptation should disclose this by altering the form of the spectral sensitivity. The technique of selective adaptation has previously been successfully employed by Goldsmith [27] to reveal that u. v. and visible photopigments were responsible for the dark adapted spectral sensitivity of the honey bee retina. Although several assumptions about the mechanism of adaptation are necessary, the negative results indicate that the u. v. and green sensitivity peaks are not the results of the summation of excitation from u. v. sensitive and green sensitive photoreceptor populations. A similar conclusion was reached by Burkhardt using a variation of the selective adaptation logic.

Several explanations are possible for the u. v. sensitivity. Florescence is one possible explanation, but it is unlikely for often the units were more sensitive to u. v. than green stimulation. Scattering of u. v. light within the retina is another possible explanation. It is now established that the reported red sensitivity (620 mμ) of the fly [14] is due to absorption properties of the shielding pigments rather than the photopigments. Shielding pigments of the fly act as sharp edge filters near 620 mμ [47] thereby allowing scattered red light within the retina to contribute to the observed response whether it be of single or multi-unit origin. The result is an apparent higher sensitivity due to the scattered red light component. Possibly a similar phenomenon occurs for u. v. light, but Langer [47] has shown that the shielding pigment of the wild-type

eye constitutes a homogeneous "grey filter" between 320 mμ and 590 mμ. Furthermore, the effect of scattered light is less significant for responses derived from fewer photoreceptors, and absolutely no indication of a red sensitivity was noted for the units studied and the light levels used. Calibration error is another possible explanation of the prominent u. v. sensitivity. However, the relatively smooth character of the spectral sensitivities and the numerous independent observations of u. v. sensitivity in flies make this explanation doubtful. The most likely explanation is that the u. v. sensitivity peak is real and due to the photopigment having absorption peaks in both the u. v. and green regions.

It has been demonstrated that honey bees utilize polarized light information for navigational purposes. It is possible that flies also use this information, for their photoreceptors have preferred orientations of the plane of polarized light. Since most photoreceptors have a dichroic ratio less than two, considerable processing of their signals seems necessary in order to attain the discrimination exhibited by the honey bee. However, neither the on-off or on-maintained units revealed any preference to the orientation of the plane of polarization.

In the past, several investigators [21, 28] have suggested that a duplicity theory of vision is applicable to the compound eye of dipterans; however, very little functional data exist to support the claim. From an anatomical standpoint, the compound eye of the fly possesses structural characteristics suggestive of a two channel

system. One channel might be mediated by photoreceptors 1-6 whose axons terminate in the first optic ganglion while the other channel would consist of photoreceptors 7 and 8 whose axons by-pass the first optic ganglion and end in the second optic ganglion. Judging from other anatomical characteristics such as rhabdomere size, microvillar orientation, and laminar synaptic organization, the channel served by photoreceptors 7 and 8 would seem to be characterized by a finer spatial resolution and a lower sensitivity than the 1-6 channel. Furthermore, it would likely carry and process polarization information. The dichotomy of the visual system into the two proposed channels has recently received support from findings other than anatomical. Langer [46] has shown that photoreceptors 7 and 8 have a different absorption spectra than do photoreceptors 1-6, and most recently, Kirschfeld [42] demonstrated that the optomotor flight torque of flies could be modulated under special stimulus conditions by rotating the plane of polarization of the light eliciting the response. The special stimulus conditions were designed to accentuate the activity of the channel served by photoreceptors 7 and 8. In light of these observations and interpretations, it is reasonable to conclude that the on-off and on-maintained units are served by photoreceptors 1-6 each of which is maximally sensitive to u. v. and green light.

Anatomical Correlates of the On-off and On-maintained Units

Based on the present knowledge about the anatomy of the

first optic ganglion, several neural elements are candidates for the anatomical counterpart of the on-off and on-maintained units. Roughly eight fibers cross the intermediate chiasma for each cartridge in the first optic ganglion. Two are the long visual fibers originating from the superior and inferior central photoreceptor cells (7 and 8). Four more are the two type I and two type II second order monopolar cells of the first optic ganglion. The centrifugal fibers of each cartridge, designated α and β, constitute the remaining two candidate fibers.

The most likely candidates can be deduced by comparing the expected functional properties of each candidate, based on its gross anatomy, with the observed functional properties of the on-off and on-maintained units. Since the centrifugal fibers are believed to carry information toward the first optic ganglion, they can immediately be eliminated from further consideration. Due to the complexity of their temporal discharge patterns and receptive field organizations, the on-off and on-maintained units can be interpreted as being at least second order units. This combined with the belief that both units are served by photoreceptors 1-6 eliminates the long visual fibers as likely candidates. Unfortunately, the anatomical details of the type II monopolar cells have not been established to the extent of those of the type I monopolar cells. However, judging from their gross morphology, they do not appear to possess the lateral communication channels required to account for the receptive field organizations of the on-off and on-maintained units. On the

other hand, the type I monopolar cells do. Before entering the cartridge, the axis fibers of the type I monopolar cells send out membrane prolongations which extend far enough to join like prolongations from monopolar cells of adjacent cartridges thereby forming the synaptic plexus. It is not known whether prolongations of the two type I monopolar cells of one cartridge make contact with those of like monopolar cells in adjacent cartridges, but the possibility is a real one. Being second order cells, the type I monopolars could conceivably support the temporal behavior patterns exhibited by the on-off and on-maintained units. Furthermore, the type I monopolar cells make numerous synaptic connections with each of the 1-6 photoreceptors serving them. Due to the summation of excitation from each of the photoreceptors, all sensitivity to the plane of polarized light would likely be lost. The most compelling reason to believe that the type I monopolar cells are the anatomical counterpart of the functionally defined on-off and on-maintained units comes from a consideration of the fiber diameters of the candidate elements. Transverse sections through the intermediate chiasma at all levels reveal bundles of fibers consisting of two large fibers (3-4 microns) and several smaller fibers (<1 micron). The two large fibers belong to the two type I monopolar cells of each cartridge [80]. Since larger fibers are expected to produce larger extracellular currents, it is likely that the discharge potentials recorded from the intermediate chiasma originated from the type I monopolar cell axons. However, it still remains to be

explained why the extracellularly recorded on-off spike potentials were always larger than the on-maintained spike potential. Nevertheless, the evidence is overwhelmingly in favor of the view that the on-off unit represents one type I monopolar cell of each cartridge and the on-maintained unit represents the other.

Assuming this identification to be correct, it is interesting to compare the anatomical properties of the type I monopolar cells with the structural configuration proposed in the model developed from considerations of the functional behavior of the on-off and on-maintained units. As illustrated in figure 7.3B, both type I monopolar cells make numerous synapses to each of the six photoreceptors serving the cartridge. In the model also illustrated in figure 7.3A, this corresponds to the excitatory synapse of the primary element on both the on-off and on-maintained units. The excitatory interaction between adjacent on-off units and the inhibitory interaction between adjacent on-maintained units are presumably mediated by the prolongations of the type I monopolar cells forming the synaptic plexus. If the synaptic plexus does mediate lateral interaction, it is likely by slow potentials. The intricate bridge structure, observed in electron micrographs, intimately associating the plasma membranes of the type I monopolar cells of each cartridge, offers a possible anatomical correlate for the proposed inhibitory synapse between the companion on-maintained and on-off units. It is, of course, quite speculative to imply that certain known anatomical

features mediate certain functional activities, for it is not even known with certainty that type I monopolar cells of adjacent cartridges make synaptic contact or that the peculiar bridge structure acts as a channel of integration, but the fact that the basic configurations of these anatomical units agree, in principle, with those suggested from the functional behavior of the on-off and on-maintained units is remarkable in itself. As more of the synaptology of the first optic ganglion is revealed, particularly pertaining to the type II monopolar cells, it will be possible to place the function-structure correlation on solid ground.

Directional Selective Motion Detection and the Chiasma Units

Although one of the original objectives of this research effort was to study units precursory to the directional selective motion detection units, very little insight into the neural mechanism of selective motion detection was gained from the study of the on-off and on-maintained units, the major reason being that these units are "too" precursory to the directional selective motion detection units. It is likely that both the on-off and on-maintained units indirectly contribute to selective motion detection, for the thresholds of the on-maintained and directional selective motion detection units agree and the crosscorrelation between on-off and directional selective motion detection units occasionally appears significant. A more fruitful approach to understanding the mechanism of selective motion detection is through the study of units, like the medulla on-off units,

which are undoubtedly of higher order than the chiasma units but still precursory to the directional selective motion detection units. It is likely that the information processing properties of the on-off and on-maintained units have nothing to do with the mechanism of selective motion detection.

LIST OF REFERENCES

1. Autrum, H. and Stumpf, H. "Das Bienenauge als Analysator für polarisiertes Licht," Z. Naturforschg., 5b, 116-122, 1950.

2. Autrum, H. and Stumpf, H. "Electrophysiologishe Untersuchungen über das Farbensehen von Calliphora," Z. vergl. Physiol., 35, 71-104, 1953.

3. Autrum, H. and von Zwehl, V. "Die Sehzellen der Insekten als Analysatoren für polarisiertes Licht," Z. vergl. Physiol., 46, 1-7, 1962.

4. Autrum, H. and von Zwehl, V. "Die spektrale Empfindlichkeit einzelner Sehzellen des Bienen auges," Z. vergl. Physiol., 48, 357-384, 1964.

5. Autrum, H. and Kolb, G. "Spektrale Empfindlichkeit einzelner Sehzellen der Aeschniden," Z. vergl. Physiol., 60, 450-477, 1968.

6. Bishop, L. G. and Keehn, D. G. "Neural correlates of the optomotor response in the fly," Kybernetik, 3, 288-295, 1967.

7. Bishop, L. G., Keehn, D. G., and McCann, G. D. "Motion detection by interneurons of the optic lobes and brain of the flies, Calliphora phaenicia and Musca domestica," J. Neurophysiol., 31, 509-525, 1968.

8. Bishop, L. G. "A search for color encoding in the responses of a class of fly interneurons," Z. vergl. Physiol., 64, 355-371, 1970.

9. Braitenberg, V. "Patterns of projection in the visual system of the fly. 1. Retina-lamina projections," Exp. Brain. Res., 3, 271-298, 1967.

10. Bullock, T. H. "The reliability of neurons," J. Gen. Physiol., 55, 563-585, 1970.

11. Burkhardt, D. and Wendler, L. "Ein direkter Beweis für die Fähigkeit einzelner Sehzellen des Insektauges, die Schwingungsrichtung polarisierten Lichtes zu analysieren," Z. vergl. Physiol., 43, 687-692, 1960.

12. Burkhardt, D. "Spectral sensitivity and other response characteristics of single visual cells in the arthropod eye," In Biological Receptor Mechanisms (ed. J. W. L. Beament), Symp. Soc. Exptl. Biol., 16, 86-109, Cambridge University Press, London, 1962.

13. Burkhardt, D. "Colour discrimination in insects," Advan. Insect. Physiol., 2, 131-173, 1964.

14. Burkhardt, D., De La Motte, I., and Seitz, G. "Physiological optics of the compound eye of the blow fly," In The Function Organization of the Compound Eye, (ed. C. G. Berhard), 51-62, Pergamon Press, Oxford, 1966.

15. Collet, T. "Centripetal and centrifugal visual cells in medulla of the insect optic lobe," J. Neurophysiol., 33, 239-256, 1970.

16. Daumer, K. "Reizmetrische Untersuchungen des Farbensehen der Bienen," Z. vergl. Physiol., 38, 413-478, 1956.

17. Daw, N. W. "Colour-coded ganglion cells in the goldfish retina: Extension of their receptive fields by means of new stimuli," J. Physiol., 97, 567-592, 1968.

18. Dethier, V. G. The Physiology of Insect Senses, Methuen, London, 1963.

19. Dill, J. C. "A computer-aided investigation of motion detection units in the fly," Ph. D. Thesis, California Institute of Technology, 1970.

20. Fermi, G. and Reichardt, W. "Optomotorische Reaktionen der Fliege Musca domestica," Kybernetik, 2, 15-28, 1963.

21. Fingerman, M. and Brown, F. A. "The 'purkinje shift' in insect vision," Science, 114, 171-172, 1952.

22. von Frisch, K. "Der Farbensinn und Formensinn der Biene," Zool. Jb. Physiol., 37, 1-238, 1914.

23. von Frisch, K. "Die Polarisation des Himmelslichtes als orientierender Faktor bei den Tänzen der Bienen," Experientia, 5, 142-148, 1949.

24. von Frisch, K. Dance Language and Orientation of Bees, Springer Verlag, Berlin-Heidelberg-New York, 1965.

25. Gerstein, G. L. and Kiang, N. Y-S. "An approach to the quantitative analysis of electrophysiological data from single neurons," Biophys. J., 1, 15-28, 1960.

26. Goetz, K. G. "Optomotorische Untersuchungen des visuellen Systems einiger Augenmutanten der Fruchtfliege Drosophila," Kybernetik, 2, 77-92, 1964.

27. Goldsmith, T. H. "The nature of the retinal action potential and the spectral sensitivities of ultraviolet and green receptor systems of the compound eye of the worker honey-bee," J. Gen. Physiol., 43, 775-799, 1960.

28. Goldsmith, T. H. "The color vision in insects," In Light and Life, (eds. McElroy, W. D. and Glass, B.), The Johns Hopkins Press, Baltimore, 1961.

29. Goldsmith, T. H. "The course of light and dark adaptation in the compound eye of the honey-bee," Comp. Biochem. Physiol., 10, 227-237, 1960.

30. Hartline, H. K. and Ratliff, F. "Spatial summation of inhibitory influences in the eye of Limulus and the mutual interaction of receptor units," J. Gen. Physiol., 41, 1049-1066, 1958.

31. Horridge, G. A., Scholes, J. H., Shaw, S., and Tunstall, J. "Extracellular recordings from single neurones in the optic lobe and brain of the locust," In The Physiology of the Insect Central Nervous System, (eds. J. E. Treherne and J. W. L. Beamont), Academic Press, 1965.

32. Horridge, G. A. "Unit studies on the retina of dragonflies," Z. vergl. Physiol., 62, 1-37, 1969.

33. Horridge, G. A. and Meinertzhagen, I. A. "The accuracy of the patterns of connexions of the first- and second-order neurons of the visual system of Calliphora," Proc. Roy. Soc. Lond. B., 175, 69-82, 1970.

34. Horridge, G. A. and Meinertzhagen, I. A. "The exact neural projection of the visual fields upon the first and second ganglia of the insect eye," Z. vergl. Physiol., 66, 369-378, 1970.

35. Hubel, D. H. "Tungsten microelectrode for recording from single units," Science, 125, 549-550, 1957.

36. Jander, R. and Waterman, T. H. "Sensory discrimination between polarized light and light intensity patterns by arthropods," J. Cell. Comp. Physiol., 56, 137-160, 1960.

37. Kaizer, W. "Zur Frage des Unterscheidungsvermögens für Spektralfarben : Ein Untersuchung der Optomotorik der Königlichen Glanzfliege Phorma regina Meig.," Z. vergl. Physiol., 61, 71-102, 1968.

38. Kaneko, A. and Hashimoto, H. "Electrophysiological study of single neurons in the inner nuclear layer of the carp retina," Vision Res., 9, 131-173, 1969.

39. Kirschfeld, K. "Das anatomische und das physiologische Sehfeld der Ommitidien in Komplexauge von Musca," Kybernetik, 2, 249-257, 1965.

40. Kirschfeld, K. "Discrete and graded receptor potentials in the compound eye of the fly Musca," In The Functional Organization of the Compound Eye, (ed. C. G. Bernhard), 291-308, Pergamon Press, Oxford, 1966.

41. Kirschfeld, K. "Die Projection der optischen Umwelt auf das Raster der Rhabdomere im Komplexauge von Musca," Expl. Brain. Res., 3, 248-270, 1967.

42. Kirschfeld, K. and Reichardt, W. "Optomotorische Versuche an Musca mit linear polarisiertes Licht," Z. Naturforshung, 25b, 228, 1970.

43. Kuffler, S. W. "Discharge patterns and functional organization of mammalian retina," J. Neurophysiol., 16, 37-68, 1953.

44. Langer, H. "Spectrometrische Untersuchung der Absorptionseigeshaften einzelner Rhabdomere im Facettenauge," Verh. Dtsch. Zool. Ges., Jena, 329-338, 1965.

45. Langer, H. and Thorell, B. "Microspectrophotometry of single rhabdomeres in the insect eye," Expl. Cell. Res., 41, 673-677, 1966.

46. Langer, H. and Thorell, B. "Microspectrophotometry assay of visual pigments in single rhabdomeres of the insect eye," In The Functional Organization of the Compound Eye, (ed. C. G. Bernhard), 145-150, Pergamon Press, Oxford, 1966.

47. Langer, H. "Über die Pigmentgranula im Facettenauge von Calliphora erythrocephala," Z. vergl. Physiol., 55, 354-377, 1967.

48. Lockeman, P. C. and Knutzen, D. W. "A multiprogramming environment for on-line data acquisition and analysis," Comm. ACM, 10, 758-764, 1967.

49. Mazokhin-Porshnjakov, G. A. Insect Vision, Plenum Press, New York, 1969.

50. Melamed, J. and Trujillo-Cenóz "The fine structure of the central cells in the ommitidia of Dipterans," J. Ultrastruct. Res., 21, 313-334, 1967.

51. McCann, G. D. and MacGinitie, G. F. "Optomotor response studies of insect vision," Proc. Roy. Soc. Lond. B., 163, 369-401, 1965.

52. McCann, G. D., Sasaki, Y., and Biedebach, M. C. "Correlated studies of insect visual nervous systems," In The Functional Organization of the Compound Eye, (ed. C. G. Bernhard), 554-584, Pergamon Press, Oxford, 1966.

53. McCann, G. D. and Dill, J. C. "Fundamental properties of intensity, form, and motion perception in the visual nervous systems of Calliphora phaenicia and Musca domestica," J. Gen. Physiol., 53, 355-371, 1969.

54. Moore, G. P., Perkel, D. H. and Segundo, J. P. "Statistical analysis and functional interpretation of neural spike data," Ann. Rev. Physiol., 28, 493-522, 1966.

55. Moore, G. P., Segundo, J. P., Perkel, D. H. and Levitan, H. "Statistical signs of synaptic interaction in neurons," Biophys. J., 10, 876-900, 1970.

56. Mote, M. "Integrative aspects of the lamina ganglionaris in the compound eye of the fly Sarcophaga bullata," Ph. D. thesis, University of California at Los Angeles, 1968.

57. Naka, K. I. and Kuwarbara, M. "Response of a single retinula cell to polarized light," Nature, 184, Suppl. 7, 455, 1959.

58. Naka, K. I. Recording of retinal action potentials from single cells in the insect compound eye," J. Gen. Physiol., 44, 571-584, 1961.

59. Naka, K. I. and Eguchi, E. "Spike potentials recorded from the insect photoreceptor," J. Gen. Physiol. 45, 663-680, 1960.

60. Naka, K. I. and Kishida, K. "Retinal action potentials during dark and light adaptation," In The Functional Organization of the Compound Eye, (ed. C. G. Bernhard), 251-266, Pergamon Press, Oxford, 1966.

61. Naka, K. I. and Rushton, W. A. H. "S-potentials from colour units in the retina of fish (Cyprinidae)," J. Physiol., 185, 536-555, 1968.

62. Naka, K. I. and Rushton, W. A. H. "An attempt to analyse colour reception by electrophysiology," J. Physiol., 185, 556-586, 1966.

63. Naka, K. I. and Kishida, K. "Simultaneous recording of S and spike potentials from fish retina," Nature, 214, 1117-1118, 1967.

64. Naka, K. I. and Kishida, K. "Amino acids and the spikes from the retinal ganglion cells," Science, 156, 648-650.

65. Naka, K. I. and Nye, P. W. "Receptive-field organization of the catfish retina: Are at least two lateral mechanisms involved?," J. Neurophysiol., 33, 625-642, 1970.

66. Perkel, D. H., Gerstein, G. L., and Moore, G. P. "Neural spike trains and stochastic point processes. I. The single spike train," Biophys. J., 7, 391-418, 1967.

67. Perkel, D. H., Gerstein, G. L., and Moore, G. P. "Neural spike trains and stochastic point processes. II. Simultaneous spike strains," Biophys. J., 7, 418-440, 1967.

68. Ratliff, F. Mach Bands: Quantitative studies on neural networks in the retina, Holden-Day Inc., San Francisco, 1965.

69. Reichardt, W. "Autocorrelation, a principle for the evaluation of sensory information by the central nervous system," In Sensory Communication, (ed. W. A. Rosenblith), 303-317, MIT Press, Cambridge, Mass., 1961.

70. Reichardt, W. "Detection of single quanta by the compound eye of the fly Musca," In The Functional Organization of the Compound Eye, (ed. C. G. Bernhard), 267-290, Pergamon Press, Oxford, 1966.

71. Roeder, K. D. "The effect of potassium and calcium on the nervous system of the cockroach Periplaneta americana," J. Cell. Comp. Physiol., 31, 327-338, 1948.

72. Scholes, J. "The electrical responses of the retinal receptors and the lamina in the visual system of the fly Musca," Kybernetik, 6, 149-162, 1969.

73. Shaw, S. R. "Simultaneous recording from two cells in the locust retina," Z. vergl. Physiol., 55, 183-194, 1967.

74. Shaw, S. R. "Organization of the locust retina," In Invertebrate Receptors, (eds. J. D. Carthy and G. E. Newell), 135-163, Academic Press, New York, 1968.

75. Strausfeld, N. J. "Golgi studies on insects. Part II. The optic lobes of Diptera," Phil. Trans. Roy. Soc. Lond. B., 258, 135-223, 1970.

76. Swihart, S. L. "The neural basis of colour vision in the butterfly, Papilio troilus," J. Insect Physiol., 16, 1623-1636, 1970.

77. Trujillo-Cenóz, O. "Some aspects of the structural organization of the intermediate retina of Dipterans," J. Ultrastruct. Res., 13, 1-33, 1965.

78. Trujillo-Cenóz, O. "Compound eye of Dipterans: Anatomical basis for integration - An electron microscope study," J. Ultrastuct. Res., 16, 395-398, 1966.

79. Trujillo-Cenóz, O. and Melamed, J. "Electron microscope observation on the peripheral and intermediate retinas of Dipterans," In The Functional Organization of the Compound Eye," (ed. C. G. Bernhard), 339-362, Pergamon Press, Oxford, 1966.

80. Trujillo-Cenóz, O. "Some aspects of the structural organization of the medulla in muscoid flies," J. Ultrastruct. Res., 27, 533-549, 1969.

81. Tunstall, J. and Horridge, G. A. "Electrophysiological investigation of the optics of the locust retina," Z. vergl. Physiol. 55, 167-182, 1967.

82. Varju, D. "A comparison of two models for lateral inhibition," Kybernetik, 1, 200-208, 1962.

83. Vowles, D. "The receptive fields of cells in the retina of the housefly Musca domestica," Proc. Roy. Soc. Lond. B., 164, 552-576, 1966.

84. Walther, J. B. and Dodt, E. "Die Spektralsensitivatät von Insekten-Komplexaugen in Ultraviolett bis 290 mμ," Z. vergl. Physiol. 146, 273-278, 1959.

85. Washizu, Y. "Electrical activity of single retinula cells in the compound eye of the blowfly Calliphora erythrocephala Meig," Comp. Biochem. Physiol., 12, 369-387, 1964.

86. Washizu, Y., Burkhardt, D., and Streck, P. "Visual field of single retinula cells and interommitidial inclination in the compound eye of the blowfly Calliphora erythrocephala," Z. vergl. Physiol., 48, 413-428, 1964.

87. Waterman, T. H. and Horch, K. W. "Mechanisms of polarized light perception," Science, 154, 467-475, 1966.

88. Werblin, F. S. and Dowling, J. E. "Organization of the retina of the mudpuppy, Nectucus maculosus. II Intracellular recording," J. Neurophysiol., 32, 339-355, 1969.

89. Wiesel, T. H. and Hubel, P. H. "Spatial and chromatic interactions in the lateral geniculate body of the rhesus monkey," J. Neurophysiol., 29, 1115-1156, 1966.

90. Zettler, F. and Järvilehto, M. "Histologishe Lokalisation der Ableiltelektrode. Belichtungspotentiale aus Retina und Lamina bei Calliphora," Z. vergl. Physiol., 68, 202-210, 1970.